2008

Identification of Loss of Specific FMRP-RNA Interactions as a Cause of Fragile X Syndrome

Julie B. Zang

Identification of loss of specific FMRP-RNA interactions as a cause of Fragile X Syndrome

A thesis presented to the faculty of
The Rockefeller University
in partial fulfillment of the requirements
for the degree of Doctor of Philosophy

by

Julie Biyuan Zang

June 2008

Identification of loss of specific FMRP-RNA interactions as a cause of Fragile X Syndrome

Julie Biyuan Zang, Ph.D.

The Rockefeller University 2008

Fragile X Syndrome presents with a clinical picture of moderate to severe mental retardation and behavioral abnormalities including autistic features resulting from the loss of function of a RNA-binding protein, Fragile X mental retardation protein (FMRP). This work is devoted to the understanding of functional roles of FMRP in normal neuronal development and in the pathogenesis of the Fragile X Syndrome. Particularly it focuses on the study of FMRP RNA binding properties, using both mouse models and biochemical analyses. The disease is usually caused by a triplet repeat expansion in the 5'UTR of the FMR1 gene leading to loss of transcription of FMR1 mRNA, but one severely affected patient has an isoleucine to asparagine point mutation in one of the RNA-binding domains of FMRP, hnRNP K homology (KH-type) domain 2. This I304N mutation has previously been shown to abrogate RNA binding. We generated and analyzed mouse models harboring the I304N mutation. The mutant protein retains some normal activities, as it is competent to bind both protein partners such as FXR1P and FXR2P and, via its RGG-domain, to G-quartet RNA, confirming it is not a completely functionless denatured protein. However, I304N protein is defective in RNA binding and is dissociated from polyribosomes. Moreover, electrophysiologic and behavioral deficits of the I304N mouse reveals that the mutation confers an FMRP-null-like phenotype on the mouse. These observations support the suggestion that a key function of FMRP in mediating normal cognition is sequence-specific RNA binding, and heightens the interest in identifying FMRP-RNA interactions.

To find mRNAs bound by FMRP in mouse brain, we have used UV crosslinking and immunoprecipitation (CLIP), a new methodology that has several advantages over conventional methods for identification of bona fide *in vivo* RNA ligands for RNA binding proteins. We obtained a defined set of FMRP RNA targets, including previously validated microtubule associated protein 1b (Mtap1b). These RNA targets encode proteins of coherent biological functions related to cytoskeletal organization and synaptic transmission, suggesting FMRP may regulate cytoskeletal dynamics, dendritic and axonal

functions that all converge at the developing synapse. Therefore, loss of FMRP KH2 domain specific RNA binding and proper regulation of RNA metabolism contributes to the synaptic dysfunction underlying the pathogenesis of cognitive and behavioral deficits observed in Fragile X Syndrome.

Acknowledgements

I owe thanks to many people over the past few years for their help, encouragement, and contributions. First and foremost, I have the utmost appreciation for the unwavering guidance of my advisors, Drs. Robert and Jennifer Darnell. Bob is always inspirational, full of great ideas and insights, always intriguing me to think about the big pictures and bringing the projects to the next level. Every day in Bob's lab is exciting and challenging. Jennifer has given me invaluable guidance, support and patience throughout the five years. She is always ready with suggestions of a good experiment or how to troubleshoot a difficult experiment. Working closely with her in the past years, she will forever be my role model.

I would also like to thank my thesis committee members, Drs. Thomas Tuschl, Michael Young for their interest in and valuable suggestions to my thesis projects. I would like to extend my appreciation to Dr. David Nelson who kindly arranged his schedule and traveled from far to serve as my outside examiner. He also generously provided the FMR1/FXR2 double knockout mouse model, which helped my projects greatly.

I am grateful to all the past and present members of the Darnell laboratory for creating a fun and stimulating work environment. Especially, Claire Fraser, Sarah van Driesche, Olga Mostovesky, and Elizabeth Stone for comprising such a wonderful FMRP group; Ru Zhong, Kiran Musunuru, Katie Staudt, Guanglin Yin for their contribution to the I304N project; Kirk Jensen, Jernej Ule, Aldo Mele, Sung-wook Chi, Xuning Wang for teaching me CLIP and their assistance; Graeme Couture, Kate Dredge, Taesum Eom, John Fak, Gulayse Ince-Dunn, Donny Licatalosi, Tiny Marney, Kevin O'Donovan, Woong-yang Park, Nishath Rehman, Matteo Ruggiu, Giovanni Stefani, Huidong Wang, Ken Wickiser, Shirley Xie, Masato Yano for their help, protocols, discussion and encouragement.

I am thankful to our collaborators, Dr. Kimberly Huber at UT Southwestern, Dr. Richard Paylor at Baylor College of Medicine, and Dr. Justin Fallon at Brown University for their work on the analysis of the I304N mouse model, linking our biochemical data to the phenotypic findings made in their laboratories.

I would like to express my gratitude to the Weill Cornell/Rockefeller/Sloan-Kettering Tri-institutional MD-PhD program that has funded my education and research. In addition, I owe many thanks to Dr. Olaf Andersen for advice and encouragement.

I am indebted to my parents, Zeng-you and Sze-wah Zang, for their love and endless support. None of this could be possible without them. Finally I would like to thank my husband, John Wang, for always being there and having faith in me. Having met him has been the best thing happened to me in my graduate school.

TABLE OF CONTENTS

LIST OF FIGURES

LIST OF TABLES

CHAPTER I. INTRODUCTION

Neuronal RNA binding proteins

Neurons are highly specialized cells that present an impressive complexity. They have a relatively small cell body but an extensive network of projections and connections, which in some instances can extend a huge distance away from the nucleus. Neurons can form neural circuitry through the relay of information between cells at synapses, in order to communicate with each other. Their complexity in structure and function requires mechanisms for spatial control and diversity of gene expression. The role of RNA binding proteins (RBPs) within the nervous system is critical. RBPs can deliver mRNAs out to neuronal processes and await proper signals to regulate local protein translation. They alternatively splice pre-mRNAs to generate a versatile repertoire of functionally different proteins. They regulate at the level of transcription, RNA editing, splicing, nuclear export, mRNA turnover, localization, and translational regulation. RBPs are essential in the mechanisms underlying neurogenesis, neurite growth, synapse formation, and plasticity in neurons. Subsequently, there is direct association between neurological diseases and perturbation of RBP activity and RNA misregulation. Here we introduce a few prototypical examples of RBPs to elucidate their diverse roles in neuronal function and development.

-Splicing (Nova)

Nova family proteins were initially discovered as target onconeural antigens of the neurodegenerative disorder paraneoplastic opsoclonus-myoclonus ataxia (POMA), found in a small fraction of patients with tumors of the breast, lung and fallopian tubes. Nova family proteins are expressed solely in the central nervous system (CNS), an immune privileged site, and for this reason they are seen by the immune system as "foreign" antigens. When they are ectopically expressed in systemic tumors, they elicit an immune response that may suppress the tumor growth but simultaneously targets the CNS leading to neuronal death and neurological impairment (Albert et al., 2000; Albert et al., 1998; Buckanovich et al., 1993; Darnell and Posner, 2003; Musunuru and Darnell,

2001). As the name suggests, POMA is a syndrome marked by a loss of inhibitory motor control in the motor neurons leading to rapid irregular eye movement (opsoclonus), muscle spasm (myoclonus) and failure of coordination (ataxia) (Darnell, 2004, 2006). Nova family proteins harbor three KH-type (hnRNP K homology) RNA binding domains (RBD) (Siomi et al., 1993a). Nova proteins, predominantly nuclear, preferentially bind to YCAY repeats in exons or introns and have been well characterized to influence alternative splicing of pre-mRNAs coding for a network of synaptic proteins (Dredge and Darnell, 2003; Jensen et al., 2000a; Jensen et al., 2000b; Ule et al., 2003; Ule et al., 2006; Ule et al., 2005b). Nova-1 knockout mice show action tremors and difficulty walking, symptoms similar to those of POMA patients. Apoptotic death of motor neurons is seen in these mice. They ultimately die at 1-2 weeks of age (Jensen et al., 2000a). Nova-2 knockout mice have a lesser degree of ataxia and die at approximately 2-3 weeks; slow inhibitory post-synaptic current (sIPSC) mediated by metabotropic GABA(B) receptors is abolished in Nova-2 null mice (Huang et al., 2005).

-mRNA stability (Hu)

Another family of RBPs, also onconeural antigens, is the Hu proteins, which are involved in the development of paraneoplastic encephalomyelitis and sensory neuropathy (PEM/SN), most commonly associated with small cell lung cancer (SCLC) (Darnell, 2004, 2006). Among the Hu family, HuB, C, and D are neuron specific while HuA (HuR) is ubiquitously expressed (Brennan et al., 2000; Deschenes-Furry et al., 2006; Keene, 1999; Okano and Darnell, 1997). Hu family proteins harbor three RNA recognition motifs (RRMs). The best understood function of Hu proteins is a cytoplasmic role in binding specifically to AU-rich elements (ARE) found in the 3'UTR thereby stabilizing a few developmentally regulated transcripts, e.g. c-fos, c-myc, N-myc, $p21^{waf1}$, neuroserpin and MARCKS (Brennan et al., 2000; Deschenes-Furry et al., 2006; Keene, 1999). Additional functions of Hu have also been shown. For instance, HuD contains a nuclear export signal and interacts with mRNA export receptor TAP/NXF1 to regulate nuclear export. Furthermore, studies show that when shuttling of HuD is blocked, neurite elongation is severely impeded, suggesting that HuD plays an important role in trafficking and localizing its transcripts, e.g. Tau mRNA is targeted to axons and GAP-43

to growth cones (Deschenes-Furry et al., 2006). Finally Hu bound mRNAs are also targeted to ribosomes and polyribosomes, e.g. HuB and neurofilament-M mRNA. Therefore, Hu could also be involved, directly or indirectly through interacting with other RBPs, in translational control (Deschenes-Furry et al., 2006). HuD knockout mice, despite the presence of other family members, still display motor/sensory defects such as abnormal clasping reflexes of the hind limbs and poor rotarod performance (Akamatsu et al., 2005). In HuD deficient primary neurospheres, the number of slowly dividing stem cells in the adult subventricular zone is increased while the number of differentiating quiescent cells is decreased (Akamatsu et al., 2005), suggesting HuD is required at multiple points during neuronal development.

-mRNA localization (ZBP1)

Zip code binding protein 1 (ZBP1) has been discovered as an RBP to the conserved 54-nucleotide element, the zipcode, in the 3'UTR of β-actin mRNA (Ross et al., 1997). ZBP1 harbors two RRM domains in its N-terminal portion and four KH domains in its C-terminal portion, placing it in the highly conserved VICKZ (Vg1 RBP/Vera, IMP-1, 2, 3 (insulin-like growth factor II mRNA binding protein), CRD-BP (c-myc coding region determinant-binding protein), KOC (KH-domain-containing protein overexpressed in cancer), ZBP-1) family of RBPs (Yisraeli, 2005). Diverse roles in RNA metabolism are seen among these closely related proteins. The main function of ZBP1 has been shown to localize β-actin mRNA to filopodia where local synthesis of β-actin and polymerization occurs in developing neurons (Bassell et al., 1998; Zhang et al., 2001a). In cultured hippocampal neurons, knocking down ZBP1 reduces dendritic β-actin mRNA levels and leads to the loss of dendritic filopodia and synapse formation (Eom et al., 2003). Conversely, overexpression of an (EGFP)-beta-actin construct, which contains the zipcode, recruits endogenous ZBP1 to dendrites and increases the density of dendritic filopodia and filopodial synapses (Eom et al., 2003). Therefore, ZBP1 appears to mediate mRNA localization, which in turn regulates dendritic morphology and synaptic growth.

-Translational control (FMRP)

Our work focuses on the study of fragile X mental retardation protein (FMRP). Functional absence of this RBP is associated with the most common form of inherited mental retardation, the Fragile X Syndrome (FRAXA). The incidence is about 1 in 4000 males and 1 in 8000 females. Affected patients have moderate to severe mental retardation, macroorchidism, autistic features, attention deficit hyperactive disorders, seizures, and connective tissue dysplasia leading to a characteristic appearance of a long narrow face and large ears (Jin and Warren, 2000, 2003; O'Donnell and Warren, 2002). In most cases the disease is caused by the expansion of a CGG repeat in the 5' UTR region and methylation of CpG islands that lead to subsequent loss of FMRP expression (Jin and Warren, 2000, 2003; O'Donnell and Warren, 2002). As a result of CGG-repeat expansion, typical fragile X patients display a folate-sensitive breakage site at chromosome Xq27.3 upon cytogenetic analysis—hence the name "fragile X."

-Fmr1 gene

FRAXA is one of the pioneer examples of one gene being responsible for one disease; however, cloning the Fmr1 gene has not been easy. A great deal of genetic and physical mapping has been done to mark the fragile site. A yeast artificial chromosome (YAC) containing markers known to flank the fragile site has been identified, and it contains a CpG island that is aberrantly methylated in fragile X patients (Heitz et al., 1991). Finally, the laboratories of Nelson, Oostra and Warren have used this same YAC to probe a human brain cDNA library and clone the Fmr1 gene responsible for the disease (Verkerk et al., 1991), and the absence of Fmr1 expression has been verified in majority of fragile X patients (Pieretti et al., 1991). Fmr1 spans 38 kilobases (kb) and encodes a 4.4kb transcript consisting of 17 exons, which are subject to alternative splicing (Ashley et al., 1993a; Eichler et al., 1993). Fmr1 has two autosomal paralogs, FXR1 and FXR2, which make up the Fragile X-related (FXR) family members (Siomi et al., 1995; Zhang et al., 1995). Gene structure is highly conserved amongst the three family members, indicating that they are derived from a common ancestral gene (Kirkpatrick et al., 2001). In Drosophila, there is only a single ortholog, dfxr (Wan et al., 2000).

-FMRP RNA and protein interactions

FMRP is almost ubiquitously expressed with the highest expression observed in brain and testes; however, in the nervous system, its expression is restricted to neurons. FMRP is characterized by multiple RNA binding motifs, two tandem KH (hnRNK homology)-type RNA binding domains (Siomi et al., 1994; Siomi et al., 1993b), a spacer region, and an arginine and glycine-rich RNA binding domain (RGG box) (Siomi et al., 1993b). The N-terminus may also have RNA binding ability as assessed by a ribohomopolymer assay (Adinolfi et al., 1999). However, the identification of FMRP RNA targets has not been a trivial task. Many laboratories have attempted this with various approaches (Brown et al., 2001; Chen et al., 2003; Darnell et al., 2005a; Darnell et al., 2001; Dolzhanskaya et al., 2003; Miyashiro et al., 2003; Muddashetty et al., 2007; Sung et al., 2003; Todd et al., 2003; Xu et al., 2004; Zalfa et al., 2003; Zhang et al., 2001b) (see Chapter IV Introduction for details), and a long list of RNA candidates has been generated. However, due to some intrinsic uncertainties underlying each technique, these targets have limited overlap, making it difficult to distinguish true FMRP targets from falsely-identified ones. Therefore, identifying a set of reliable FMRP RNA targets is still highly necessary. So far the most believed and functionally-validated target, combining both biochemical analysis and Drosophila genetics, is Mtap1b mRNA (Brown et al., 2001; Zhang et al., 2001b).

Aside from binding to RNA, FMRP has been reported to be in complex with many other proteins. Its N-terminal domain has been characterized by NMR structures and deletion studies as a platform for protein-protein interactions (Adinolfi et al., 2003; Mazroui et al., 2003; Ramos et al., 2006). FMRP interacts with FXR1P and FXR2P in mouse brain (Ceman et al., 1999; Tamanini et al., 1999; Zhang et al., 1995). Yeast 2 hybrid assays have also identified NUFIP1 (Bardoni et al., 1999), CYFIP1 and CYFIP2 (Schenck et al., 2001), which are shown in Drosophila to interact with Rac GTPase pathway that controls actin cytoskeleton remodeling (Schenck et al., 2003), and 82-FIP (Bardoni et al., 2003). Nucleolin, YB1/p50, Purα, mStaufen, and myosin Va have also been shown to be components of FMRP containing complexes (Ceman et al., 1999; Ceman et al., 2000; Ohashi et al., 2002), although evidence for their direct interaction

with FMRP is not sufficient. In Drosophila, dFXR has been found to interact biochemically with Argonaute 2 (dAgo2), a key component of the RNA-induced silencing complex (RISC) (Caudy et al., 2003; Caudy et al., 2002; Ishizuka et al., 2002) and genetically with dAgo1 (Jin et al., 2004). In mammalian cell cultures, FMRP and FXR1P have been shown to co-immunoprecipitate with mAgo2 (ortholog of dAgo1) (Jin et al., 2004; Vasudevan and Steitz, 2007).

-FMRP role in translational control

Despite our knowledge of FMRP multiple functional domains and interacting partners, the precise physiological functions of FMRP have not been defined. The most likely function of FMRP, given the sum of the current literature in the field, is in translational regulation. A strong piece of evidence is that FMRP is on polyribosomes in cell culture and mouse brain in an RNA-dependent manner (Corbin et al., 1997; Feng et al., 1997a; Feng et al., 1997b; Khandjian et al., 1996; Khandjian et al., 2004; Stefani et al., 2004). FMRP has been shown to be a translational inhibitor in rabbit reticulocyte lysate and in over-expressed cell culture, but these studies used candidate mRNAs which have little overlap with identified FMRP targets (Laggerbauer et al., 2001b; Li et al., 2001; Mazroui et al., 2002; Zhang et al., 2001b); both systems are also considerably different from endogenous cellular environment. The best *in vivo* evidence comes from combined biochemical data and Drosophila genetics. Mutations of futsch/Mtap1b or dfxr alone lead to aberrations in architecture of neuronal synapses, but double mutation restores synaptic architecture (Zhang et al., 2001b). Together with the findings that Mtap1b mRNA coprecipitates with FMRP and has increased association with polyribosomes (Brown et al., 2001), these data have support the model that FMRP negatively regulates translation of Mtap1b mRNA. In addition, FMRP has been proposed to regulate local translation. The evidence comes from FMRP trafficking to dendrites and synapses after stimulation of metabotropic glutamate receptor (mGluR) and is dependent on microtubules (Antar et al., 2004; Antar et al., 2005; De Diego Otero et al., 2002). A few FMRP target mRNAs encoding synaptically localized proteins (PSD95, GluR1/2, and CamKIIa) have been shown to have increased polyribosome association in synaptoneuorosome preparations in absence of FMRP (Muddashetty et al., 2007),

suggesting FMRP as a local translational repressor. Moreover, the relatively new finding of dFXR association with RISC components implies that FMRP may also repress translation via microRNAs (miRNAs) (Caudy et al., 2003; Caudy et al., 2002; Ishizuka et al., 2002; Jin et al., 2004). Recently, one unbiased screen has identified FXR1P in complex with mAgo2 binding to AREs. Instead of repressing translation, FXR1P and mAgo2 were shown to up-regulate translation, likely through a different miRNA mediated mechanism (Vasudevan and Steitz, 2007). Due to the common ancestry of FMRP and FXR1P, this finding suggests that FMRP may be a translational enhancer, too.

Understanding translational regulation

Translation of mRNA into protein represents the final step in the gene expression pathway. Control of translation is a mechanism to fine-tune protein expression levels in both time and space in a wide range of biological situations. Two general modes of control can be envisioned: 1) global control, in which the translation of most mRNAs in the cell is regulated, and 2) mRNA specific control, whereby the translation of a defined group of mRNAs is modulated without affecting general protein synthesis or translational status as a whole.

Translation of an mRNA to cognate protein proceeds in three sequential steps of initiation, elongation, and termination and regulation can occur at any of these steps. During initiation, an eIF2·GTP·Met-tRNA$_i$ ternery complex binds to 40S ribosomal subunit to form a 43S pre-initation complex. The 43S complex is recruited to the initiation condon of the mRNA to form a stable 48S complex, which is assisted by a set of factors from the eIF4 family. These factors subsequently dissociate, the 60S ribosomal subunit joins the 40S subunit to form the 80S complex, and elongations ensues. During elongation, eEF1A and eEF1B guide aminoacyl-tRNAs to the A site on the ribosome; following peptide bond formation, eEF2 mediates the ribosome translocation by one codon along mRNA. Finally, termination at a stop codon is mediated by a set of release factors. eEF1 structurally and functionally mimics tRNA to decode stop codons and promote ribosome-catalyzed peptidyl-tRNA hydrolysis, releasing nascent polypeptide chain (Sonenberg et al., 2000).

-Global translational control

Global regulation mainly occurs by the modification of translation initiation factors. One prototypical example is of cap-binding protein eIF4E availability. Interaction of eIF4E with scaffold protein eIF4G is required for cap-mediated recruitment of the 43S ribosomal complex to mRNA. eIF4E-binding proteins (4E-BPs) compete with eIF4G for the interactions with eIF4E, preventing recruitment of the 43S complex and resulting in translational inhibition. Following brain-derived neurotrophic factor (BDNF) stimulation, activation of PI3K/Akt/mTOR signaling pathway has reported in neurons to phosphorylate 4E-BPs rendering it to dissociate from eIF4E, therefore enable eIF4E and eIF4G interaction to start translation (Takei et al., 2004; Takei et al., 2001).

-mRNA specific regulation of translation

mRNA specific regulation of translation on the other hand is driven by regulatory protein complexes that recognize particular elements present on the target mRNA. A special and very interesting example of mRNA specific regulation is the local regulation of translation that occurs in polarized cells, such as neurons. The purpose is to generate a protein gradient or to restrict protein expression to a small defined region, e.g. synapses.

Translational initiation is typically rate limiting and thus often a target for regulation. Here are a few well-characterized examples of mRNA specific translational control at various steps of the initiation stage. Cytoplasmic polyadenylation element binding protein (CPEB) binds to a uridine rich cytoplasmic polyadenylation element (CPE) located in the 3'UTR of target mRNA, e.g. dendritic CamKIIα (Wu et al., 1998). In response to NMDAR activation, CPEB is phosphorylated by aurora kinase. After phosphorylation, CPEB binds CPE in CamKIIa 3'UTR and recruits poly(A) polymerase to polyadenylate the mRNA. Polyadenylation promotes the dissociation of Maskin from eIF4E, thus "unmasking" eIF4E, so local translation of CamKIIα is activated (Huang et al., 2002; Wells et al., 2001; Wu et al., 1998). Iron regulatory proteins (IRP)1 and 2 bind a stem loop sequence, iron responsive element (IRE), in the 5'UTRs of ferritin heavy and light-chain mRNAs within 40 nucleotides of the cap structure. IRP1 and 2 sterically block the 43S ribosomal complex recruitment to ferritin mRNA that is engaged with eIF4F complex, thereby preventing translation initiation (Gray and Hentze, 1994;

Muckenthaler et al., 1998). CPEB targets the formation of eIF4F complex, whereas IRPs allow the cap binding complex eIF4F to bind mRNA, but blocks 48S ribosomal complex recruitment. Still a later step of translation initiation, formation of the 80S ribosomal complex is regulated by hnRNP K and hnRNP E1. They bind to a CU-rich repeat element, also known as differentiation-control element (DICE) that is located in the 3'UTR of 15-lipoxygenase (LOX) mRNA. Sucrose gradient analysis has been used to show that 48S complex formation occurrs, but 80S momosome formation is inhibited. hnRNP K and hnRNP E1 prevented joining of the 60S ribosomal subunit by interfering with translational initation factors. hnRNP K and E1 translational regulation of LOX mRNA is bypassed in IRES-dependent translation, since IRES does not require any translational initiation factors (Ostareck et al., 2001; Ostareck et al., 1997; Ostareck-Lederer and Ostareck, 2004).

Translational control can also be achieved through regulation at the elongation stage mainly for two reasons. First is to maintain translational fidelity, since it is inversely related to elongation activity (Carr-Schmid et al., 1999). Second, when translational elongation is inhibited, polyribosomes are still retained, which will allow translation to resume rapidly when needed. One such protein that regulates elongation is eEF2, which mediates ribosome translocation from one codon to the next. Two major signaling mechanisms—Ca^{2+} (shown in amphibian tectum and rat inferior colliculi) and cAMP (shown in cardiac myocytes) activate Ca^{2+}/calmodulin dependent kinase III (CamKIII), which phosphorylates eEF2. Phosphorylated eEF2 becomes inactive and switches off elongation (McLeod et al., 2001; Scheetz et al., 1997, 2000). Increased cAMP by activation of protein kinase A (PKA) is usually seen under conditions of increased energy demand, therefore putting a brake on elongation, which is the most energy consuming step of translation in order to conserve the energy for more urgent purposes.

-miRNA mediated translational control

Perhaps the most recent and exciting area of translational control is miRNA dependent translational repression. They are small RNA molecules of ~22 nucleotides in length that hybridize by incomplete base pairing, usually to the 3'UTR of target mRNAs.

The first miRNAs discovered were lin-4 and let-7, which are crucial for regulating developmental timing in Caenorhabditis elegans. Because the target mRNA remains intact after miRNA binding, miRNAs are believe to repress translation rather than degrading mRNA. The mechanism for repression is largely unknown. The initial hypothesis has been that miRNAs mediate repression of gene expression after the initiation step, since translational repression of lin-14 mRNA by lin-4 miRNA does not alter lin-14 mRNA association with polyribosomes (Engels and Hutvagner, 2006). This, however, has been challenged when a few laboratories have reported miRNA mediated repression can skew some mRNAs toward the top of the polyribosome gradient and can be bypassed in IRES-dependent translation, suggesting miRNA inhibition of translation can also happen at the initiation step (Humphreys et al., 2005; Pillai et al., 2005). Yet another development is that Argounate proteins, miRNAs, and their target mRNAs can accumulate in cytoplasmic foci, known as P-bodies (processing bodies), where translational repression happens (Jackson and Standart, 2007). It is still unknown how RBPs may play a role in miRNA dependent translational regulation, but a role in helping miRNAs bind the correct mRNA is worth exploring.

Modeling human neurological disease in animals

Identification of disease-associated genes has facilitated the understanding of many diseases, especially in the realm of diagnosis. Animal models provide a link between the lesion of a gene and the pathologic manifestation of a disease. Mice, for instance, share important physiological, anatomical, and genomic similarities with humans. Fine genetic manipulation in animal models enables us to tease out the steps of disease-causing mechanisms in a physiologically-relevant system. Lastly, animal models also allow us to test possible treatments in a living organism. Here we provide a few examples of modeling a few neurological diseases using transgenic, knockout, knock-in, and conditional knockout mice.

-Modeling Spinal muscular atrophy

Spinal muscular atrophy (SMA) is a recessive genetic disease of spinal motor neuron degeneration, muscle denervation, and atrophy. More than 95% of patients have

been identified to carry a partial or complete deletion of the telomeric survival of motor neuron gene (SMN1). SMN1 has a highly homologous centrimeric copy, SMN2, of which all SMA patients carry at least one intact copy. As SMA is a recessive disorder, it is believed that remaining levels of SMN protein can govern the severity of the disease in patients. A combination of different SMA mouse models has provided valuable insights to the understanding of the disease. Unlike in human, there is only one mouse SMN ortholog, and knockout of mouse SMN results in early embryonic lethality (Schrank et al., 1997). Transgenic mice, which allow ectopic expression of human SMN2, have been generated, and these mice have been crossed onto the SMN knockout background. These SMN knockout and human SMN2 transgenic mice have survived and recapitulated the motor neuron death in the spinal cord and skeletal muscle abnormalities of the human disease (Hsieh-Li et al., 2000; Monani et al., 2000). Transgenes can insert in the genome in tandem repeats, resulting in lines of high and low expressers. Utilizing differential SMN expression of these transgenic mice, it has been shown that high expressers produce a milder phenotype than low expressers, confirming belief that the level of SMN protein inversely correlates with the disease severity. Conditional knockout mice of SMN, which utilize the Cre-LoxP recombination system and allow tissue specific knockdown of the gene, have further elucidated the mechanism behind muscle denervation. Neuron specific ablation of SMN resulted in morphological changes in motor neuron and skeletal muscle denervation, providing evidence that motor neurons are the primary target of SMN (Frugier et al., 2000). Interestingly, muscle specific SMN knockout mice have a dystrophic phenotype that causes paralysis, indicating that SMN defect in skeletal muscle may also have a role in SMA pathogenesis (Cifuentes-Diaz et al., 2001).

-Modeling Rett Syndrome

Rett syndrome (RTT) is a neurodevelopment disorder that predominantly affects females who show normal development for 6-18 months but then enter a period of regression in which motor and language skills are lost. Mutations in the gene encoding methyl-CpG binding protein 2 (MeCP2) cause RTT. MeCP2 is on the X chromosome, therefore the affected females are mosaic due to X chromosome inactivation (XCI). Patients with XCI skewed toward mutant allele inactivation have milder symptoms. The

same mutation in males causes a more severe phenotype, e.g., neonatal encephalopathy or infantile death. To model the disease, MeCP2 knockout mice have been generated and show hypoactivity, abnormal breathing, uncoordinated gait, and death at 6-12 weeks of age (Guy et al., 2001), replicating the severe disease found in infant males. Brain specific MeCP2 knockout mice show a similar phenotype as the MeCP2 knockout (Chen et al., 2001), indicating the loss of MeCP2 in the CNS alone is sufficient to cause the disease, despite MeCP2 expression in many other tissues. Finally, a knock-in strategy has been used for generation of a hypomorphic truncation mutation of MeCP2 308 recapitulating many features of classic RTT in male mice, bypassing the complication of XCI of heterozygote females (Shahbazian et al., 2002). These RTT mouse models, complementing one another, are valuable systems in which functions of MeCP2 are examined.

-Fragile X Syndrome animal models

A pathogenetic link between the lesion in the FMR-1 gene and the fragile X phenotype has been established by the generation of FMR-1 knockout mice. These mice bear many similarities to human patients. They have significant macroochidism (Dutch-Belgian Fragile X Consortium, 1994) and abnormally-long, tortuous dendritic spines (Comery et al., 1997; Nimchinsky et al., 2001). They exhibit defects in behavior and learning, e.g., hyperactivity, decreased level of anxiety (Dutch-Belgian Fragile X Consortium, 1994; Peier et al., 2000), and increased sensitivity to audiogenic seizure (Chen and Toth, 2001; Musumeci et al., 2000). Electrophysiologic studies on these mice have shown they have enhanced mGluR-dependent long term depression (LTD) in the hippocampus that persists in the absence of *de novo* protein synthesis (Huber et al., 2002; Nosyreva and Huber, 2006), suggesting a synaptic plasticity defect underlying the fragile X biology. Enhanced mGluR dependent LTD has also been observed at parallel fiber synapses in cerebellum in Purkinje cell specific Fmr1 knockout mice. Purkinje specific knockout of FMRP alone is sufficient to cause defect in classical delay eye-blink conditioning in these mice (Koekkoek et al., 2005), which later has been demonstrated in human patients. In addition to modeling the various defects of the Fragile X Syndrome, the knockout mice have already been used widely in comparison to wild type mice in

various validation assays to elucidate functional roles of FMRP. Furthermore, trials of clinical treatments targeting mGluR signaling pathway have already been undertaking using these mice as a model system for the human disease.

In addition to Fmr1 knockout mice, Fmr1 YAC transgenic mice, an over-expresser of human FMR1, have been generated and functionally rescued the knockout phenotype, shown by behavioral assays and testicular phenotype (Peier et al., 2000). Additionally, over-expression of FMRP causes an opposite phenotype, implying the level of FMRP is likely to be tightly regulated in vivo; a moderate overproduction can harbor its own phenotype.

FMRP has two functional paralogs, FXR1P and FXR2P, which are derived from the same ancestral gene (Kirkpatrick et al., 2001). A genetic system like Drosophila where there is only one ortholog, dfxr, can be used to knock out all three family members. Dfxr mutant flies exhibit phenotype in many ways similar to Fmr1 knockout mice. They have increased synaptic growth at the neuromuscular junction, arrhythmic circadian activity, reduced courtship, and impaired coordinated behavior (Dockendorff et al., 2002; Inoue et al., 2002; Morales et al., 2002; Zhang et al., 2001b). However, no one has yet rescued the Drosophila phenotype with a mammalian Fmr1 gene. Therefore, FXR1 and FXR2 knockout mouse models have each been generated. FXR1 knockout mice have a striated muscle defect and unfortunately die shortly after birth likely due to cardiac or respiratory failures (Mientjes et al., 2004). FXR2 knockout mice exhibit many behavioral abnormalities overlapping with Fmr1 knockout mice (Bontekoe et al., 2002; Spencer et al., 2006). Indeed, Fmr1/FXR2 double knockout mice showed an exaggerated behavioral phenotype (Spencer et al., 2006), suggesting that FXR family proteins may function synergistically; one possibility for the relatively mild phenotype in the Fragile X Syndrome may be due to the functional redundancy of its paralogs.

All these mouse models so far are a loss or gain of the entire FMRP protein. Because FMRP consists of multiple functional domains, it has been difficult to determine which domain's loss of function is critical for the pathogenesis of the disease until a single fragile X patient was reported to harbor a *de novo* isoleucine to asparagine mutation in KH2 RNA binding domain (DeBoulle et al., 1993). He has the clinical stigmata of severe fragile X syndrome: coarse acromegaloid features, a large forehead, an

asymmetric long face, large ears, thick lips, mandibular prognathism, focal seizures, and impressive macroorchidism with both testicles exceeding 100ml volume. This I->N mutation has previously been shown by our lab and others to abolish RNA binding by this and similar KH-type RBDs, therefore offering hope of focusing FMRP studies in a key functional domain. A mouse model of this specific mutation will be highly valuable to understand how the loss of specific functions of FMRP in normal neuronal biology contribute to the defects in neuronal function seen in Fragile X Syndrome.

CHAPTER II. EXPERIMENTAL PROCEDURES

Generation of targeted Fmr1 I304N knock-in mutation

A genomic clone encoding Fmr1 was isolated from a BAC library derived from a 129 mouse (ES-129/SvJ BAC library, clone address 217I21, Incyte Genomics). To generate a Fmr1 KH2 I304N targeting vector, we first cloned a 7.2 kb BamHI-XhoI 5' homology arm spanning from intron 5 to intron 9 into pBSK plasmid. Simultaneously we cloned a 1.9kb XhoI-KpnI fragment including the I304N mutation and 3'homology arm (1.3kb). On the XhoI-KpnI fragment, PCR mutagenesis generated the I304N mutation in exon 10 (as well as a new HindIII site) as well as a new XbaI site in the middle of intron 10 that showed divergence in the mouse and human sequences. The loxP-Auto-Cre-Neo^{R}-loxP (ACNF) cassette was inserted in this novel XbaI site. Finally, the 5' homology arm and the XhoI-(I304N)-(ACNF)-KpnI fragment were ligated together into pBSK plasmid. The plasmid was linearized by NotI and used to electroporate ES cells at the Transgenic Services Laboratory at The Rockefeller University. Genomic DNA from individual colonies was digested with BamHI and screened by Southern blot analysis. The Southern probe overlapping exon 12, which had no corresponding sequences in FXRs (Kirkpatrick et al., 2001), would distinguish the targeted allele, 2.7kb, from wild type locus, 9.6 kb. Correctly targeted clones were selected for blastocyst injection and transferred to pseudopregnant females, from which germline chimeras were obtained.

Generation of Fmr1 I304N BAC transgenic mice

The I304N mutation was inserted into BAC clone encoding Fmr1 by the homologous recombination protocol of Heintz and colleagues (Yang et al., 1997). In short, a shuttle vector was cloned comprising 1kb of genomic sequence centered on the I304N mutation, the *recA* recombinase gene, tetracycline resistance cassette, and a temperature-sensitive origin of replication. E coli of DH10B strain harboring Fmr1 BAC, which also contains a chloramphenicol resistance cassette, were transformed with the shuttle vector and doubly selected for tetracycline and chloramphenicol first at 30^{o}C and then 43^{o}C for co-integration of Fmr1 BAC and I304N shuttle vector. Co-integrated clones were then

grown at 43°C in the presence of chloramphenicol to allow the resolution of shuttle vector from BAC. Resolved clones were screened by PCR for the presence of I304N mutation. I304N BAC plasmid DNA was then prepared by cesium chloride gradient ultracentrifugation, digested with NotI, purified, buffer exchanged to high salt injection buffer, and finally injected into pronuclear oocytes of the inbred FVB/N strain by the Transgenic Services Laboratory at The Rockefeller University. Germline transmission of the transgene was seen with two female Fmr1 I304N founders, A and B, which were then bred to the Fmr1 null background. One wild type transgenic founder was also obtained as control.

Histopathology and testicular measurement

Three I304N knock-in mice and three wild type littermates were sacrificed and tissues fixed in 10% formalin overnight and embedded in paraffin blocks. Tissue sections were deparaffinized, rehydrated, stained with hematoxylin & eosin, and visualized with a Zeiss Axioplan microscope by the Animal Phenotyping Core Facility at the Rockefeller University. For testicular analysis, seminiferous tubule diameters were measured and interstitial cell numbers were counted under randomly selected 20X power field blind of genotype. Macroorchidism was assessed by combined weight of both testes of I304N knock-in mice compared to that of either wild type or Fmr1 knockout littermates. Measurements from multiple litters of similar ages were pooled and subjected to statistical analysis.

RNA preparation

RNA from mouse tissues or polyribosome fractions was both extracted using Trizol LS Reagent (Invitrogen). 10ng luciferase RNA was spiked into each polyribosome fraction as a control for RNA recovery. 49:1 chloroform:isoamyl alcohol was added to facilitate aqueous and phenol-chloroform organic phase separation. After 15min 12,000xg centrifugation, the aqueous phase where RNA remained was collected and precipitated with ethanol at -20°C overnight. After precipitation, RNA was pelleted at 20,000xg for 20min at 4°C, washed with 75% ethanol, and then was dissolved in H_2O. Extracted RNA

was then RQ1 DNase (Promega) treated at 37^{o}C for 1hr and underwent a second round of phenol-chloroform extraction and ethanol precipitation.

Quantitative RT-PCR

Purified RNA was reverse transcribed using random hexamers (Roche) and superscript III reverse transcriptase (Invitrogen). cDNA products were amplified using SYBR green PCR master mix (Applied Biosystems) with 200nM of the following primers.

Fmr1 1F (spanning exon 2 to 3) 5'-TGAAAACAACTGGCAACCAGAGAG-3'
Fmr1 1R (spanning exon 2 to 3) 5'-CAGGTGGTGGGAATCTCACATC-3'
Fmr1 2F (spanning exon 10 to 11) 5'-GTCAGGAGTTGTGAGGGTGAGG-3'
Fmr1 2R (spanning exon 10 to 11) 5'-GGAAGGTAGGGAACTTGGTGGC-3'
GAPDH F 5'-CATGGCCTTCCGTGTTCCTA-3'
GAPDH R 5'-GCGGCACGTCAGATCCA-3'
Luc F 5'-GCCTTGATTGACAAGGATGGA-3'
Luc R 5'-CAGAGACTTCAGGCGGTCAAC-3'
Mtap1B F 5'-CATCACTGAACCACAGACTTGCG-3'
Mtap1B R 5'-AGCTGCCACTGAGAAGTTTGCC-3'
APC F 5'-TGAGAATACCGATGACAAACACC-3'
APC R 5'-CCACTGGTCCCCTTGACC-3'
Rab6ip F 5'-GTTCACCAACAGGGAACAGATG-3'
Rab6ip R 5'-GGGCAGGTAGGGCTCAGG-3'
Kif5c F 5'-GGAGGAGGAGGTGGCTCTTC-3'
Kif5c R 5'-GGGACAGAAAGGAACTGGTGAC-3'
Arhgap5 F 5'-CGCGCCGGGAGAGATG-3'
Arhgap5 R 5'-TGTAGTTCCCTCATTGCCAAAG-3'

Quantitative PCR amplification of was performed using 7900HT sequence detection system (Applied Biosystems) at Genomic Resource Center at The Rockefeller University. Fluorimetric intensity of SYBR green was monitored during each cycle of amplification to quantify mRNA level. Regression curves were drawn for each sample and relative amount of mRNA was calculated from the threshold cycles using the instrument's

software, SDS 2.0. For expression level in total brain, relative Fmr1 mRNA level was measured using standard curve method and normalized to internal control GAPDH mRNA. For polyribosome distribution, relative Fmr1 mRNA or FMRP target mRNA level in each fraction was normalized to spiked in luciferase RNA analyzed using ΔΔCt method. mRNA in each fraction was then plotted as a percentage of its total over the entire polyribosome gradient to illustrate its translational profile.

Northern blot

Northern blot was performed following NorthernMax-Gly protocol (Ambion). Briefly, 30ug of brain RNA and 10ug of testes RNA were denatured by with Glyoxal load dye at 50^{o}C for 30min and then were separated on a 0.8% agarose gel in 1X Gel Prep/Gel Running buffer. The RNA then was transferred from the agarose gel to a GeneScreen Plus hybridization transfer membrane (Perkin Elmer) in 10XSSC. P^{32}-labeled Fmr1 probe was hybridized to membrane at 68^{o}C for 2hrs in QuikHyb hybridization solution (Strategene). β-actin probe was hybridized at 42^{o}C for 1hr with in Ultra-Hyb Oligo solution (Ambion). Membrane was then washed with 2XSSC, 0.1% SDS and 0.1XSSC, 0.1% SDS at room temperature. Radiolabeled signals were detected and quantified by phosophoimager (Bio-Rad).

Fmr1 probe, complementary to 3'UTR region, was synthesized by T7 *in vitro* transcription with trace P^{32}-α-UTP using Maxiscript Kit (Ambion). Template DNA for transcription was generated using a reverse primer that had the T7 core promoter sequence appended (underlined).

Fmr 3UTR F 5'-TCAGCAGTATGTTTCAGTCTTTCGG-3'

Fmr 3UTR R 5'-

<u>TAATACGACTCACTATAGGGGAGA</u>GTTTTCAAAGTTGAAATTCGTCATCAGG

-3'

20nt long DNA anti-sense to β-actin exon 4 was 5' end radiolabeled with T4 PNK (NEB) and used as Northern probe for β-actin.

Antibodies

The following antibodies were used throughout this work:

mouse monoclonal anti-FMRP 1C3 (1:1000, IB). Chemicon.

mouse monoclonal anti-FMRP 2F5 (1:100, IB) (Gabel et al., 2004).

rabbit polyclonal anti-FMRP 17722 (1:500, IB). Abcam.

mouse monoclonal anti-FMRP 7G1-1 (1:100, IB, IP) (Brown et al., 2001; Ceman et al., 2003b) (Developmental Studies Hybridoma Bank (DSHB), University of Iowa.

rabbit polyclonal anti-FXR1P ML13 (1:10,000, IB). A generous gift from Dr. E. Khandjian (Université Laval).

mouse monoclonal anti-FXR2P 1G2 (1:100, IB). DSHB, University of Iowa.

mouse monoclonal anti-hsp90 (1:5000, IB). BD Bioscience.

mouse monoclonal anti-β-actin (1:20,000 IB) Abcam.

mouse monoclonal anti-γ-tubulin (1:10,000) Sigma.

mouse monoclonal anti-ribosomal S6 protein. Cell Signaling.

human POMA patient serum against Nova (1:1000, IB)

mouse monoclonal anti-His-tag HRP conjugated (1:5000, IB). Novagen.

mouse monoclonal N-APC antibody (1:500, IB) and rabbit polyclonal M-APC antibody (1:500, IB). A generous gift from Dr. I. Nathke (University of Dundee).

mouse monoclonal anti-Kif1a (1:500, IB). BD Bioscience.

rabbit polyclonal anti-Kif5a (1:1500, IB). Affinity Bioreagents.

rabbit polyclonal anti-Akap6 (1:2000, IB). Abcam.

rabbit polyclonal anti-Grin2b (1:1000, IB). Covance.

mouse monoclonal anti-Psd95 (1: 1,000,000, IB). Upstate.

mouse monoclonal anti-Munc13 (1:200, IB). BD Bioscience.

mouse monoclonal anti-β-catenin (1:500, IB). BD Bioscience.

Mouse monoclonal anti-active β-catenin (1:1000, IB). BD Bioscience.

Mouse monoclonal anti-NMDAR1 (1:2000, IB). Chemicon.

Rabbit polyclonal anti-Synaptophysin (1:2000, IB). Chemicon.

Mouse monoclonal anti-CamKIIα (1:20,000, IB). Chemicon.

Rabbit polyclonal anti-Ago1 and Ago2 (1:250, IB). A generous gift from Dr. T. Tuschl, (The Rockefeller University).

secondary anti-mouse, rabbit, or human antibodies. Jackson Immunoresearch.

Total tissue extract

Tissues were each Dounce homogenized in RIPA lysis buffer (0.5% NP-40, 0.5% deoxycholic acid, 0.1% SDS in PBS, 50% glycerol, and Complete protease inhibitor cocktail (Roche)) sonicated, and spun 20,000xg at 4^{o}C for 15min. Protein concentration was determined by Bradford assay. 50ug of protein from each sample was boiled in SDS-sample loading buffer and continued for Western analysis.

Western Analysis

Samples were run on SDS polyacrylamide gels and transferred onto nitrocellulose membranes (Millipore). Membranes were blocked for 1hr at room temperature in 10% non-fat milk in Western blot wash buffer (WBWB) (23mM Tris, pH 8.0, 190mM NaCl, 0.1% w/v BSA, 1mM EDTA, 0.5% Triton X-100, 0.02% SDS). Respective primary antibodies and horseradish peroxidase-labelled secondary antibodies (Jackson Immunoresearch) in 10% milk-WBWB were used during incubation from 1hr at room temperature to overnight at 4^{o}C. Blots were washed with WBWB 5min for 5 times after each antibody incubation. Signals were detected by Chemiluminescence (Perkin Elmer) and quantified with Versadoc Imaging System (Bio-Rad).

T7 transcription and directed UV crosslinking IP

96 nt long GQ and KC RNAs (Darnell et al., 2005a; Darnell et al., 2001) were generated by T7 *in vitro* transcription of with P^{32}-α-UTP and P^{32}-α-GTP RNAs were urea-polyacrylamide gel purified and spiked into 100ul supernatant S2 brain lysate prepared as for polyribosome analysis below. RNAs were incubated with the brain lysates for 15min at room temperature and then UV crosslinked with Stratalinker. Lysates were then diluted with RIPA buffer (0.5% NP-40, 0.5% deoxycholic acid, 0.1% SDS in PBS) to increase the stringency for the following IP. IP was performed the same way as co-immunoprecipitation below, with the exception that RIPA buffer was the IP and wash buffer. Immunoprecipitates were run on 4-12% SDS-PAGE, transferred to nitrocellulose membrane, and exposed for autoradiograph.

Co-immunoprecipitation of FMRP and FXRPs

1:1 slurry of protein A sepharose beads (Sigma) were first bound to 120ug of rabbit anti-mouse Fcγ bridging antibody (Jackson Immunoresearch) and then bind to 10ul of anti-FMRP monoclonal 7G1-1 ascites (5mg/ml). Brain cytoplasmic lysates (0.5% Triton X-100, 10mM Hepes, pH 7.4, 200mM NaCl, 30mM EDTA, Complete protease inhibitor cocktail (Roche)) were incubated with beads and antibodies at 4^{o}C for 2 hrs. Immunoprecipitates were washed four times with the same lysis buffer to remove non-specific binding. Proteins were eluted off the protein A-Sepharose beads by boiling in SDS sample loading buffer and analyzed by Western analysis.

Mouse brain polyribosome analysis

Mouse brain polyribosomes were prepared according (Darnell et al., 2005a; Stefani et al., 2004). Briefly, post-natal 2 week-old mice were sacrificed by decapitation. The brain was removed and placed in ice-cold dissection buffer (10mM Hepes-KOH, pH 7.4, 150mM KCl, 5mM $MgCl_2$, 100ug/ml cycloheximide). Cortex and cerebellum were dissected free of underlying white matter, homogenized in 1ml per cortex lysis buffer (10mM Hepes-KOH, pH 7.4, 150mM KCl, 5mM $MgCl_2$, 0.5mM DTT, 100ug/ml cycloheximide, 1X Complete EDTA-free protease inhibitor cocktail (Roche), 40U/ml rRNAsin (Promega)) with 12 strokes at 900rpm in a motor-driven glass-Teflon homogenizer. Homogenate was spun at 2000xg for 10min at 4^{o}C. The supernatant (S1) from the homogenized material was collected and adjusted to 1% NP-40, v/v. After incubation for 5min on ice, S1 lysate were spun at 20,000xg for 10min at 4^{o}C and the supernatant (S2) was loaded onto a 20-50% w/w linear density gradient of sucrose in 10mM Hepes-KOH pH 7.4, 150mM KCl, and 5mM $MgCl_2$. Gradients were ultracentrifuged at 40,000xg for 2hrs at 4^{o}C in a Beckman SW41 rotor. Fractions of 0.75ml volume were collected with continuous monitoring at 260nm using ISCO UA-6 UV detector. Proteins in each fraction of sucrose gradients were TCA precipitated and analyzed by Western blot.

Superose 6 gel filtration

We used a pre-packed Superose 6 Precision column PC 3.2/30 in a SMART system (GE Healthcare) to determine the molecular masses of protein complexes. The optimal separation range of globular proteins in this column is 5kD to 5000kD with its exclusion limit of 40,000kD. Mouse brain cytoplasmic lysates (0.3% NP-40, 10mM Hepes, pH 7.4, 150mM KCl, either with or without 30mM EDTA) were spun over a 0.22um Costa SpinX column (Corning Incorporated) before loaded onto the Superose 6 column with a flow rate of 30ul/min. Protein profile was monitored at A280nm and fractions of 75ul were collected. Fractions were TCA precipitated for Western analysis. To calibrate the column, protein markers (GE Healthcare) were run and gave the following results: blue dextran (void ≥40,000kD) in fraction 4, thyroglobulin (669kD) in fraction 10 to 11, ferritin (440kD) in fraction 13, albumin (67kD) in fraction 15, and ribonuclease (13.7kD) in fraction 18. Molecular mass was extrapolated for each fraction according to the migration of these protein markers and used for identification of protein complex sizes we studied. For complete RNase digest, recombinant RNase A (Ambion) and T1 (Ambion) were added to mouse brain lysates to a final concentration of 20ug/ml and 10,000U/ml respectively. Lysates were incubated at room temperature for 30min before gel filtration.

Behavioral analysis

Mice were derived from crosses between I304N/+ female and wild type male mice on c57/b genetic background. All assays were done blind of the genotype essentially as described (Peier et al., 2000; Spencer et al., 2006).

Electrophysiology

Hippocampal slices (400uM) were prepared from 30-90 day old I304N knock-in mice and their wild type littermates bred to congenic C57bl/6 strain. All experiments were performed blind of the genotypes. Extracellular field potentials (FPs) were measured in the stratum radiatum of hippocampal CA1 elicited by Schaffer collateral stimulation.

mGluR-LTD was induced by application of 100uM DHPG for 5min or by PP-LFS at 1Hz for 20min, 50ms interstimulus interval. Synaptic strength was measured as the initial slope (10-40% of the rising phase) of the FP. LTD magnitude was compared at 60-70min after the onset of DHPG or PP-LFS. Independent t-tests were used to determine statistical significance.

CLIP (in vivo Cross-link and Immunoprecipitation) method

FMRP CLIP and Argonaute CLIP were adapted from Nova CLIP (Ule et al., 2005a).

UV crosslinking of mouse brains

Cortex, cerebellum and hippocampus from P8 mice were harvested and sat in cold HBSS (50ml 10X Hank's balanced salt solution, Ca-Mg-free, (Invitrogen), 5ml 1M Hepes, pH 7.4, 445ml ddH_2O) until harvest was complete. Tissues were triturated with a 5ml pipette and resuspended in 10 volumes of HBSS. Suspension was irradiated using 10ml per 10cm tissue culture plate six times for 400mJ/cm^2 in Stratalinker (Strategene model 2400). After irradiation, tissue suspension was collected and pelleted at 2500rpm 10min at 4^{o}C. Pellets were resuspended in HBSS (~2X pellet volume), distributed to Eppendorf tubes (1 brain per tube), quick pelleted at 4^{o}C. Pellets (~0.6ml/tube) were kept frozen at -80^{o}C until needed.

Immunoprecipitation with anti-FMRP 7G1-1 antibody

For each tube of crosslinked lysate 400ul protein A dynabeads (Dynal) were used. Beads were washed 3x with 0.1M Na-phosphate pH 8.0 and then were resuspended in 400ul of same wash buffer with 50ul of rabbit anti-mouse Fcγ bridging antibody, 2.4mg/ml (Jackson Immunoresearch), rotating at room temperature for 45min. After binding bridging antibody, beads were again washed 3x with 0.1M Na-phosphate pH 8.0 and then resuspended in the same buffer with 8ul of FMRP "specific" 7G1-1 antibody, 5mg/ml rotating at 4^{o}C over night. Antibody bound beads were washed 3x with 1XPXL (0.1% SDS, 0.5% deoxycholate, 0.5% NP-40, PBS tissue culture grade, Ca-Mg-free).

Each tube of crosslinked brain bits was lysed with 700ul of 1XPXL with 1X Complete EDTA-free protease inhibitor cocktail (Roche) and let sit on ice for 10min. 15ul RNAsin (Promega) and 20ul of RQ1 DNase (Promega) were added to each tube and incubated in Thermomixer R (Eppendorf) at 37^{o}C for 5min, 1000rpm. 10ul of 1:10,000 dilution of

RNase A, 5mg/ml (USB) was used to limiting digest RNA at 37^{o}C fro 10min, 1000rpm. Lysates were spun in pre-chilled ultra-microcentrifuge (polycarbonate tubes in TLA 120.2 rotor) at 30,000rpm for 20min at 4^{o}C. Supernatants were carefully removed and added to prepared tubes of beads for immunoprecipitation for 1.5hrs at 4^{o}C. Beads were washed with ice-cold buffer: 2x with 1XPXL, 2x with 5XPXL (0.1% SDS, 0.5% deoxycholate, 0.5% NP-40, 5XPBS tissue culture grade, Ca-Mg-free) and 2x with 1XPNK (50mM Tris-Cl pH 7.4, 10mM $MgCl_2$, 0.5% NP-40).

CIP treatment (on bead)

After immunoprecipitation, beads were resuspended in 80ul of 1X dephosphorylation buffer and 3ul of calf intestinal alkaline phosphatase (CIP) (Roche) were added. Beads were incubated in Thermomixer R at 37^{o}C for 20min, programmed 1000rpm for 15sec every 4min. Beads were washed with 1x with 1XPNK, 1x with 1XPNK/EGTA (50mM Tris-Cl pH 7.4, 20mM EGTA, 0.5% NP-40) and 2x with 1XPNK.

Hot 3' RNA linker ligation (on bead)

3' RNA linker, L33 without 5' phosphate, was 5' radiolabeled with T4 phosphonucleotide kinase (PNK). 1ul of L33 no phosphate at 50pmol/ul, 15ul P^{32}-γ-ATP, 6ul of T4 PNK (NEB), and 2ul RNasin (Promega) in PNK buffer (NEB) were incubated at 37^{o}C for 30min. The reaction was let go for additional 5min with 10ul 1mM ATP. Radiolabeled 3'RNA was then spun through a G25 column (Amersham) to remove free ATP. Each 10pmol of the labeled 3' RNA linker were used for ligation reaction for one tube of beads, in addition, 8ul of 10X T4 RNA ligase buffer (Fermentas), 8ul of BSA (0.2ug/ul), 8ul 10mM ATP, 2ul T4 RNA ligase (Fermentas), 2ul of RNasin (Promega) and H_2O up to total volume of 80ul were added. On bead ligation reactions were incubated at 16^{o}C for 1hr at Thermomixer R programmed 1000rpm for 15sec every 4min. After 1hr, 4ul of 3'RNA linker, L33 with 5' phosphate at 20pmol/ul were added to each tube of reaction and incubation was continued over night. The next day beads were washed 3x with 1XPNK.

PNK treatment (on bead)

80ul of PNK mix (1ul 10mM ATP, 4ul T4 PNK enzyme (NEB), 2ul RNasin and 8ul of 10XPNK buffer (NEB), H_2O up to 80ul) were added to each tube. Mixture was incubated for 20min 1000rpm 15sec every 4min and washed 3x with 1XPNK.

SDS-PAGE and transfer to nitrocellulose

Each tube of beads was resuspended in 13ul of LDS NuPAGE loading buffer (Invitrogen), 4ul of 10X reducing agent (Invitrogen) and 13ul 1XPNK and incubated at 70^{o}C for 10min at 1000rpm. Supernatant were taken off the beads for loading to Novex NuPAGE 10% Bis-Tris gel (Invitrogen). After running at 175V for 3hr, the protein gel was transferred to S&S BA-85 nitrocellulose using Novex wet transfer apparatus (Invitrogen). After transfer, nitrocellulose was quickly rinsed with PBS, blotted with Kimwipes, wrapped in plastic wrap and exposed to film.

Most of radiolabeled unligated L33 linker would run close with the gel front. Free RNA ligated with L33 linker, which would have an average size of 70 nt, will migrate on the gel mostly between 10-30kD. Using 1:10000 RNase A dilution would generate RNAs of average size of 50 nt. As the tags contained 20 nt long L33 linker, their average size would be 70 nt. Thus with our RNase A digest, FMRP-RNA complex would migrate on average approximately 20kD higher than the molecular weight of FMRP alone due to the bound RNA tags. Because RNase digestion is random, RNA tag sizes could vary from 30-150 nt, FMRP-RNA complex would therefore appear as a diffused radioactive smear.

Nitrocellulose membrane was aligned carefully with the exposed film and thin bands approximately at 85, 90, 95 (ideal for FMRP-RNA complex), and 115kD (ideal for Ago-miRNA complex) were cut out using a clean scalpel blade.

RNA isolation and purification

Each band of nitrocellulose membrane was further cut into smaller pieces and proteinase K treated (200ul of 4mg/ml of proteinase K (Roche) in 1XPK buffer (100mM Tris-Cl pH 7.5, 50mM NaCl, 10mM EDTA)) at 37^{o}C, 1100rpm for 20min. Then 200ul of 1XPK+7M urea solution were added and incubated for another 20min at 37^{o}C 1100rpm. Finally, 400ul RNA phenol (Ambion) and 130ul of 49:1 $CHCl_3$:isoamyl alcohol were added and incubated at 37^{o}C, 1100rpm for additional 20min. Tubes were spun at 20000xg in desktop microcentrifuge and aqueous phase is carefully taken. 0.5ul of glycogen (Ambion), 50ul 3M NaOAc pH 5.2 and 1ml of 1:1 ethanol:isopropanol were added and RNAs were precipitated overnight at -20^{o}C.

5' RNA linker ligation

RNAs were spun down, washed; pellet dried and dissolved in 6ul H_2O. RNA ligation was performed with 1ul 10X T4 RNA ligase buffer (Fermentas), 1ul BSA (0.2ug/ul), 1ul ATP (10mM), 0.1ul T4 RNA ligase, 3U (Fermentas), 1ul L51 RNA linker at 20pmol/ul and 6ul of RNA in H_2O at 16^oC overnight.

DNase treatment and RT-PCR

To the ligation reaction, 77ul H_2O, 11ul 10X RQ1 DNase buffer, 5ul RQ1 DNase (Promega) and 5ul RNasin (Promega) were added and incubated at 37^oC for 20min. 300ul H_2O, 300ul RNA phenol (Ambion) and 100ul $CHCl_3$ were added, vortexed, spun and aqueous layer taken. RNAs were precipitated with 50ul 3M NaOAc pH 5.2, 1ul glycogen (Ambion) and 1ml 1:1 ethanol:isopropanol over night at -20^oC. Next day, RNAs were spun down, pellet was washed, dried, and resuspended in 8ul of H_2O.

8ul of RNA were mixed with 2ul of P33 at 5pmol/ul, incubated at 65^oC for 5min, chilled, and spun. 3ul 3mM dNTPs, 1ul 0.1M DTT, 4ul 5X SuperScript RT buffer, 1ul RNasin, and 1ul SuperScript III (Invitrogen) were added and incubated at 50^oC for 30min, 90^oC for 5min and left at 4^oC.

PCR reactions were performed with 27ul Accuprime pfx supermix (Invitrogen), 1ul P51 primer, 5pmol/ul, 1ul of P33 primer, 5pmol/ul and 2ul of the RT reaction, cycled 20-25 cycles with 95^oC 20sec, 61^oC 30sec, and 68^oC 20sec.

Polyacrylamide gel separation of RNA

A 10% denaturing polyacrylamide was poured and the entire PCR reaction was run. 3ul Amplisize Molecular Ruler (Biorad) were used. To visualize DNA, the gel was immersed in 10000-fold dilution of SYBR Gold (Molecular Probes) in TBE for 10min. DNA of 60-100 nts was cut out. DNA was extracted with Qiaex II kit (protocol for polyacrylamide gel) (Qiagen) and resuspended in 15ul of H_2O.

TOPO Cloning and sequencing

A overhang was generated by incubating 2.5ul DNA with 2.5ul Accuprime Taq Supermix (Invitrogen) for 10min at 72^oC in Thermomixer R. Cloning was done with 4ul DNA, 1ul salt solution, and 1ul pCR4-TOPO vector (Invitrogen), which was incubated 5min at room temperature and transformed into TOP 10 cells. Plasmids were isolated using DNA mini-prep, and sequenced using the T7 primer.

Concatamerization

Samples with good sequences (mouse sequences and ideal sized tags for FMRP, 50-70 nt long inserts) were concatermized and sequenced on a larger scale. 3ul Qiaex II purified RT-PCR DNA were amplified using 95ul Accuprime pfx supermix (Invitrogen) and 1ul P51BanIa, 100pmol/ul and 1ul P33BanI 100pmol/ul, cycled 15 cycles with 95^{o}C 20sec, 61^{o}C 30sec, and 68^{o}C 20sec. PCR product was extracted using 200ul DNA phenol/chloroform (Sigma), then 200ul 24:1 chloroform:isoamyl alcohol. Aqueous fraction was collected and DNAs were precipitated by add 14ul 5M NaCl (0.1M final) and 500ul ethanol (2.5 volume) at -20^{o}C over night. DNAs were pelleted, washed, dried and resuspended in 80ul of 1X NEBuffer 4 (NEB) and 4ul of Ban I enzyme (20U/ul) (NEB) were added; DNAs were digested at 37^{o}C for 3hr. Then DNAs were phenol/chloroform (Sigma) extracted and ethanol precipitated. Pellet was resuspended in 66ul of H_2O, 8ul 10X T4 DNA ligase buffer (NEB), 1.2ul P51BanIa, 100pmol/ul, 1.2ul P33BanIa 100pmol/ul were added. Before adding ligase, the reaction was incubated at 65^{o}C for 10min and chilled on ice immediately, in order to quench short cleaved ends to prevent re-ligation. Then 4ul T4 DNA ligase (2000U/ul) (NEB) were added and incubated at 16^{o}C over night. The next day, 1ul of T4 DNA ligase was added to let the reaction continue for an additional hour. The reaction was desalted on G-25 column (Amersham) and run on a 2% low melting (NuSieve) agarose gel. Concatemer products were purified using Qiaex II (Qiagen) and TA cloned and sequenced.

Linker and primer sequences

RNA linkers (from Dharmacon):

R51: 5'-OH AGG GAG GAC GAU GCG G 3'-OH

R33: 5'-P CGG UUG CGA GGU GAG UGA A 3'-puromycin

R33 no P: 5'-OH CGG UUG CGA GGU GAG UGA A 3'-puromycin

DNA primers (from Operon):

P51: AGGGAGGACGATGCGG

P33: CTTCACTCACCTCGCAACCG

Concatermization primers:

P51BanIa: CAGCCAACAGGCACCAGGGAGGACGATGCGG

P33BanIa: CACTAGCTTGGTGCCTTCACTCACCCTCGCAACCG

Synaptoneurosome preparation (filtration method)

We used filtration method for synaptoneurosome preparation from mouse brains (Ceman et al., 2003b; Shin et al., 2004). Cortex and hippocampus were dissected in cold PBS free of underlying white matter. Tissue was immediately Dounce homogenized in 2ml of ice cold buffer ((10mM Hepes pH 7.4, 2mM EDTA, 2mM EGTA, 0.5mM DTT, 100mM sucrose, and Complete protease inhibitor cocktail (Roche), detergent free). Homeogenate was filtered sequentially through two 100 micron nylon mesh filters (Small Parts, Inc.); and filtrate centrifuged at 2000xg for 1min at desktop centrifuge. Supernatant was collected and passed through a 5 micron pore filter (Millipore) and filtrate was centrifuged at 1000xg for 10min. The pellet was resuspended in SDS sample loading buffer for Western blot analysis.

CHAPTER III. GENERATION AND CHARACTERIZATION OF I304N MOUSE MODELS FOR FRAGILE X SYNDROME

Introduction

Fragile X mental retardation, the most common form of inherited mental retardation, presents with a clinical picture of moderate to severe mental retardation, macroorchidism, seizures, connective tissue dysplasia, and complex behavioral and cognitive deficits. In most cases, the disease is caused by transcriptional silencing of the fragile X mental retardation 1 (Fmr1) gene as a result of CGG repeat expansion and hypermethylation of CpG islands in the 5'UTR region (O'Donnell and Warren, 2002). Multiple functional domains have been characterized in the Fragile X mental retardation protein (FMRP). These include two tandem KH-type RNA binding domains (named for their homology to hnRNPK) (Siomi et al., 1994; Siomi et al., 1993b), an arginine and glycine-rich RNA binding domain (RGG box) (Siomi et al., 1993b), and an N-terminal domain (NDF), similar to Tudor/Agenet domains, that may be involved in both RNA binding and protein-protein interactions (Adinolfi et al., 2003; Mazroui et al., 2003; Ramos et al., 2006; Zalfa et al., 2005).

The presence of multiple functional domains within FMRP has made it difficult to determine which lost functions are sufficient for causing Fragile X Syndrome. A single severely affected patient with a missense mutation in FMRP has offered hope of focusing FMRP studies in a key functional domain. This patient has severe mental retardation with IQ measured below 20 and impressive macroorchidism with both testes exceeding 100ml volume (DeBoulle et al., 1993). The patient harbors a single nucleotide mutation in a conserved isoleucine, changing it to an asparagine (I304N), within the KH2 domain.

Our interest in FMRP, and this I304N mutation in particular, arose from studies of a structurally related neuronal RNA binding protein termed Nova (Darnell, 2006). Nova harbors three RNA binding domains with a similar spacing to those in FMRP—two paired (tandem) KH domains, intervening sequence, and a third KH domain (Burd and

Dreyfuss, 1994; Lewis et al., 1999). The RNA binding specificity of Nova's KH domains have been well defined, including determination of the structure of one Nova KH domain co-crystallized with its RNA ligand (Lewis et al., 2000). This study revealed that Nova binds RNA in a sequence-specific manner, using amino acid side-chains to precisely coordinate two nucleotides (CA) in the midst of a pyrimidine-rich region. This binding pocket is supported by three conserved hydrophobic amino acids, one of which, a leucine, is found to be the corresponding amino acid to the isoleucine in the I304N FMRP mutation (Lewis et al., 2000; Ramos et al., 2003).

Extrapolating the results from Nova to FMRP, these results suggest the possibility that the key defect in FMRP loss-of-function is the loss of sequence-specific RNA binding, mediated through the FMRP KH2 domain, and requiring isoleucine-304 in particular. This interpretation has been complicated by questions of whether such a mutation might lead to an unfolded protein and the loss of other functions of the protein in addition to RNA binding, as analogous mutations in vigilin KH6, Nova KH3, FMRP KH1 (Lewis et al., 1999; Musco et al., 1997; Musco et al., 1996) have been reported to result in the complete unfolding of the domain. Other KH domains remain well structured with this mutation including SF1 and dFXR KH1-KH2 (Liu et al., 2001; Pozdnyakova and Regan, 2005; Ramos et al., 2003), yet specific RNA binding is lost. Here we address these issues by generating and analyzing mouse models harboring the I304N mutation. We will examine whether the mouse models support the production of I304N FMRP, whether the mutant protein is completely denatured or still retains some functions, and whether this point mutation in FMRP KH2 domain causes loss of RNA binding, as we may have predicted. Lastly, we will assess whether I304N mouse models phenocopy the Fragile X Syndrome.

Results

Generation and general description of Fmr1 I304N mice

Two mouse models were generated to phenocopy the I304N patient. Initially we generated BAC transgenic mice harboring the I304N mutation **(Figure 3.1)**. BAC transgenic technology has several advantages over conventional transgenics (Yang et al., 1997). First, BAC trangenes are present on a large piece of DNA, when they insert in the

genome, they are relatively immune from positional effects caused by the neighboring sequences. Second, BAC transgenes include the most distal enhancers and all intronic elements. They are spliced and regulated like the endogenous gene, which is a huge improvement over traditional cDNA transgenics. At the time, when our Fmr1 BAC transgene was obtained, it was the only one available (Musunuru, K, PhD thesis). It is unfortunate because the BAC gene is so close to the 5' end Fmr1 gene that it is no better (but also no worse) than a traditional transgene in terms of positional effects, therefore we need several lines of transgenic mice, just as for a traditional transgene. Two lines of I304N BAC transgenic mice and one control line of wild type Fmr1 BAC transgenic mice were obtained and bred to the FVB Fmr1-null background. Despite their considerable advantages over traditional transgenics, BAC transgenic mice have at least one potential drawback, which is gene dosage variability, as they tend to incorporate in the genome as tandem repeats. We were only able to generate three lines of mice despite several attempts at injection, perhaps because overexpression of FMRP is toxic to the nervous system. Therefore, we may have selected for mice with lower expression in brain due to positional effects.

At this point it was unlikely for us to generate multiple lines of I304N and wild type control BAC transgenic mice to properly control for gene dosage and positional effects in our BAC transgenics. Therefore, we generated a second and "cleaner" mouse model, the I304N knock-in (KI) mouse, using conventional gene targeting **(Figure 3.2A)**. An Fmr1 KH2 I304N targeting cassette, including a self-excising loxP-Auto-Cre-Neo^{R}-loxP (ACNF) cassette (Bunting et al., 1999) was electroporated into ES cells and 53 homologous recombinants were identified by Southern blot **(Figure 3.2B).** Germline chimeras were bred to generate I304N knock-in male mice. These mice were backcrossed ten generations into both FVB and C57/BL6 backgrounds. As we were successful in knocking in this mutation by homologous recombination most of our subsequent analysis focused on the I304N knock-in mice. I304N BAC transgenic mice were used when appropriate to support the findings in the knock-in model.

I304N knock-in mice were viable and did not exhibit an overt phenotype. Mutant mice were fertile with normal litter sizes, and transmitted the mutant allele in an X-linked Mendelian pattern (data not shown). Histological examination of heart, spleen, liver,

lung, kidney, adrenal glands, stomach, intestines, muscles, diaphragm, bladder, thymus of I304N KI mice revealed no abnormalities (data not shown). We especially focused on the brain and testes, as both organs are functionally and anatomically abnormal in fragile X patients, and the I304N patient in particular. The cerebellum **(Figure 3.3A, B, C and D)**, cortex (**Figure 3.3E, F, G and H)** and hippocampus **(Figure 3.3I, J, K and L)** of I304N knock-in mice were macroscopically and microscopically normal. Microscopic examination of testes of the I304N mouse revealed no structural difference compared with wild type mice **(Figure 3.3M, N, O and P)**. Macroorchidism is present in more than 90% of adult males with Fragile X Syndrome, and is particularly severe in the I304N patient whose testicular volume exceeds 100 ml (DeBoulle et al., 1993). Fmr1 knockout mice also exhibit progressively more severe macroochidism with age; their testicular weights are up to 30% heavier than wild type mice at 6 months, the oldest age measured (Dutch-Belgian Fragile X Consortium, 1994). Consistent with these observations, testicular weights of adult I304N knock-in mice were found to be 15-30% heavier than those of their wild type littermates, with the most pronounced difference seen at the oldest age group **(Figure 3.4A, B and E)**. Because the human I304N patient has a much more severe macroorchidism than most Fragile X patients whose disease results from loss of expression of FMRP, we compared the testicular weights of I304N knock-in mice and Fmr1 knockout littermates. We found that they were not significantly different in mice up to 600 days old. **(Figure 3.4C, D, and E)**. There was no significant difference in body weights between I304N knock-in mice and wild type or Fmr1 knockout littermates **(Figure 3.5)**.

I304N mRNA and protein expression

We examined the expression level of Fmr1 mRNA in I304N knock-in mice. Northern blot and quantitative RT-PCR analysis showed that I304N Fmr1 mRNA was expressed at wild type levels in both brain and testes **(Figure 3.6A and B)**. The I304N mRNA appeared to be of the correct size in both brain and testes, compared with wild type littermates and in agreement with previous work (Ashley et al., 1993a; Pieretti et al., 1991). Sequencing of RT-PCR products from the I304N mouse confirmed the correct sequence of the introduced mutation **(Figure 3.6C)**.

Western blot analysis was used to compare I304N protein expression in the brain, testes, liver, and spleen with wild type levels at different post-natal ages. At 2 months of age, I304N FMRP was expressed at ~50% of the normal level in brain **(Figure 3.7A)** and remained at ~50% in brain at 6 months of age **(Figure 3.7B)**. We noted that in younger mice (P14), I304N was expressed at lower levels (~20% of the wild type level in brain; **Figure 3.8)**. For this reason, behavioral analyses and electrophysiologic studies of the I304N mice were done in adults. Outside the brain I304N FMRP was expressed at somewhat lower levels as well--~30% in testes, ~30% in spleen at 2 months of age **(Figure 3.7A)** and ~40% in testes, ~90% in spleen, 70% in liver at P14 **(Figure 3.8A and B)**. Interestingly, expression levels of FXR1P and FXR2P, autosomal paralogs of FMRP, did not increase to compensate for the low I304N protein levels **(Figure 3.9)**.

To further address the variable protein levels in I304N relative to WT mice, we also analyzed BAC transgenic mice harboring either I304N or wild type FMRP. Transgene expression was studied by Western blot and quantitative RT-PCR. One line of the I304N transgenic mice (TG I304N-B) expressed normal levels of the mutant protein in adults **(Figure 3.10A)**. However, analogous to the knock-in mice, at P14, there was roughly a 4 fold decrease of I304N protein relative to mRNA in two lines of the I304N BAC transgenic mice, but not in wild type Fmr1 BAC transgenic mice **(Figure 3.10B)**. These consistent findings, in both the knock-in and transgenic mice, together with similar data in Drosophila harboring an analogous I307N mutant protein (Banerjee et al., 2007), suggest that post-transcriptional regulation may lead to reduced levels of the mutant I304N protein.

Decreased protein expression with normal mRNA levels suggests that I304N FMRP may have either a slower protein synthesis rate or a faster protein turnover rate in the mouse brain. We analyzed the I304N translational profile by examining its mRNA distribution on polyribosome sucrose gradients compared with wild type littermates. Quantitative RT-PCR of RNA from different fractions showed that I304N Fmr1 mRNA had a similar distribution on polyribosomes to wild type Fmr1 mRNA **(Figure 3.11)**. These observations suggest that lower I304N expression is not likely due to translational regulation, but may instead relate to increased turnover of the mutant protein.

I304N FMRP retains some RNA and protein binding activities

In vitro RNA selection studies have identified a kissing complex RNA that is bound with high affinity by the FMRP KH2 domain (Darnell et al., 2005a). Recombinant I304N protein produced in bacteria has been shown to be competent to bind G-quartet RNA, the high affinity RNA ligand for the RGG box of FMRP (Brown et al., 2001; Darnell et al., 2001; Schaeffer et al., 2001), but not the kissing complex RNA (Darnell et al., 2005a). We examined endogenous I304N protein in mouse brain to see whether it would mimic these RNA binding abilities. Radiolabeled G-quartet or kissing complex RNA was spiked into mouse brain lysates, UV-crosslinked, and immunoprecipitated with FMRP antibody. When samples were run on SDS-PAGE gels, a radiolabeled FMRP:RNA complex was seen specifically in the immunoprecipitate of the I304N extract crosslinked to the G-quartet RNA, but not the kissing complex RNA **(Figure 3.12A and B)**. When compared with the wild type, the reduced radioactive signal from G-quartet RNA crosslinked to the I304N extract was consistent with the lower I304N protein level in the knock-in mice **(Figure 3.12C)**. Point mutations in G-quartet or mutant kissing complex RNAs, which are not bound by recombinant I304N FMRP in vitro (Darnell et al., 2005a; Darnell et al., 2001) also did not crosslink to either wild type or I304N FMRP in mouse brains **(data not shown)**.

We also evaluated whether the I304N FMRP was competent to interact with its known protein partners. In vitro studies indicate that I304N FMRP is able to heterodimerize with FXR1P and FXR2P (Laggerbauer et al., 2001a; Zhang et al., 1995) and we analyzed these interactions in the brains of I304N knock-in mice. Co-immunoprecipitation from mouse brains confirmed that I304N binds in vivo to FXR1P and FXR2P **(Figure 3.13)**, demonstrating that I304N FMRP has an intact protein-protein interaction domain. Taken together, these data indicate that the I304N protein in mouse brain retains some normal activities, as it is competent to bind both protein and, via its RGG-domain, to bind G-quartet RNA. Therefore the defect in the I304N protein may be selective for defective KH2:sequence-specific RNA binding.

I304N FMRP is dissociated from polyribosomes

The laboratories of Warren and Khandjian have provided the first evidence that FMRP is on polyribosomes (Corbin et al., 1997; Feng et al., 1997a; Khandjian et al., 1996) suggesting a role in translational regulation of specific mRNAs. , Significantly, in I304N patient lymphoblastoid cells, mutant FMRP no longer associates with polyribosomes (Feng et al., 1997a). Transfected reporter constructs also suggested that the I304N mutation inhibits the ability of FMRP to associate with polyribosomes (Darnell et al., 2005b). We examined whether the I304N mutation affected endogenous FMRP-polyribosome association in brain (Feng et al., 1997b; Khandjian et al., 2004; Stefani et al., 2004). Polyribosome profiles were identical for wild type and I304N mouse brain extracts **(Figure 3.14A)**, indicating comparable global translation status. Similar to previous findings in the patient lymphoblastoid cells as well as I304N FMRP- transfected neuronal cell lines (Darnell et al., 2005b; Feng et al., 1997a), I304N FMRP was largely dissociated from polyribosomes in mouse brain **(Figure 3.14A and B)**. A negligible amount of wild type FMRP was present in fractions lighter than 80S monoribosomes (fractions 1-5) and more than 55% was on the very heavy polyribosomes (fractions 9-12), while 44% of total I304N FMRP was in the corresponding light fractions and only 24% on the polyribosomes. This result was further confirmed using I304N-FMRP transgenic mice bred to the Fmr1 null background. One line of I304N BAC transgenic mice (TG I304N-B) expressed the mutant protein at normal level in adult brain **(Figure 3.10A)** and its polyribosome association was significantly decreased as well **(Figure 3.15)**, indicating that lack of polyribosome association is independent of steady state protein level, but specific to the mutation. Also consistent with previous findings in patient lymphoblastoid cell lines (Feng et al., 1997a), the I304N mutation in FMRP does not affect FXR1P or FXR2P polyribosome association in mouse brain **(Figure 3.14A)**.

I304N FMRP complex is abnormally small due to a loss of RNA binding

It has been suggested that the I304N mutation renders the protein incapable of forming normal mRNP particles (Feng et al., 1997a). We analyzed endogenous I304N particle size in brain by Superose 6 gel filtration of mouse brain cytoplasmic extracts. Wild type FMRP was found in the void volume of the Superose 6 column, indicating that

FMRP is normally associated with an mRNP of greater than 40,000 kDa **(Figure 3.16A)**. On the contrary, the vast majority of I304N FMRP was found in an abnormally small complex eluting with standards of approximately 150-300 kDa **(Figure 3.16B)**, which correlated well with <440 kDa observed with patient lymphoblastoid cells (Feng et al., 1997a).

To assess whether this small complex containing I304N might result from a loss of protein-RNA interaction (Lewis et al., 2000; Liu et al., 2001; Ramos et al., 2003) versus protein-protein interactions (Feng et al., 1997a; Laggerbauer et al., 2001a), we treated brain cytoplasmic extract with excess RNase and then repeated Superose 6 gel filtration. Under these conditions, the wild type FMRP mRNP apparent size was reduced to the size of I304N complex **(Figure 3.16C)**, while this RNase treatment did not further alter the size of the I304N complex **(Figure 3.16D)**. This data suggests that the I304N FMRP in mouse brain has lost majority of its ability to associate with RNA. This likely explains the dissociation of I304N mutant FMRP from polyribosomes.

We further examined the nature of the I304N complex by comparing its size with denatured, recombinant His-tagged I304N protein added to mouse brain extract and sized by Superose 6 gel filtration. Mouse brain I304N FMRP was found in a complex significantly larger than the His-tagged I304N monomer **(Figure 3.17)** suggesting that interactions with other proteins (most likely homodimerization with itself or heterdimerization with FXR1P and FXR2P) are intact. These data and the finding that the I304N protein coprecipitates with FXR1P and FXR2P demonstrate that I304N FMRP is still capable of protein:protein interactions while most if not all of its RNA-binding capacity is lost. This suggests that the loss of polyribosome association is due primarily to a loss of RNA binding due to the I304N mutation in the KH2 RNA-binding domain.

I304N knock-in mice show similar behavior to Fmr1 knockout mice

I304N knock-in male mice and wild type littermates were subject to a battery of behavioral assays, which included locomotor activity, anxiety related responses, sensorimotor gating, learning and memory, analgesia, obsessive-compulsive activity, and audiogenic seizure. Results of I304N knock-in mice were compared with historical findings on Fmr1 knockout mice (Brennan et al., 2006; Kooy, 2003; Peier et al., 2000;

Spencer et al., 2005; Spencer et al., 2006) in the same genetic background *ad hoc* (Brennan et al., 2006; Kooy, 2003; Peier et al., 2000; Spencer et al., 2005; Spencer et al., 2006). These experiments were performed by our collaborator Dr. Richard Paylor and the results are summarized in **Figure 3.18M**.

Locomotive activity in an open field. A single mouse was placed in the open-field arena and its activity was recorded over a period of 30min. I304N knock-in mice traveled a greater total distance in the open field compared with their wild type littermates **(Figure 3.18A)**, suggesting that I304N knock-in mice had increased exploratory behavior, similar to Fmr1 knockout mice (Peier et al., 2000). There was no difference between I304N and wild type mice for rearing, as measured by vertical activity **(Figure 3.18B)**.

Anxiety related responses. The center:total distance ratio in the open field test is a measurement of anxiety related response to a brightly-lit open arena. Wild type mice preferred to stay along the perimeter of the arena while I304N knock-in mice traveled a greater proportion of their distance in the center of the open field **(Figure 3.18C)**. Light and dark exploration test is another anxiety response test. Mice were allowed to move freely between a large, open, and brightly lit chamber and a small, closed and dark chamber. I304N knock-in mice exhibited a greater number of light-dark transitions than their wild type littermates **(Figure 3.18D)**. Both tests indicated that I304N knock-in mice had a lower level of anxiety, like Fmr1 knockout mice (Peier et al., 2000). No difference was observed between I304N knock-in and wild type littermates for the total time spent in the dark **(Figure 3.18E)**.

Startle habituation. Prepulse inhibition (PPI) of the acoustic response was used to measure sensorimotor gating. A weak non-startling sound presented immediately before a startling sound will suppress the startle response of an animal. I304N knock-in mice exhibited significantly lower startle responses than their wild type littermates **(Figure 3.18F)**, analogous to Fmr1 knockout mice (Peier et al., 2000; Spencer et al., 2006). As the prepulse level increases, there is greater suppression of the startle response. There was no significant difference in PPI between I304N knock-in mice and their wild type littermates **(Figure 3.18G)**, although Fmr1 knockout usually showed increased PPI (Paylor, R unpublished data). This was one of the very few discrepancies of I304N and Fmr1 knockout mice amongst a whole collection of behavioral tests.

Conditioned fear. Conditioned fear test, based on a Pavlovian learning and memory paradigm, was used to examine cognitive functions. In the context test, mice were given two mild foot shocks in a chamber, and 24 hours later they were placed back in the same chamber and their freezing bouts as an index of fear were measured for 5min. In the auditory conditioned stimulus (CS) test, mice were trained to associate an auditory cue, conditioned stimulus (CS), with an aversive unconditioned stimulus (US), foot shocks. 24 hours later mice were place in a novel chamber, but given the auditory cue (CS) and their freezing bouts were measured. As observed in Fmr1 knockout mice, I304N knock-in mice displayed no difference of conditioned fear in either context test or auditory CS test compared with wild type littermates **(Figure 3.18H and I)** (Peier et al., 2000; Spencer et al., 2006).

Hotplate. The hotplate test provides an assessment of sensitivity to pain. Mice were placed on a 55^{o}C hotplate and the latency of their first hindlimb response was recorded. I304N knock-in mice showed a greater latency to hindlimb response than wild type mice ($p=0.076$) **(Figure 3.18J)**, suggesting they are less sensitive to pain, similar to Fmr1 knockout mice (Paylor, R unpublished data).

Marble bury. Marble burying tests for obsessive-compulsive behavior and perseveration. I304N knock-in mice buried more marbles than their wild type littermates **(Figure 3.18K)**, although Fmr1 knockout mice tended to bury less marbles (Paylor, R unpublished data).

Audiogenic seizure. On C57BL/6 genetic background, 18% of I304N knock-in mice showed audiogenic seizure **(Figure 3.18L)**, unlike wild type or Fmr1 knockout mice, none of which were susceptible to audiogenic seizure (Paylor, R unpublished data).

With the exception of these few discrepancies, these data suggest that I304N knock-in mice are very similar to Fmr1 knockout mice in the majority of behavioral assays.

I304N knock-in mice have altered synaptic plasticity in hippocampus

Metabotropic glutamate receptor dependent long term depression (mGluR-LTD) in hippocampal CA1 area is a form of synaptic plasticity that relies on dendritic protein synthesis. Previous work has shown that mGluR-LTD was enhanced in Fmr1 null mice

(Huber et al., 2002) and that it no longer required *de novo* protein synthesis (Nosyreva and Huber, 2006). We investigated the protein synthesis requirement for both chemically induced (100uM 3,4-dihydroxyphenylglycine (DHPG), 5min) and synaptically induced [using paired pulse low frequency stimulation (PP-LFS)] mGluR-LTD in acute hippocampal slices prepared from I304N knock-in mice and their wild type littermates. These experiments were performed by Dr. Kim Huber and colleagues using paired littermates supplied by our lab. Pre-incubation with the protein synthesis inhibitor anisomycin (20uM) inhibited both DHPG- ($p=0.02$) and PP-LFS- ($p=0.004$) induced LTD in wild type mice as expected **(Figure 3.19A and C)**. In contrast, anisomycin had no effect on either form of LTD in I304N knock-in mice **(Figure 3.19B and D)**, as observed in Fmr1 knockout mice (Nosyreva and Huber, 2006). Our data suggests that the I304N KI mice are similar to Fmr1 knockout mice in that in both, in contrast to wild type mice, mGluR-LTD is no longer dependent upon new protein synthesis.

Discussion

Fragile X Syndrome presents with a clinical picture of moderate to severe mental retardation and behavioral abnormalities including autistic features resulting from the loss of function of an RNA-binding protein, FMRP. Although the disease is usually caused by a triplet repeat expansion in the 5'UTR of the Fmr1 gene leading to loss of transcription of Fmr1 mRNA, one severely affected patient has a point mutation in KH2 RNA binding domain of FMRP (DeBoulle et al., 1993). This isoleucine to asparagine mutation (I304N) has previously been shown by our lab and others to abolish RNA binding by this and similar KH-type RBDs. Symptoms of Fragile X Syndrome in this patient therefore suggest that the disease is caused by loss of sequence-specific RNA binding by this KH domain in FMRP. However, it has not been formally demonstrated that this point mutation caused Fragile X symptoms in this individual, as his clinical picture is complicated by an unrelated familial liver disease.

To address this issue, we have generated and analyzed mouse models harboring the I304N mutation. We find that the protein is present, albeit at somewhat reduced levels in adult mice. It retains some normal activities, as it is competent to bind both protein partners such as FXR1 and FXR2 and, via its RGG-domain, to G-quartet RNA. However,

it is defective in polyribosome association and RNA binding. These findings, together with FMRP null-like behavioral deficits and altered synaptic plasticity seen in the I304N mouse, suggest that loss of RNA binding by the second KH domain contributes to the dysfunctions underlying the Fragile X Syndrome.

I304N mutant protein is present, albeit at a lower level

Our genetic engineering of the I304N knock-in mouse model has been made such that an Auto-Cre-Neo^{R} (ACNF) cassette was inserted in a non-conserved region of Fmr1 intron 10 and it was entirely excised during spermatogenesis in male chimeric mice. Only one loxP site remains in the Fmr1 intron of the I304N knock-in mouse, which does not affect I304N Fmr1 mRNA transcription or splicing, as the mRNA is expressed at the correct length and normal level. We have mutated ATT that corresponds to isoleucine-304 to AAC to encode asparagine, a commonly used codon in mouse with a usage frequency of 20.7% that is comparable to the 15.6% frequency of the ATT (Ile) codon. Wobble mutations of CTG (Leu) to CTT (Leu) and CAA (Gln) to CAG (Gln) have been made for the amino acid residues leucine and glutamine before and after the I->N mutation. Mutated codons are also common codons with a comparable usage frequency as the original codons in mouse.

The production of endogenous I304N mutant protein has been rigorously assessed using multiple antibodies against FMRP. The protein is present in all tested tissues, albeit at lower levels than in wild-type littermates. The post-transcriptional reduction in steady state levels of I304N protein compared with mRNA levels has not only been observed in I304N knock-in mice, both lines of I304N BAC transgenic mice, but also in I307N dFXR flies (Banerjee et al., 2007), suggesting that it is intrinsic to the mutation rather than a result of our genetic manipulation. Lower steady state levels of I304N FMRP in brain and testes is surprising in light of previous data demonstrating that I304N FMRP is expressed at normal levels in the patient, as detected using EBV transformed patient lymphoblastoid cells (Feng et al., 1997a). Reasons for the differences between our findings and previously published data are that immortalized cell culture systems do not necessarily mimic the context of the endogenous protein in a living organism, and that the we also detect relatively normal levels of I304N expression in some tissues. Therefore, I304N

FMRP levels may be normal in the patient's primary blood cells (a clinically unaffected tissue) as well,. In light of these findings it would be interesting to assess FMRP levels in the patient's nervous system, but not feasible.

I304N Fmr1 mRNA has a normal translational profile on polyribosomes, suggesting its low protein levels is not likely due to translational repression. This is an issue of interest because it has been reported that FMRP can bind a G-quartet in the coding sequence of its own mRNA, possibly inhibiting its translation (Schaeffer et al., 2001). Our genome wide screen for FMRP RNA targets has not identified its own mRNA as a target (see Chapter IV). We hypothesize the observed low protein level is due to faster turnover of the mutant protein.

I304N FMRP retains some characterized functions

Structural biologists have studied the I304N mutation in many similar KH-type RBDs. Vigilin KH6, FMRP KH1, and Nova KH3 (Lewis et al., 1999; Musco et al., 1997; Musco et al., 1996) are completely unfolded as judged by circular dichroic spectroscopy, while SF1 and dFXR KH1-KH2 (Liu et al., 2001; Pozdnyakova and Regan, 2005; Ramos et al., 2003) are correctly folded. Structural studies using recombinant proteins cannot definitively prove the outcome of I304N folding *in vivo*. These contradictory findings make it difficult to determine the direct cause of the patient's disease, whether it is due to a denatured and completely functionless I304N protein or due specifically to the lack of KH2 domain-mediated RNA binding.

We have shown that mouse brain I304N protein retains its ability to bind G-quartet RNA via its C-terminal RGG box (Darnell et al., 2001) and its ability to heterodimerize with FXR1P and FXR2P, mediated by its N-terminal domain (Adinolfi et al., 2003; Mazroui et al., 2003; Ramos et al., 2006). These functional assays prove to us I304N protein in mouse brain is not a completely denatured functionless protein, but retains some normal activities. While I304N protein still binds G-quartet RNA, it has lost binding to kissing complex RNA (Darnell et al., 2005a), suggesting the defect in the I304N protein is selective for KH2 sequence specific RNA binding. *In vitro* ligand binding experiments support our mouse model, since a previously known dysfunction of the I304N protein is observed in these mice. Concurrently we have demonstrated that the

in vitro-selected RNA motifs previously characterized with I304N FMRP produced from bacteria and baculovirally infected insect cells, are indeed bound by endogenous brain FMRP.

I304N FMRP is defective in polyribosome association and RNA binding

We have confirmed previous findings that vast majority of I304N protein is dissociated from polyribosomes in mouse brain (Darnell et al., 2005b; Feng et al., 1997a). In addition to showing that I304N FMRP no longer binds kissing complex RNA, we also show that I304N FMRP is in a 150-300 kDa complex in mouse brain, and that is not reduced in size after treatment with RNases, suggesting it has lost RNA binding. In contrast, the wild type FMRP mRNP is >40,000 kDa in size and after RNase treatment, it decreases to the size of the I304N complex. All these data suggest to us that loss of RNA binding due to the I304N mutation in the KH2 domain is likely to be the primary cause for polyribosome dissociation, thus loss of correct translational control.

Here we have reported two seemingly contradictory findings—the I304N FMRP protein is capable of binding G-quartet RNA, but it is found mostly in an RNase resistant complex. One possibility is that FMRP may bind differently to endogenous than to SELEX ligands, which usually are the highest affinity binders. RBPs are usually composed of multiple combinations of just a few basic domains and these domains can function together in various ways to achieve specificity and affinity that is not possible for a single domain or if the domains did not cooperate (Lunde et al., 2007). Since an RGG box mutation does not affect FMRP polyribosome association (Darnell et al., 2005b; Mazroui et al., 2003), we hypothesize that the binding of FMRP to endogenous RNAs may require a hierarchical binding of the KH2 domain before the RGG box. When two RBDs are separated by a flexible spacer, after the first domain binds RNA, the second domain can just sweep within the sphere of the spacer length, which will have a much increased effective concentration compared to free solution. For instance, hnRNP A1 has two RRMs separated by a flexible linker; the increase in the avidity of the protein for RNA is not simply the additive affinity of the two domains, but is increased 1000 fold by the presence of two binding sites in the same molecule. (Shamoo et al., 1995; Shamoo et al., 1997). Second, upon first RNA binding, initially disordered regions in the RNA,

protein, or both can change conformation to facilitate further binding, thereby increasing the affinity by hundreds to thousands of folds—the induced fit model (Leulliot and Varani, 2001; Williamson, 2000).

Lastly, homodimerization of tagged I304N fusion protein has been reported to be defective (Laggerbauer et al., 2001b), but this has only been shown with tagged fusion proteins. We have not been able to assess homodimerization of I304N FMRP in mouse brain. Transgenic FMRP in our BAC mice is tagged but with a Flag tag which is too small to discern from endogenous FMRP, especially in light of the multiple isoforms of FMRP present. However, the I304N FMRP is in a complex larger than His-tagged monomer, and we have demonstrated its ability to heterodimerize with FXR1P and FXR2P showing that I304N FMRP is still capable of protein:protein interactions. In conclusion, defective KH2 domain mediated RNA binding is likely the primary cause that leads to the loss of polyribosome association, and hence loss of proper translational control in I304N mouse brain.

I304N mice have a Fmr1 null-like phenotype

The I304N knock-in mouse phenocopies the disease in most of the phenotypical analyses we have conducted so far. We have demonstrated their behavioral abnormalities, e.g. hyperactivity and decreased anxiety, with a battery of assays and their altered synaptic plasticity such that mGluR induced LTD no longer requires new protein synthesis. Behavioral and electrophysiologic analysis qualitatively suggest that I304N knock-in mice are similar to Fmr1 null mice. Comparable macroorchidism to knockout mice quantitatively shows I304N knock-in mice bear a Fmr1 null like phenotype.

Our behavioral and hippocampal LTD analysis have been performed using adult male I304N knock-in mice, in which the mutant protein is about 50% of normal levels in the brain. Attempts have been made using the line of I304N BAC transgenic mice (FVB background) that has normal levels of the mutant protein in adult brain, but C57BL/6 strain specificity of both behavioral studies and hippocampal LTD findings unfortunately prevent us from characterizing these BAC mice, which are currently only in the FVB background.

Studies have shown that 42% of FMRP expression in peripheral blood smears is nearly a perfect cut-off for differentiating functional normal males from fragile X males (Willemsen et al., 1997). All male full mutation patients that express 50% of normal FMRP protein levels have a non-retarded IQ (>70) (Tassone et al., 1999). Heterozygotes of many loss-of-function mutations, e.g. the Nova gene, are also much more mildly affected if at all. Therefore, the phenotypical abnormalities seen in the I304N knock-in mice are not just due to a 50% decreased protein level, but also the loss of function of the remaining I304N FMRP, namely RNA binding ability mediated by the KH2 domain.

More phenotypic analyses, for example, classical delayed eye blinking conditioning (Koekkoek et al., 2005), circadian rhythm (Dockendorff et al., 2002; Inoue et al., 2002; Morales et al., 2002), dendritic spine morphology (Comery et al., 1997; Nimchinsky et al., 2001) will be to our interest to further characterize the I304N mutation.

I304N FMRP does not have a dominant negative effect

Despite the defect of I304N FMRP in association with polyribosomes or binding to RNAs, the mutant protein does not affect its autosomal paralogs, FXR1P and FXR2P, as their expression levels, polyribosomal association and mRNP complex sizes are unchanged. Unlike the I304N patient who has more severe manifestations of Fragile X Syndrome (DeBoulle et al., 1993), I304N knock-in mice have a Fmr1 null like phenotype and analogous I307N mutation in Drosophila results in a partial loss of function phenotype (Banerjee et al., 2007). Biochemical analyses and phenotypical findings in both mouse and fly suggest that I304N FMRP does not have a dominant negative effect on FXR1P or FXR2P, but is consistent with a loss of function mutation. Severe Fragile X symptoms, like IQ below 20 and impressive macroorchidism, observed in the I304N patient that have not been reproduced elsewhere can be a result of the patient's genetic background or an exacerbated effect by the patient's familial liver disease.

A new and more specific mouse model for the Fragile X Syndrome

Our I304N knock-in mouse models closely after the I304N patient and phenocopies the disease. It provides a new and more specific mouse model for the Fragile

X Syndrome. I304N knock-in mouse model has led us to understand that a KH2 mediated defect in RNA binding is likely the primary cause for polyribosome dissociation and thus loss of proper translational control, which can in turn contribute to the pathogenesis underlying the cognitive and behavioral deficits observed in the Fragile X Syndrome. Therefore identification of the RNA ligands of FMRP in mouse brain would be key to ultimately understand the pathogenesis of the disease. Once a reliable and comprehensive set of *in vivo* RNA targets of FMRP is obtained, the I304N mouse model, in conjunction with the Fmr1 knockout (Dutch-Belgian Fragile X Consortium, 1994), Fmr1 conditional knockout (Mientjes et al., 2006), and FMR1 YAC transgenic mice (Peier et al., 2000), would be a valuable mammalian animal model for the validation of these FMRP RNA targets and for the study of defined functional roles of FMRP in RNA metabolism in the process of gene expression. Lastly, trials of clinical treatment can also be tested on the I304N knock-in mice, since it provides a physiological relevant living system that phenocopies Fragile X Syndrome.

Figure 3.1.

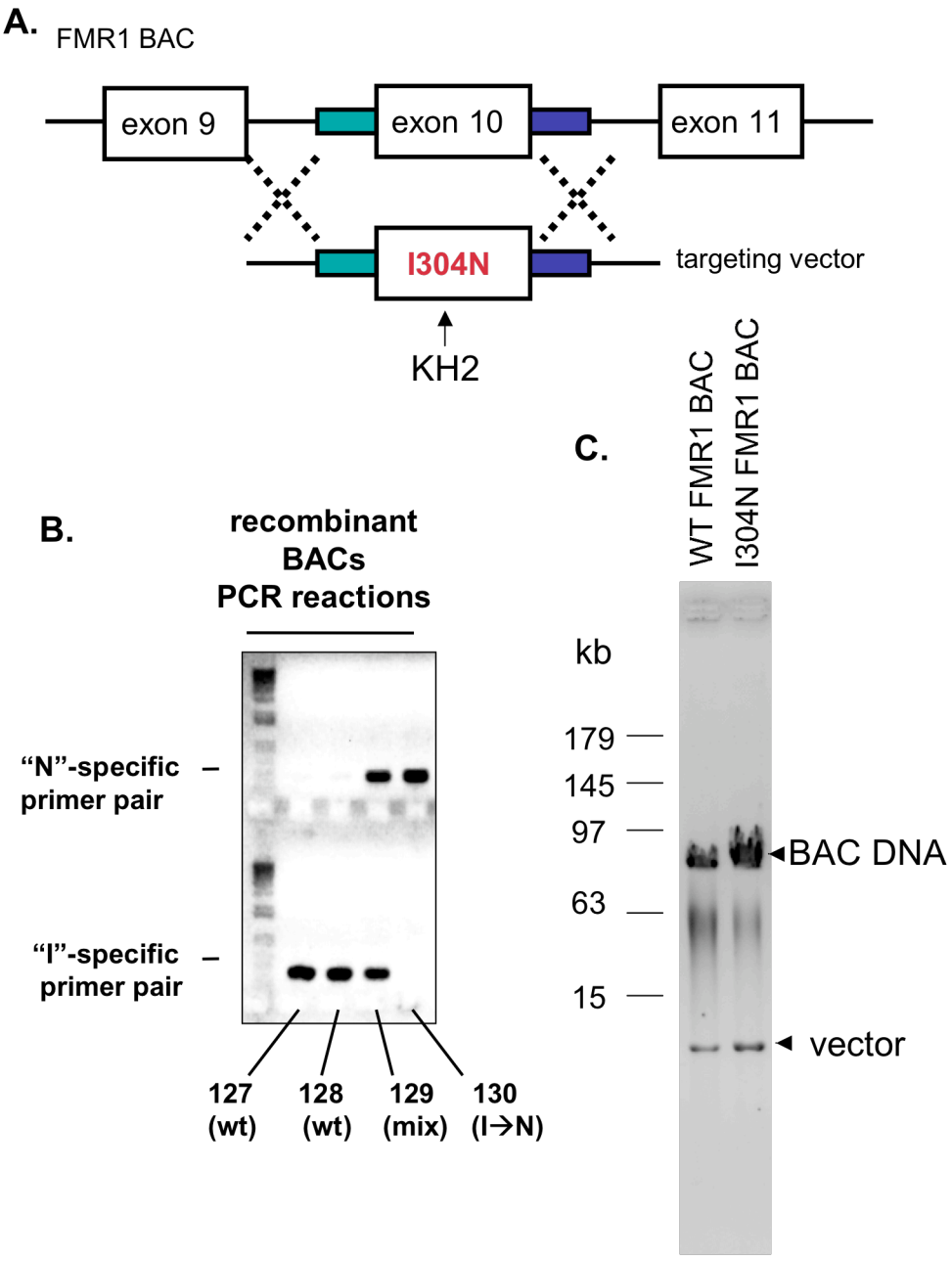

Figure 3.1. Generation of Fmr1 BAC transgenic mice. (A) Schematic representation of the strategy used to insert I304N into Fmr1 BAC via homologous recombination. ~500bp of sequence on either side of the site of the mutation in exon 10 were cloned into a targeting vector. **(B)** I304N recombinant Fmr1 BAC clones were screened with wild type and mutation specific PCR primers. Clone #130 was selected for pronuclear oocyte injections to generate transgenic founder mice. **(C)** Pulsed field gel electrophoresis to check integrity of BAC I304N Fmr1 DNA (digested by NotI) before pronuclear injection.

Figure 3.2.

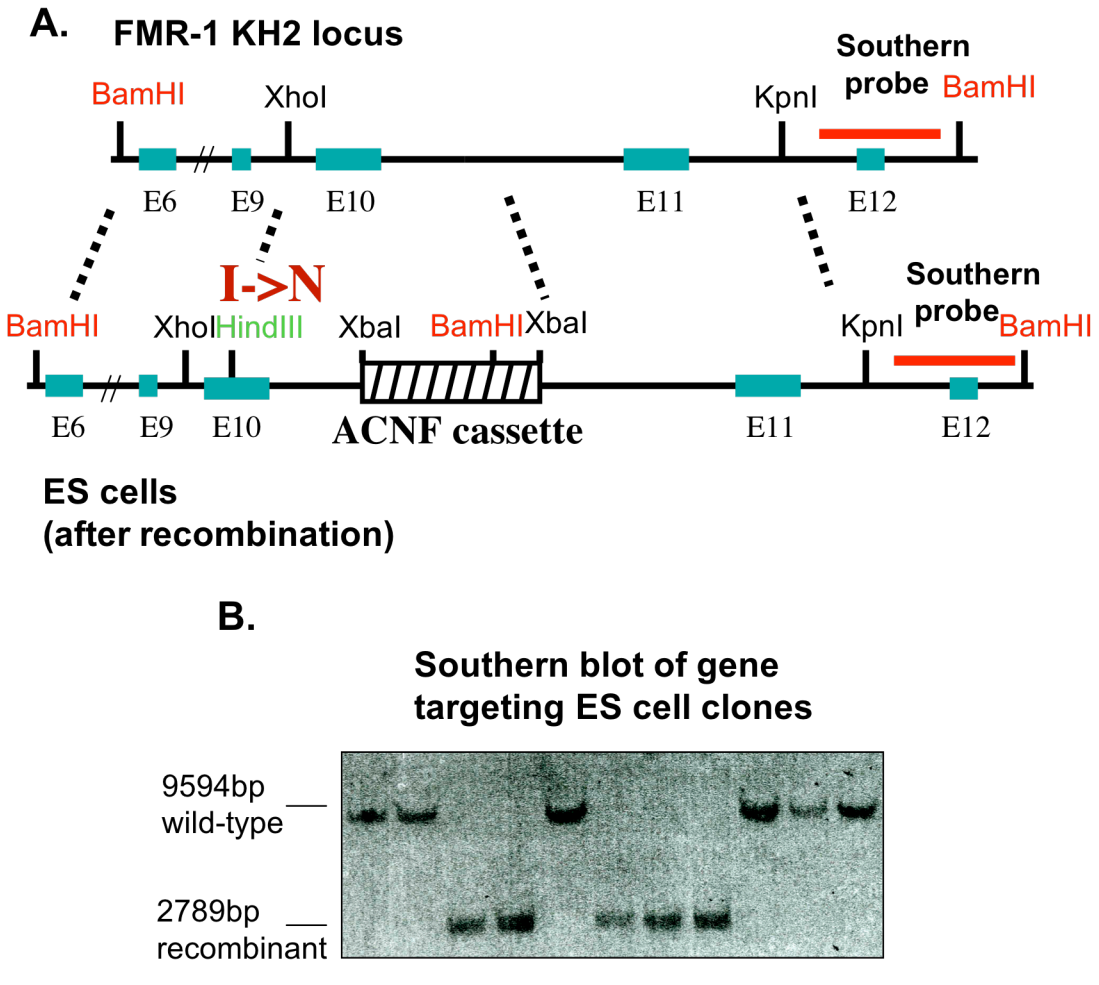

Figure 3.2. Generation of the Fmr1 I304N knock-in mouse model. (A) I304N Fmr1 targeting construct at the KH2 locus of the Fmr1 allele changes an isoleucine to asparagine in exon 10. An Auto-Cre-Neo^{R} (ACNF) cassette was inserted in a non-conserved region of intron 10. Testis-specific Cre recombinase expression drives auto-excision of the entire ACNF cassette during spermatogenesis in male chimeric mice. **(B)** Southern blot analysis of ES cells transfected with the I304N Fmr1 targeting construct. ES cell clones digested with BamHI were probed with an outer Southern probe overlapping exon 12. The targeted allele, 2.7kb, can be distinguished from the wild type locus, 9.6kb.

Figure 3.3.

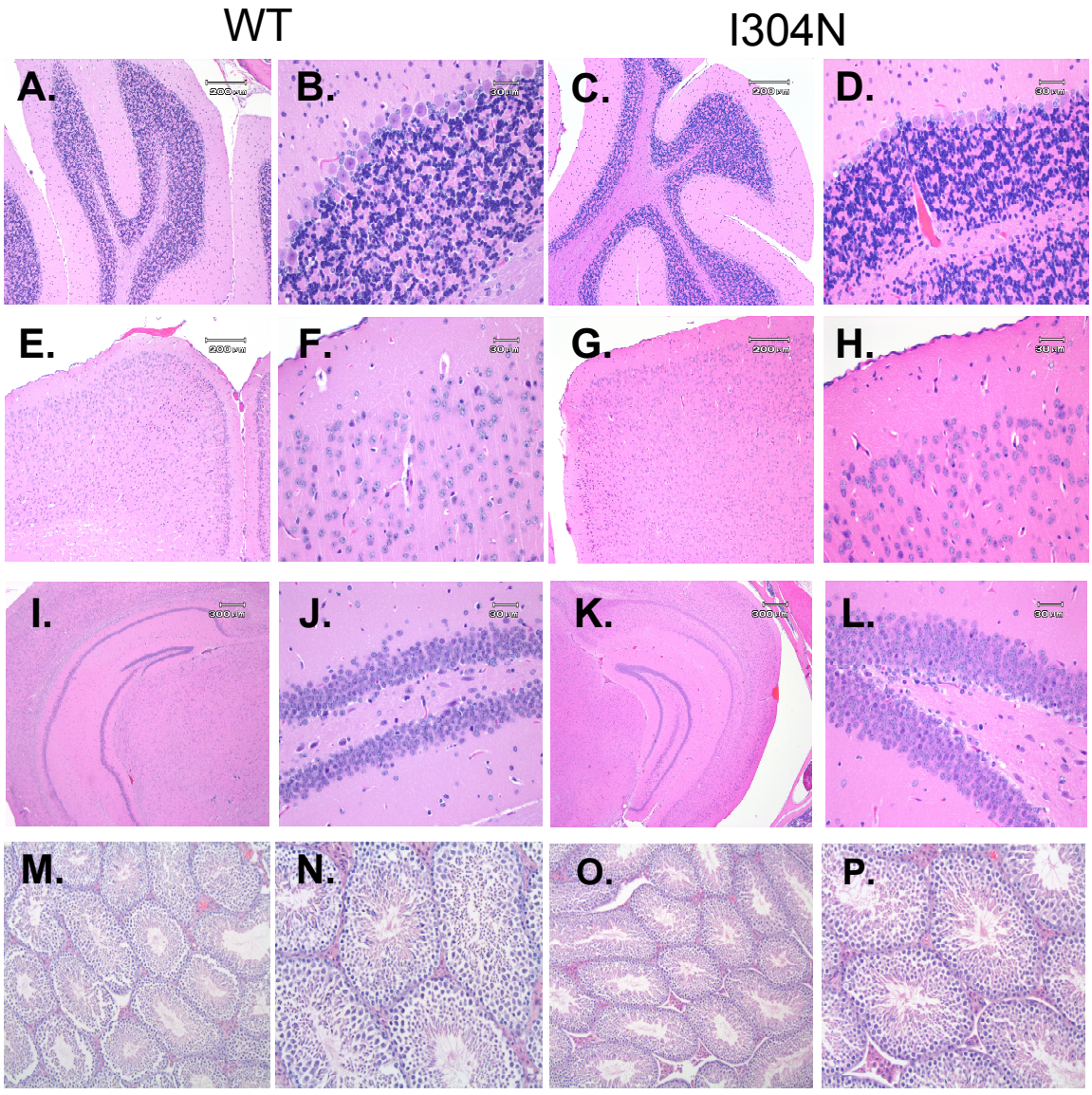

Figure 3.3. Light micrographs of sagittal sections of I304N knock-in mouse brains and testes revealed no microscopic abnormality. Post mortem mouse organs were fixed in 10% formalin, paraffin embedded, sectioned, stained with hematoxylin & eosin. **(A) (B)** wild type cerebellum, **(C) (D)** I304N cerebellum, **(E) (F)** wild type cortex, **(G) (H)** I304N cortex, **(I) (J)** wild type hippocampus, **(K) (L)** I304N hippocampus, **(M) (N)** wild type testes, and **(O) (P)** I304N testes.

Figure 3.4.

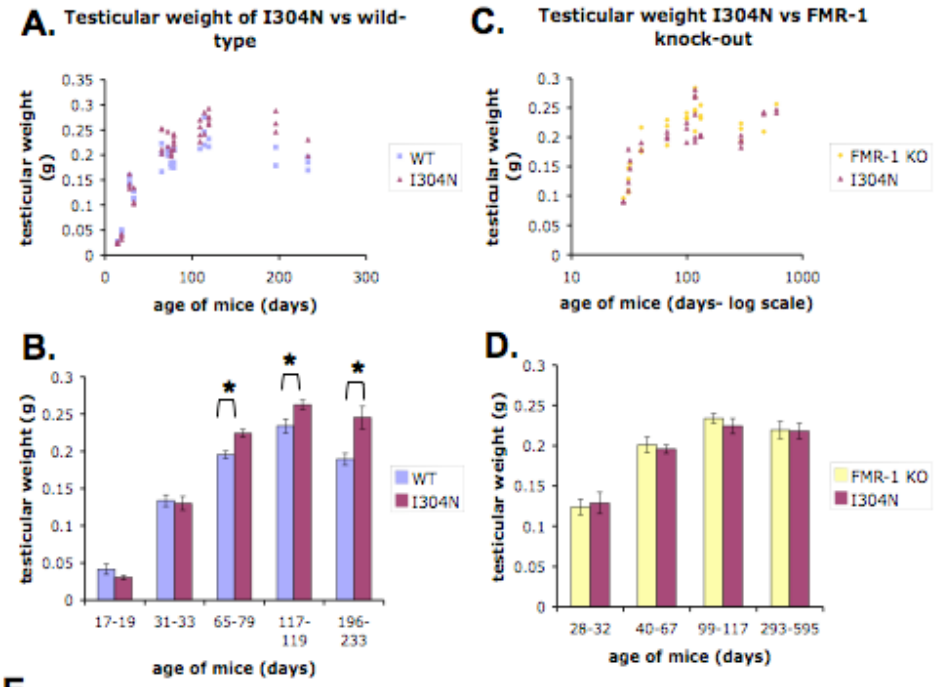

E.

Age (days)	I304N knock-in mice (g)	Wild-type littermates (g)	P value
17-19	0.031 ±0.003 (n=6)	0.042 ±0.007 (n=3)	P>0.05
31-33	0.130 ±0.009 (n=6)	0.134 ±0.008 (n=6)	P>0.05
65-79	0.224 ±0.005 (n=14)	0.195 ±0.005 (n=13)	P<0.03
117-119	0.263 ±0.006 (n=11)	0.234 ±0.010 (n=6)	P<0.03
196-233	0.245 ±0.015 (n=5)	0.189 ±0.008 (n=5)	P<0.03

Age (days)	I304N knock-in mice (g)	FMR-1 KO littermates (g)	P value
28-32	0.129±0.013 (n=7)	0.123 ±0.010 (n=6)	P>0.05
40-67	0.196 ±0.005 (n=5)	0.201 ±0.010 (n=6)	P>0.05
99-131	0.224 ±0.009 (n=12)	0.234 ±0.006 (n=11)	P>0.05
293-595	0.218 ±0.010 (n=8)	0.220 ±0.010 (n=5)	P>0.05

Figure 3.4. Combined weight of both testes of I304N knock-in mice compared with their wild type or Fmr1 knockout littermates. (A) I304N knock-in mice (42 total) shows macroorchidism when compared to their wild type littermates (33 total). Testicular weights were plotted against the age of mice. Data were derived from multiple litters. **(B)** For statistical analysis, litters of similar ages were grouped together and data were subject to student's t-test. * $p<0.03$. **(C)** and **(D)** The same analysis was applied to I304N knock-in mice (32 total) and their Fmr1 knockout littermates (28 total). However, there is no statistical difference in their testicular weights, up to 600 days of age. **(E)** Tabulation of testicular weight analysis of I304N versus wild type or Fmr1 knockout littermates.

Figure 3.5.

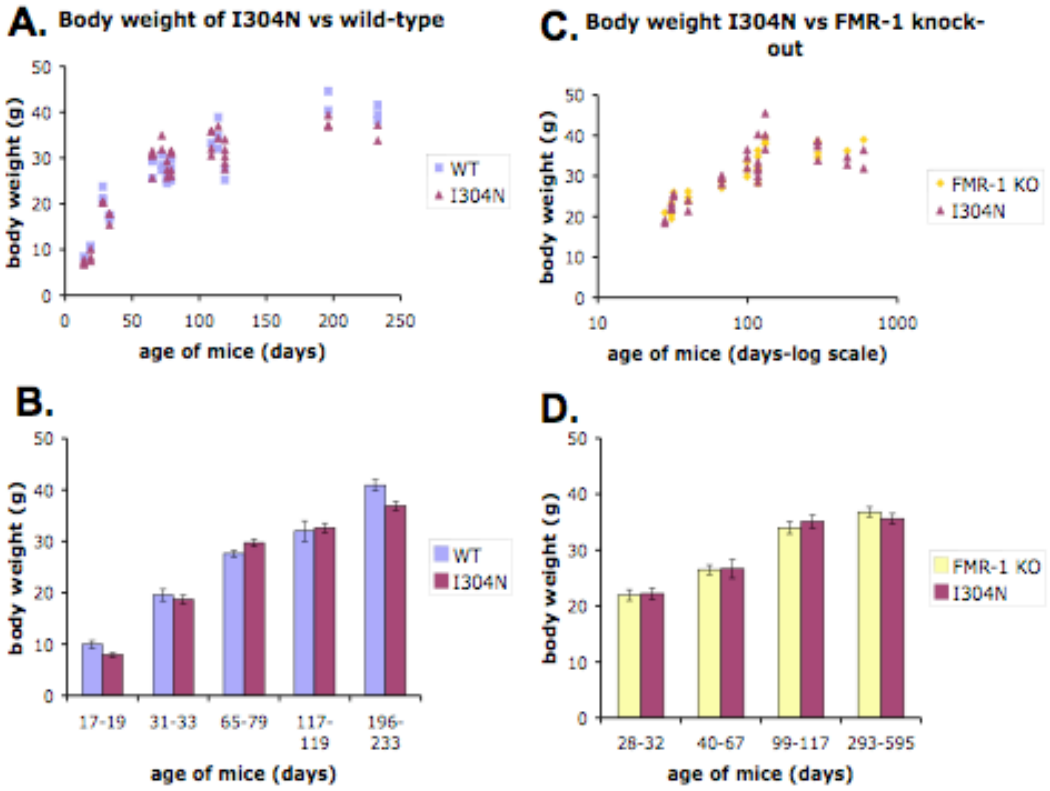

Figure 3.5. Body weight of I304N knock-in mice compared with their wild type or Fmr1 knockout littermates shows no statistical difference. These are the same male mice we used to analyze the testicular weight difference.

Figure 3.6.

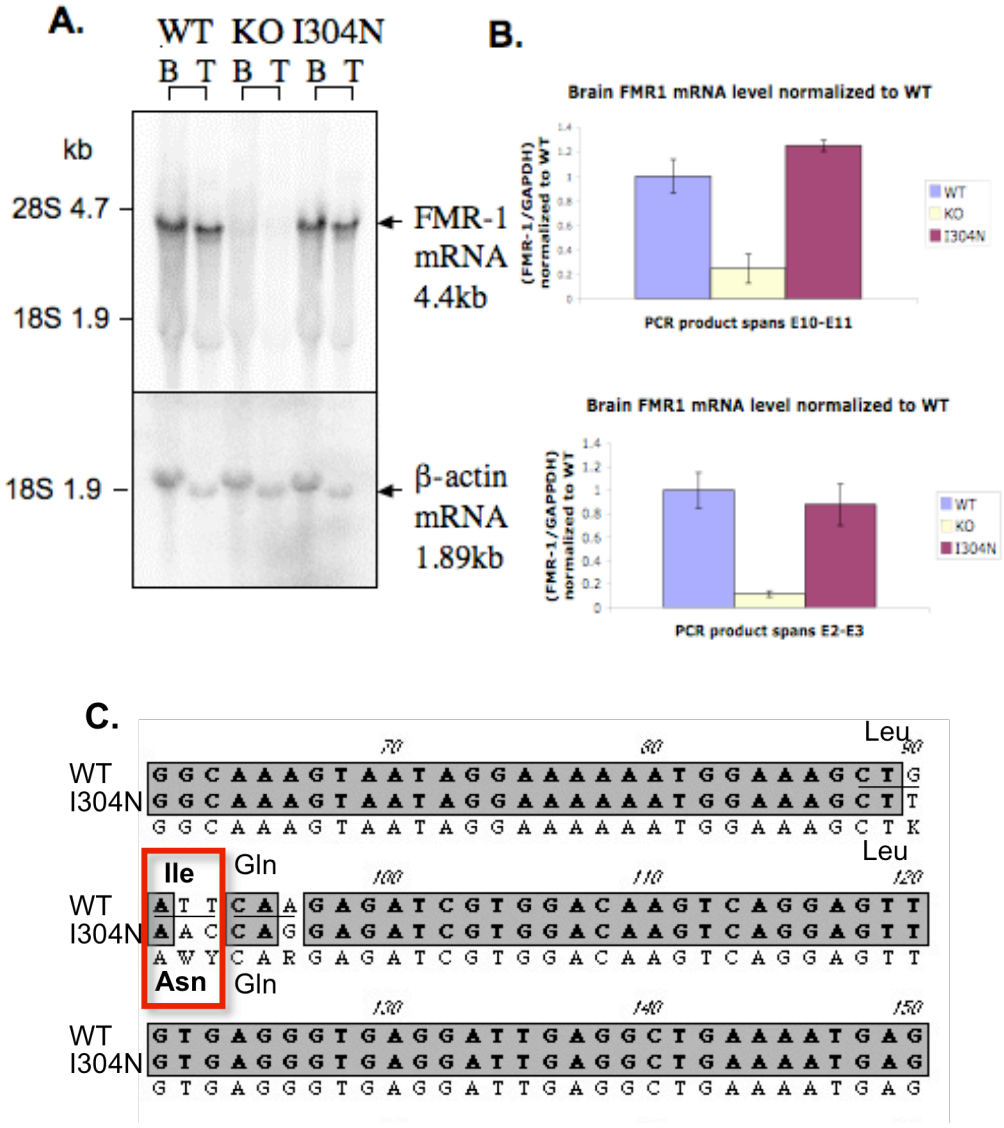

Figure 3.6. mRNA analysis of I304N knock-in mouse model. (A) Northern blot of mouse brain and testicular mRNA shows that I304N Fmr1 mRNA has normal length and level. Fmr1 mRNA was detected using an *in vitro* transcribed radiolabeled RNA probe anti-sense to the 3'UTR of the Fmr1 transcript. β-actin mRNA served as a loading control. **(B)** Quantitative RT-PCR confirms that I304N Fmr1 mRNA is expressed at normal levels. Two sets of primers (left panel primers spanning exon 10 to 11 and right panel primers spanning exon 2 to 3) were used to amplify the Fmr1 transcript. Data were quantified by the standard curve method. **(C)** Sequence alignment of RT-PCR products from wild type and I304N knock-in mouse brain RNA confirms the presence of the I304N point mutation. Partial sequence where the I304N mutation is present is shown.

Figure 3.7.

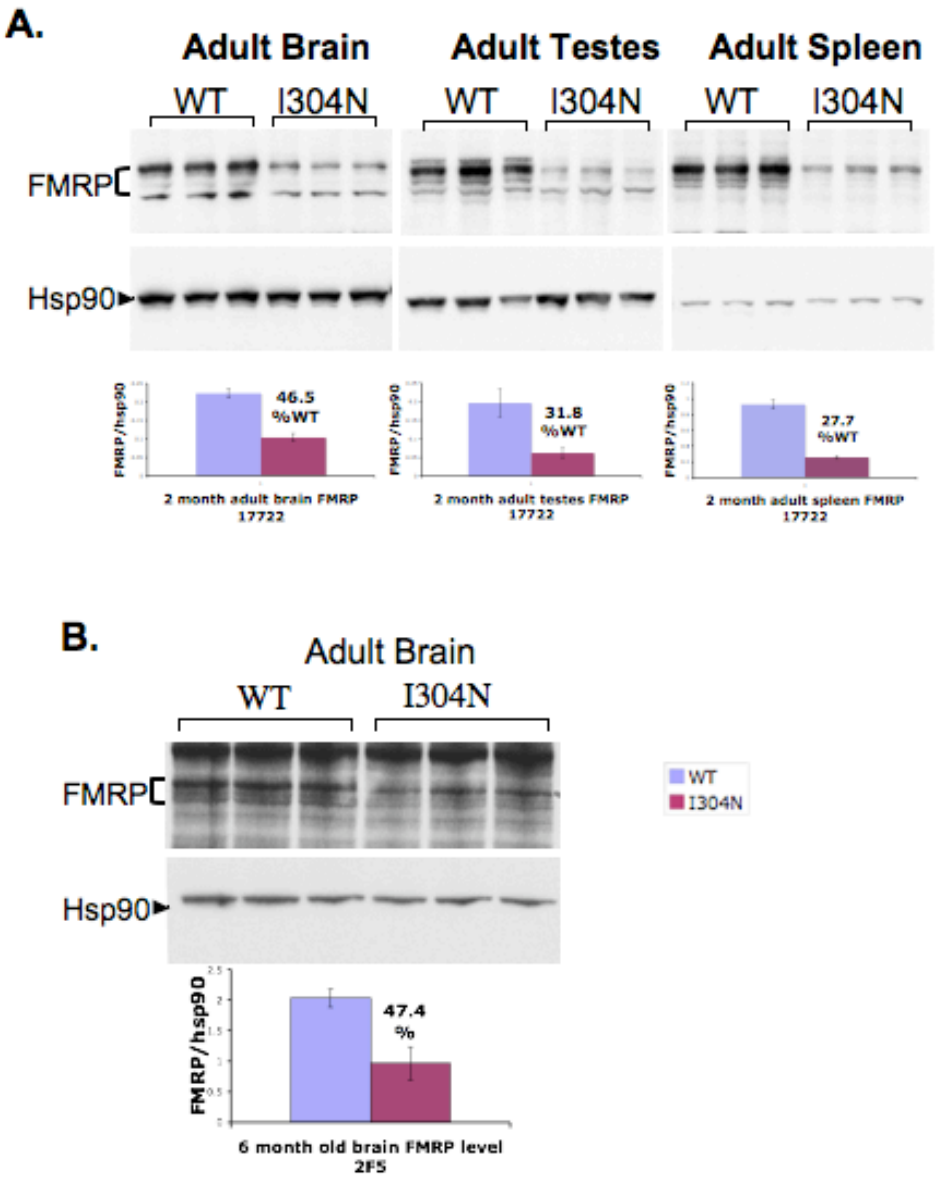

Figure 3.7. Analysis of mutant protein in adult I304N knock-in mice. (A) Western analysis and quantification of I304N FMRP in 2 month old mouse brain, testes , and spleen, probed with FMRP polyclonal antibody, ab17722 (Abcam). Hsp90 served as the loading control. Signals were quantified by chemiluminescence using Versadoc imaging. The percentage of I304N FMRP expression compared to wild type in each tissue is indicated. **(B)** Western analysis and quantification of I304N FMRP in 6 month old mouse brain using 2F5 FMRP monoclonal antibody.

Figure 3.8.

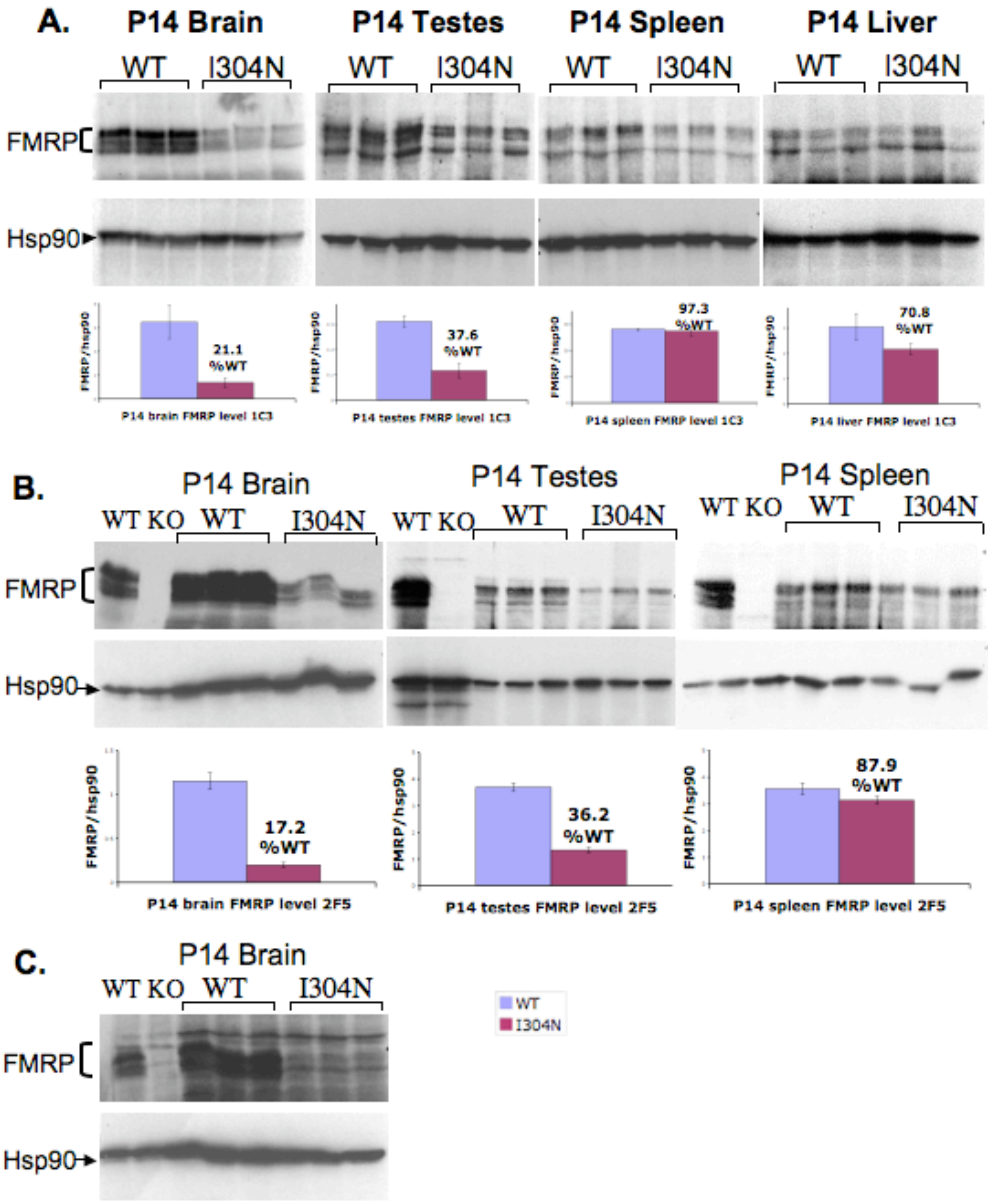

Figure 3.8. Analysis of mutant protein in P14 I304N knock-in mice. (A) Western blot and quantification of FMRP expression in brain, testes, and spleen of three P14 I304N knock-in mice versus three wild type littermates. Western blots were probed with FMRP monoclonal antibody 1C3. **(B)** Western blot and quantification of I304N FMRP in P14 mouse brain, testes, and spleen, probed with 2F5 FMRP monoclonal antibody, confirming relatively lower level of the mutant FMRP. **(C)** Western blot of I304N FMRP steady state levels in P14 mouse brain with 7G1-1 FMRP monoclonal antibody.

Figure 3.9.

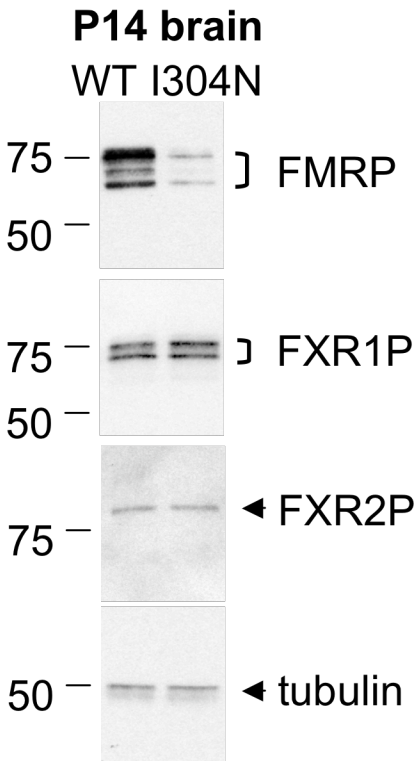

Figure 3.9. FXR1P and FXR2P have normal expression in I304N mouse brain. Western blot analysis of FXR1P probed with ML13 and FXR2P probed with 1G2 antibody in P14 I304N vs. wild-type mouse brains.

Figure 3.10.

A.

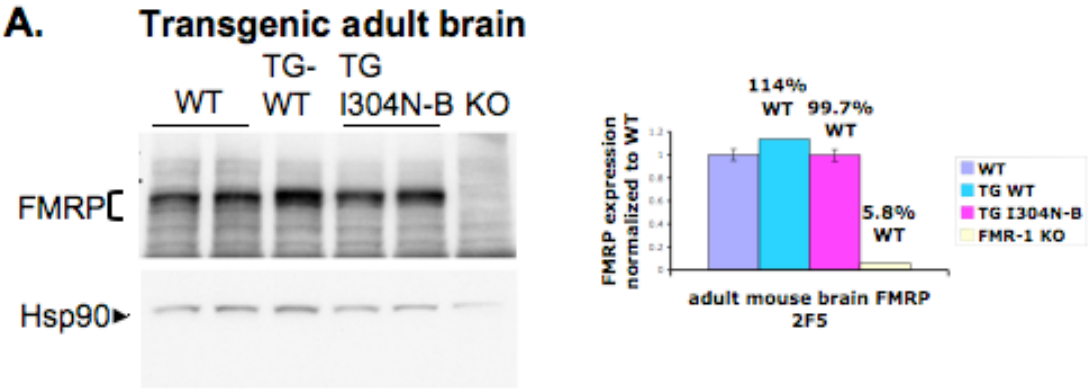

B.

	TG WT	TG I304N-A	TG I304N-B
FMRP relative to WT	76.5%	18.2%	41.8%
FMR-1 mRNA relative to WT	90.7%	69.2%	168%
Protein/mRNA ratio relative to WT	~ 1	~1/4	~1/4

Figure 3.10. Expression analysis of I304N BAC transgenic mice. (A) Western blot (left panel) and quantification (right panel) of I304N expression in adult transgenic mice, probed with 2F5 antibody. One line of transgenic I304N (TG-I304N-B) has normal I304N expression in adult brain. **(B)** At P14, a 4 fold decrease of I304N FMRP protein to its mRNA ratio was observed in both lines of transgenic I304N mice mimicking the I304N knock-in, but not in wild type transgenic control mice. Protein level was measured by Western blot with 2F5 antibody. mRNA level was measure by quantitative RT-PCR with standard curve method, normalized to GAPDH mRNA.

Figure 3.11.

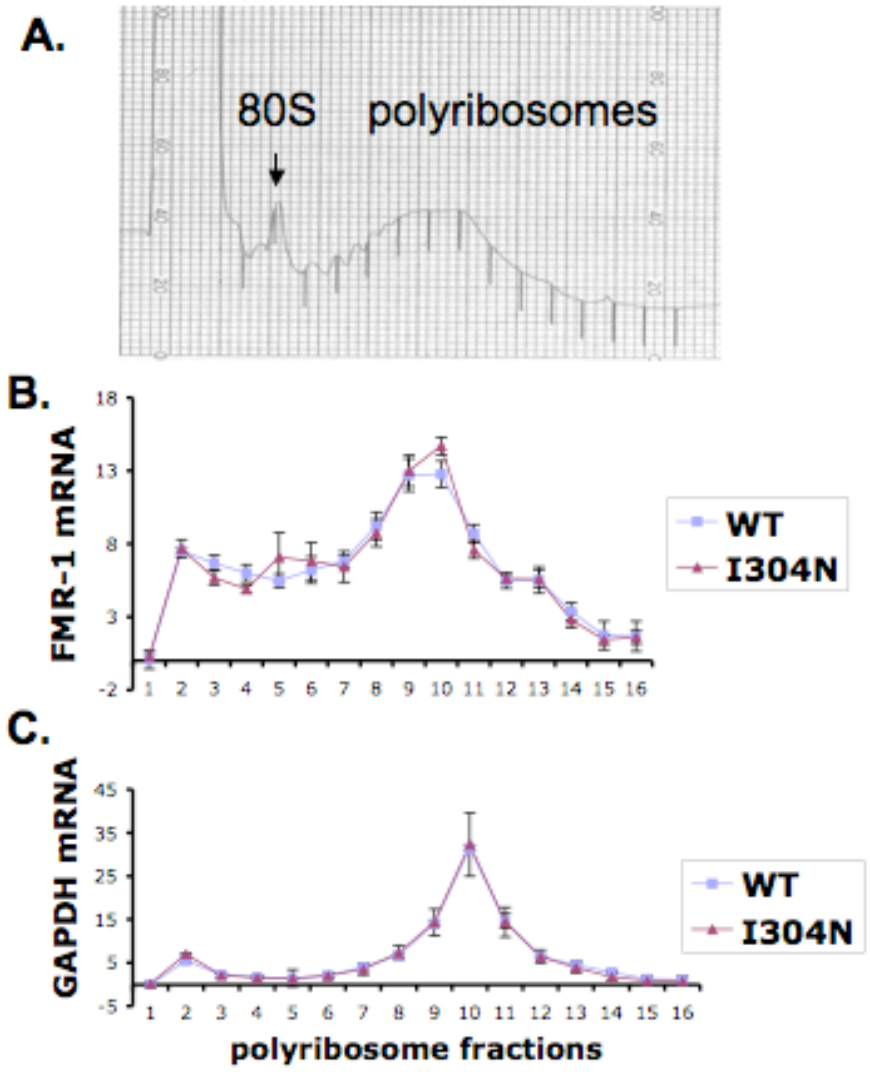

Figure 3.11. I304N mRNA has a normal translational profile. I304N and wild type mouse brain cytoplasmic lysates were centrifuged on a w/w 20-50% linear sucrose gradient. A260 absorption profiles are shown in **(A)**, 80S monosome and polyribosomes are indicated. **(B)** Gradients were fractionated and RNA was collected from each fraction. Quantitative RT-PCR was performed (ΔΔCt method) for Fmr1 mRNA. Relative Fmr1 mRNA level in each fraction was plotted as a percentage of total Fmr1 mRNA to illustrate its distribution over the polyribosome gradient. **(C)** GAPDH was the control mRNA that did not show distribution changes over I304N vs. wild type polyribosome gradients.

Figure 3.12.

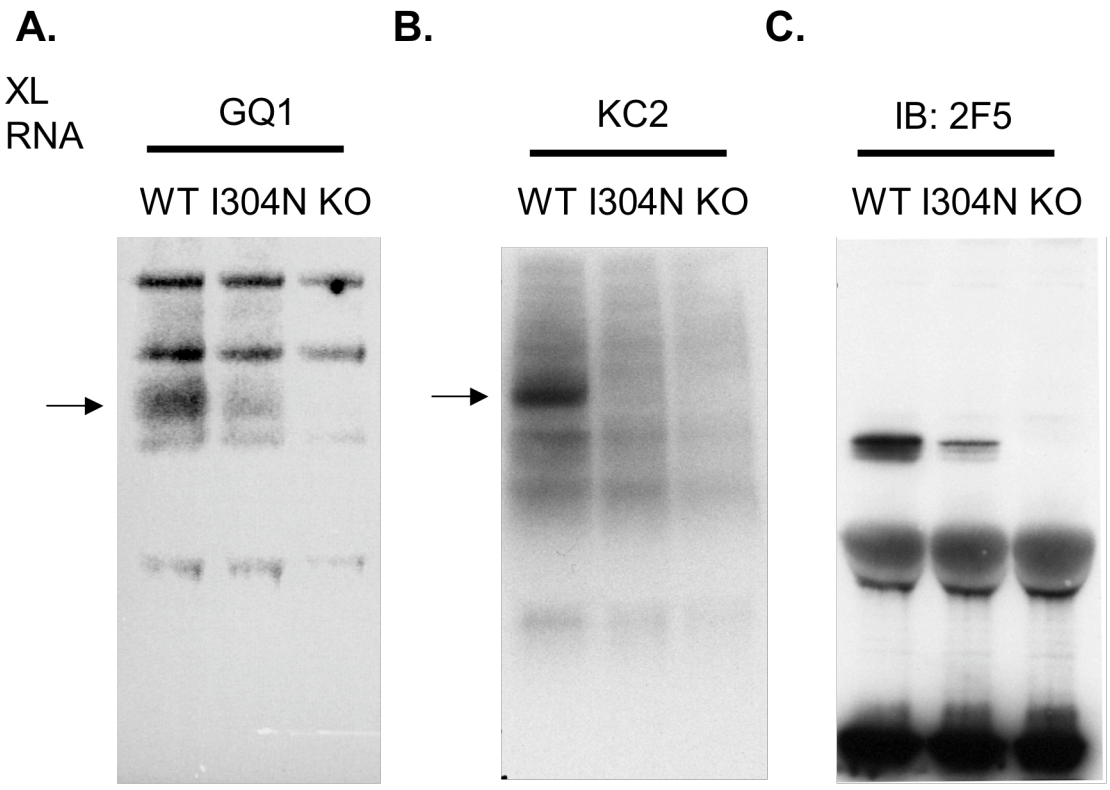

Figure 3.12. Mouse brain I304N protein is able to bind G-quartet RNA, but not kissing complex RNA. Extracts from wild type, I304N knock-in, and Fmr1 knockout mouse brains were incubated with 96nt radiolabeled RNA generated by in vitro transcription encoding **(A)** G-quartet RNA and **(B)** kissing complex RNA. Samples were UV crosslinked, RNase treated, immunoprecipitated with FMRP specific 7G1-1 antibody, run on SDS-PAGE gels, transferred to nitrocellulose and exposed to phosphoimager to detect radiolabeled RNA. The arrow indicates immunoprecipitated FMRP-radiolabeled G-quartet RNA complex in **(A)** and FMRP-kissing complex RNA in **(B)**. **(C)** 7G1-1 immunoprecipitated wild type and I304N FMRP were detected using anti-FMRP 2F5 antibody.

Figure 3.13.

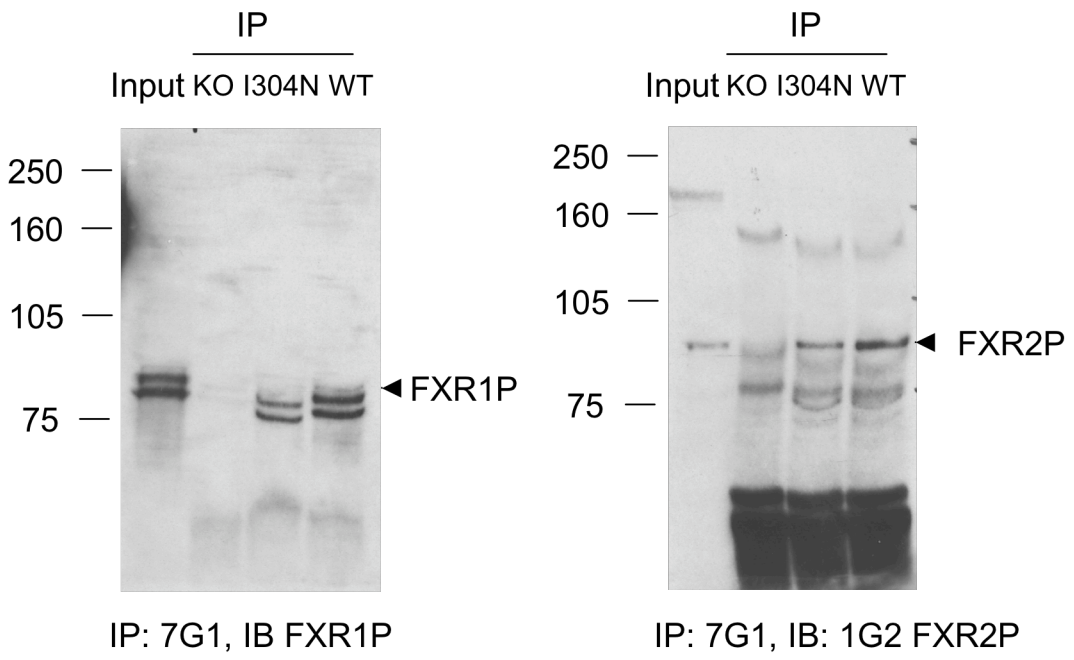

Figure 3.13. Co-immunoprecipitation of I304N with its autosomal paralogs, FXR1P and FXR2P. FMRP was immunoprecipitated using the 7G1-1 antibody. FXR1P and FXR2P were detected using antibody ML13 (gift from Dr. Eduoard Khandjian) and 1G2, respectively. Wild type and Fmr1 knockout mice were used as positive and negative controls.

Figure 3.14.

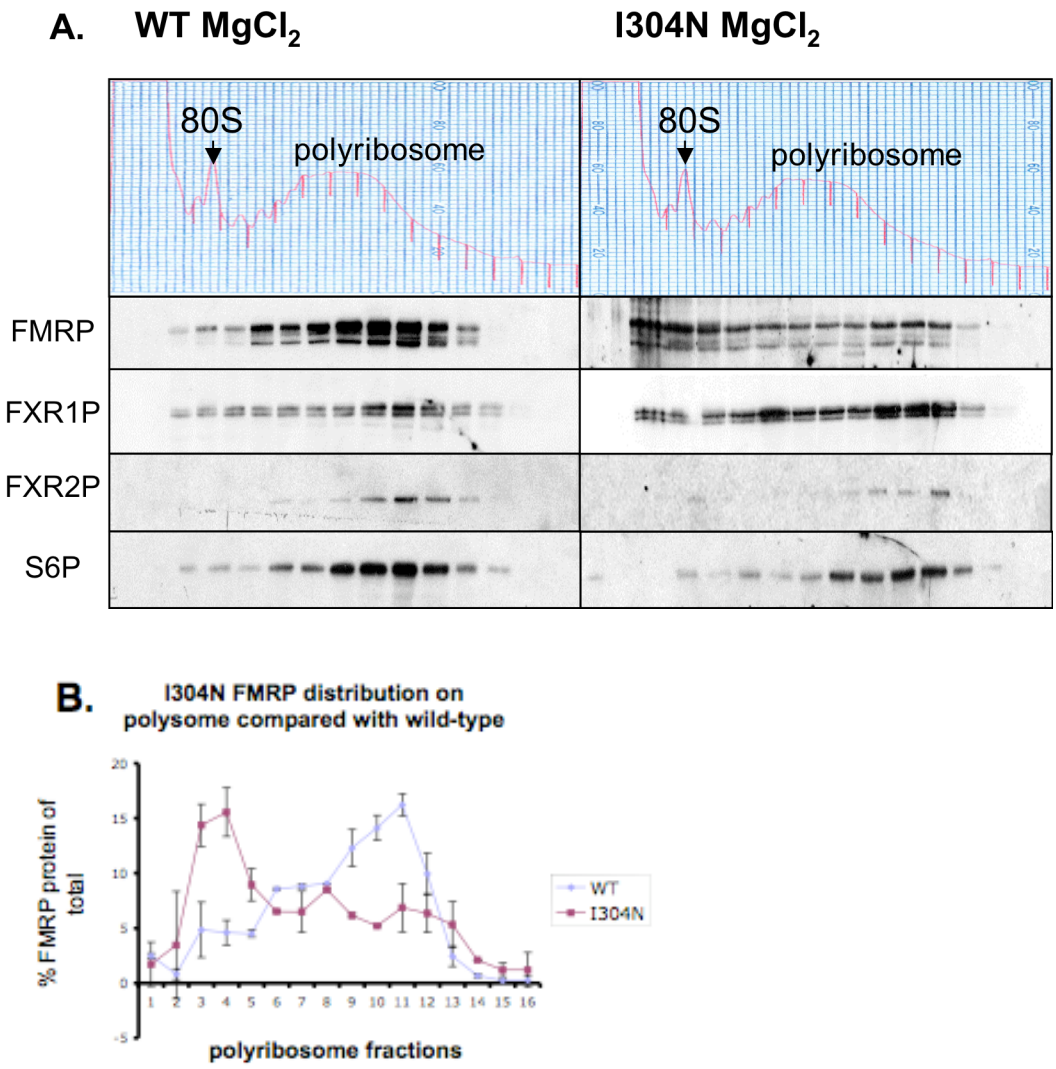

Figure 3.14. The majority of I304N FMRP is dissociated from polyribosomes while FXRPs are still on polyribosomes in I304N knock-in mouse brain. (A) Mouse brain cytoplasmic extracts were centrifuged on a w/w 20-50% linear sucrose gradient. Fractions were collected; positions of the 80S monosome and polyribosomes are indicated on the A260 profile. FMRP (7G1-1 antibody), FXR1P, and FXR2P migration were analyzed by Western blot. Ribosomal protein S6 distribution further confirms the polyribosome sedimentation profile. **(B)** Quantification of chemiluminescence by Versadoc imaging of the Western blot of I304N knock-in vs. wild type FMRP in (**A**), the percentage of FMRP present in each fraction as a function of the total FMRP signal in the gradient is indicated.

Figure 3.15.

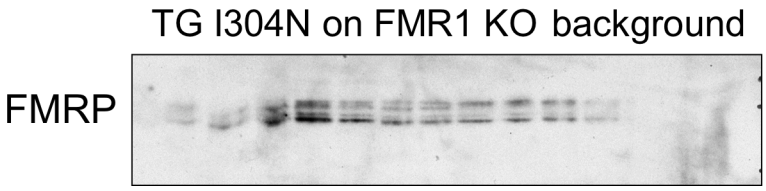

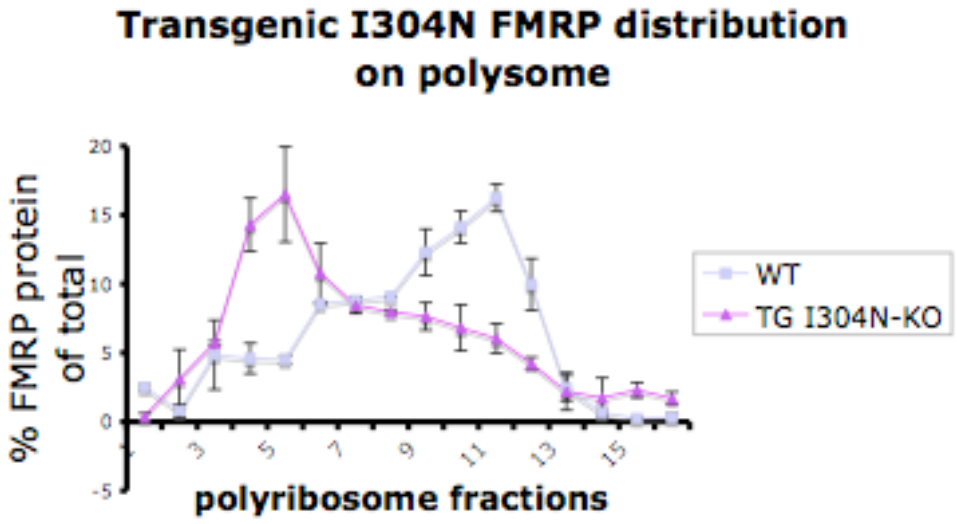

Figure 3.15. Most of the I304N FMRP in I304N BAC transgenic mice does not cosediment with polyribosomes. Proteins from 400 ul of each sucrose gradient fraction were TCA precipitated and resolved by SDS-PAGE. FMRP was detected by Western blot using 7G1-1 antibody.

Figure 3.16.

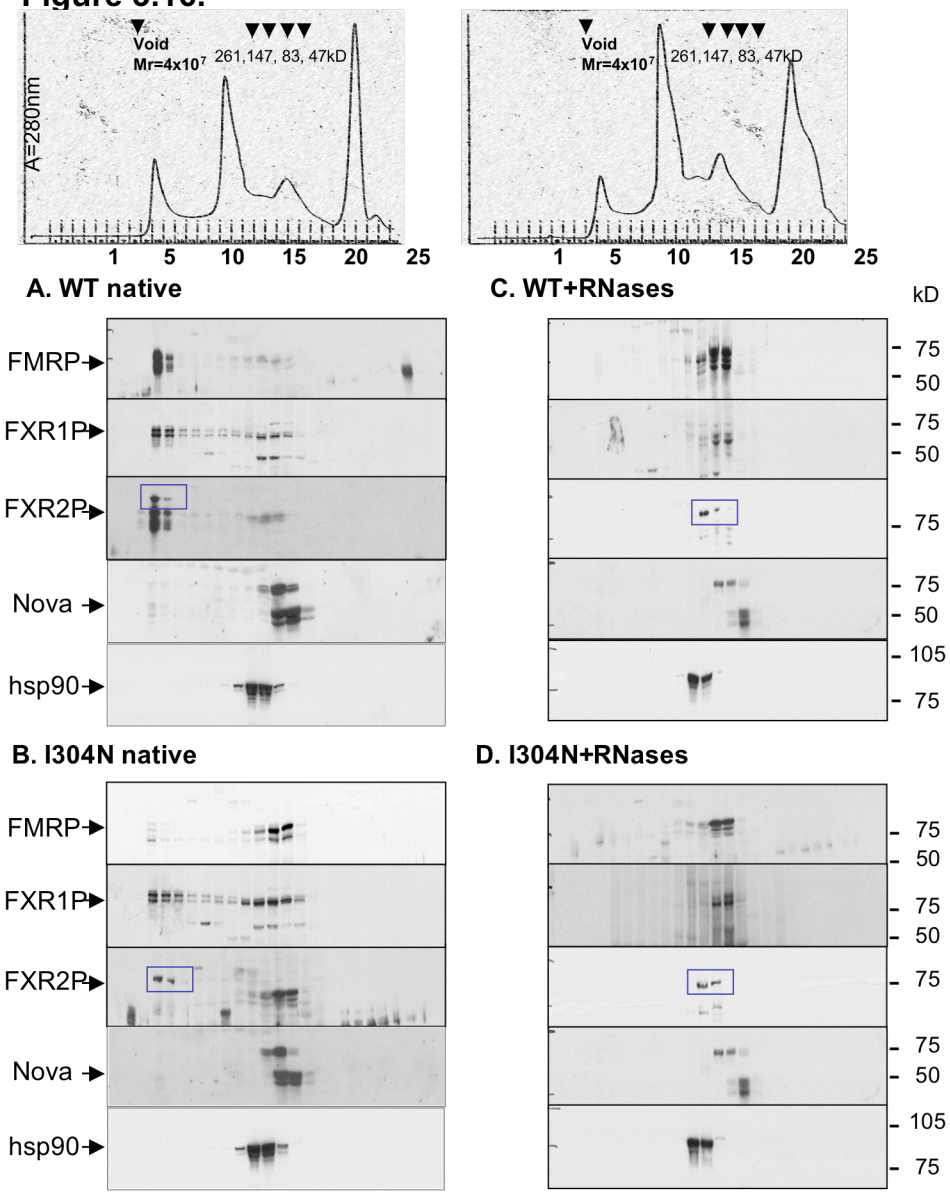

Figure 3.16. The majority of I304N FMRP is in an abnormally small RNase-resistant complex. Top panels show the absorption profiles at 280nm of Superose 6 gel filtration of wild type and I304N mouse brain lysates, without and with RNase treatment. The molecular sizes in kDa depicted on top of the profile were calibrated using molecular weight markers. Bottom panels are Western blots of wild type or I304N FMRP, FXR1P, FXR2P corresponding to the fractions of the absorption profiles. The RNA binding protein Nova and hsp90 are controls. **(A)** The wild type FMRP-mRNP eluted in the void volume of the column corresponding to a relative size > 40,000 kDa. **(B)** I304N is in a much smaller complex of 100-300 kDa. After complete RNase A and T1 digest, the large wild type FMRP complex falls apart to the size of the native I304N FMRP complex **(C)** and the I304N complex does not shift in its relative size **(D)**.

Figure 3.17.

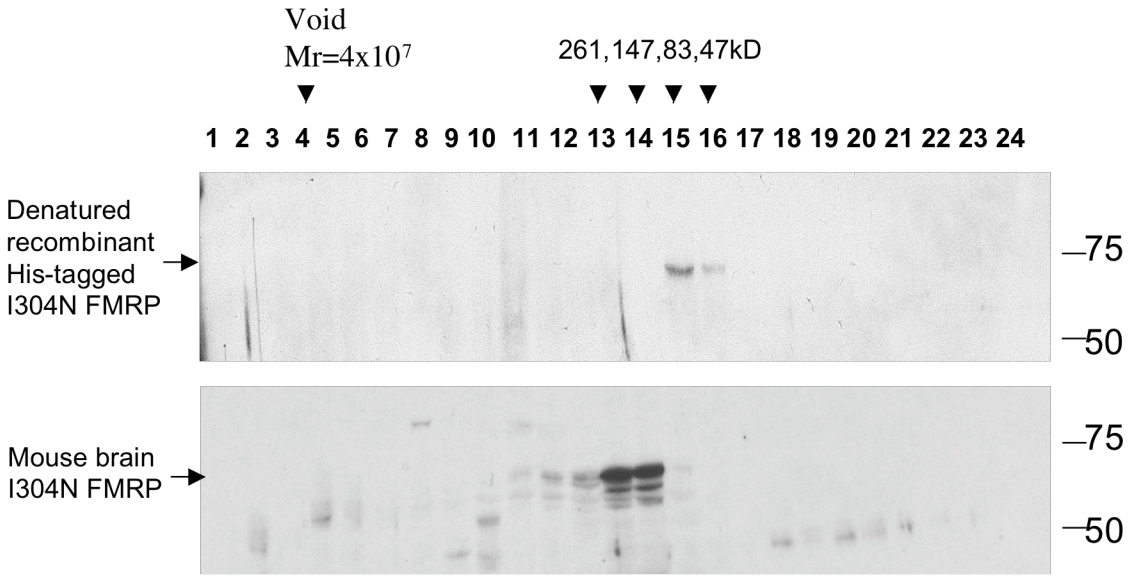

Figure 3.17. The I304N FMRP core particle is in a complex larger than the I304N monomer. Full length His tagged I304N FMRP was denatured by heating at 95^{o}C for 10min and spiked into mouse brain lysate. Lysate was then run on a Superose 6 column; fractions were collected and subject to Western blot analysis. Denatured I304N FMRP was detected using HRP conjugated anti-His antibody.

Figure 3.18.

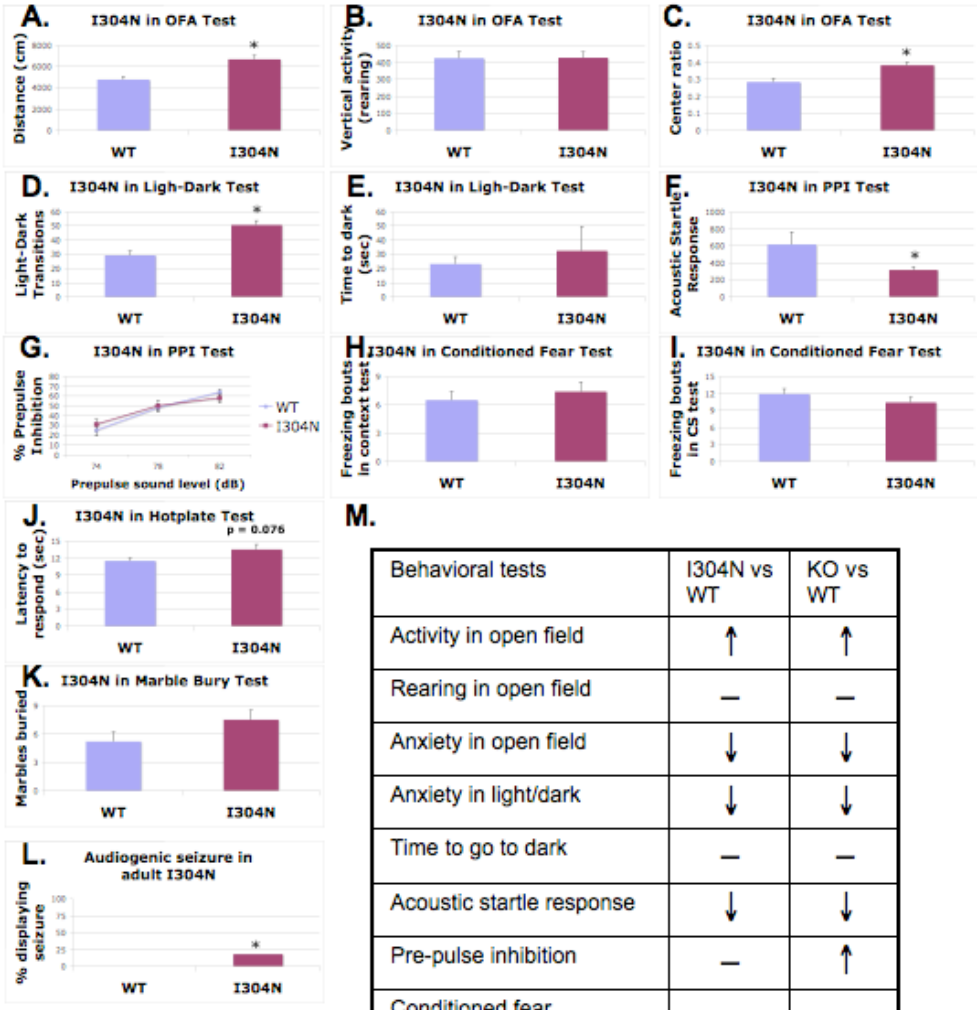

M.

Behavioral tests	I304N vs WT	KO vs WT
Activity in open field	↑	↑
Rearing in open field	–	–
Anxiety in open field	↓	↓
Anxiety in light/dark	↓	↓
Time to go to dark	–	–
Acoustic startle response	↓	↓
Pre-pulse inhibition	–	↑
Conditioned fear	–	–
Hotplate sensitivity to pain	↓	↓
Marble burying	↑	↓
Audiogenic seizure	18%	none

Figure 3.18. Behavioral assays comparing I304N knock-in mice and their wild type littermates. Activity in open field test: **(A)** total distance traveled, **(B)** vertical distance (rearing). Anxiety related responses: **(C)** center:total distance ratio in an open field, **(D)** light to dark transition, **(E)** time spent in the dark chamber. Startle habituation: **(F)** acoustic startle response in PPI test, **(G)** %PPI with increasing prepulse level. Conditioned fear: **(H)** fear response in context test**, (I)** fear response in acoustic conditioned stimulus test. **(J)** Hotplate test for sensitivity to pain. **(K)** Marble burying for obsessive-compulsive behavior. **(L)** Audiogenic seizure. **(M)** Tabulation of behavioral test summary and comparison with historical findings on Fmr1 knockout mice.

Figure 3.19.

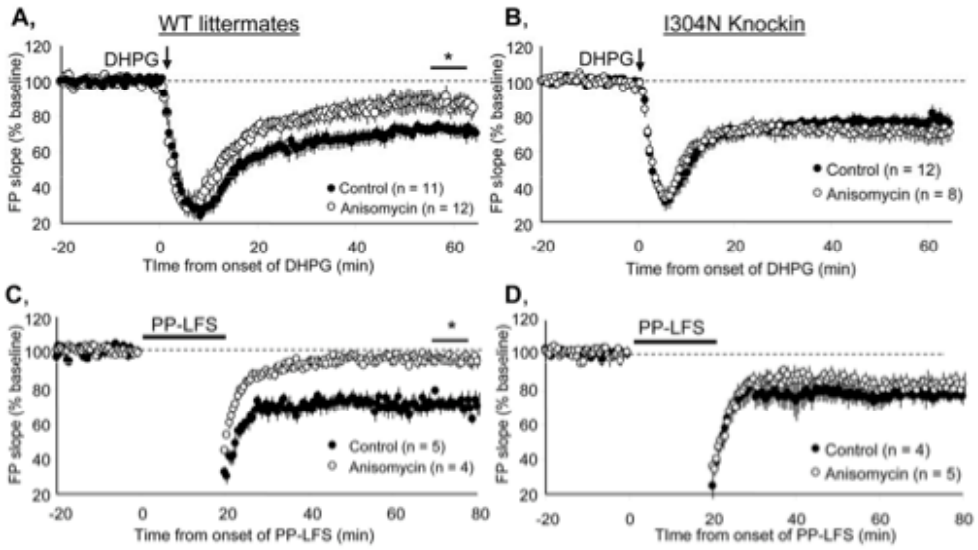

Figure 3.19. Protein synthesis-independent mGluR-LTD in I304N knock-in mice. Evoked extracellular field potentials (FPs) from CA1 of acute slices from 30-90 day old wild type and I304N knock-in littermates are plotted as a percent of baseline (pre-DHPG or PP-LFS). **(A) (B)** Anisomycin inhibits DHPG-induced LTD in wild type littermates, but has no effect in I304N knock-in mice (*; p=0.02). **(C) (D)** Anisomycin inhibits synaptically induced LTD (with PP-LFS; *; p=0.004) in wild type mice, but not I304N knock-in mice. The magnitude of LTD between wild type and I304N knock-in mice is not different under control conditions, but is enhanced in the presence of anisomycin (ANOVA and subsequent Fisher PLSD; $p<0.05$).

CHAPTER IV. IDENTIFICATION AND VALIDATION OF FMRP *IN VIVO* RNA TARGETS

Introduction

FMRP has been well-characterized as an RNA binding protein; both *in vitro*-translated and purified FMRP bind RNA ribohomopolymers and ~4% of fetal brain mRNAs *in vitro*, (Ashley et al., 1993b; Brown et al., 1998; Siomi et al., 1993b). Like the majority of RBPs, FMRP harbors multiple RNA binding motifs, two tandem KH (hnRNPK homology)-type RNA domains (Siomi et al., 1994; Siomi et al., 1993b), a spacer and an arginine- and glycine-rich RNA binding domain (RGG box) (Siomi et al., 1993b). The N-terminus may also have RNA binding ability as assessed by a ribohomopolymer assay (Adinolfi et al., 1999) and recent data suggesting that the N-terminus binds BC1, a neuron-specific noncoding RNA (Zalfa et al., 2005). In both cell lines and brain lysates subjected to sedimentation in sucrose gradients, FMRP has been found to associate with translating polyribosomes as part of a large messenger ribonucleoprotein (mRNP) complex, and this has been shown to be an RNA-dependent interaction (Corbin et al., 1997; Eberhart et al., 1996; Feng et al., 1997a; Feng et al., 1997b; Khandjian et al., 1996; Khandjian et al., 2004; Stefani et al., 2004). Since the study of the I304N mouse model suggests that a key function of FMRP in mediating normal cognition is sequence-specific RNA binding, the interest in identifying RNA ligands for FMRP is heightened. Identification of the RNA targets that FMRP binds to *in vivo* would be a key step in ultimately understanding the normal function of the protein and the mechanistic defects caused by the protein's absence.

However, identification of FMRP targets has not been easy and many labs have attempted with various approaches. Our lab has used *in vitro* RNA selection assays (SELEX) and identified G quartet and kissing complex RNA motifs as RNA ligands of the FMRP RGG box and KH2 domain respectively (Darnell et al., 2005a; Darnell et al., 2001). The G quartet motif has been independently identified by the candidate gene approach in the 3' end of Fmr1 coding sequence that FMRP specifically binds (Schaeffer et al., 2001). Co-immunoprecipitation (IP) of FMRP-mRNP complexes and extraction of

RNA for microarray analysis has identified a repertoire of neuronal RNAs (Brown et al., 2001), some of which also contained G quartet elements. Among these candidates, Mtap1b (MAP1B) has been validated as a target RNA *in vivo*, using a *Drosophila* model of the fragile X syndrome. Aberrations in the architecture of neuronal synapses were noted in flies in which the dFxr gene (the *Drosophila* homologue of FMR-1) had been disrupted. Double deletion of dfxr and futsch, the homologue of Mtap1b, restored normal synaptic architecture, supporting the hypothesis that FMRP negatively regulates translation of Mtap1b mRNA (Zhang et al., 2001b). Despite the fact that these targets are widely studied, there are still some uncertainties. Fusion proteins lack post-translational modification and both phosphorylation and methylation status of RGG box has shown to affect FMRP RNA binding (Ceman et al., 2003a; Denman, 2002; Stetler et al., 2006). Problems with co-IP of mRNPs include precipitation (which must be done under low to moderate stringency to avoid loss of associated RNAs) of additional associated RBPs along with their targets, creating signal to noise problems, and reassociation of RBPs with aberrant RNAs after cell lysis (Mili and Steitz, 2004). Other different techniques, including antibody-positioned RNA amplification (APRA) (Miyashiro et al., 2003), yeast 3-hybrid (Dolzhanskaya et al., 2003; Sung et al., 2003), and cDNA SELEX (Chen et al., 2003) have identified distinct sets of mRNAs associated with FMRP-mRNP complexes adding to the repertoire of FMRP's potential RNA targets. Moreover, a few more targets have been identified by candidate gene approach (Todd et al., 2003; Xu et al., 2004; Zalfa et al., 2003). The long lists of RNAs with limited overlap from different laboratories make it difficult to distinguish true FMRP targets from falsely identified ones and would necessitate an enormous amount of work of rigorous validation.

To overcome this, our laboratory has developed *in vivo* UV crosslinking and immunoprecipitation (CLIP) analysis (Fig. 4.1) (Ule et al., 2005a; Ule et al., 2003). It has been used successfully to identify the genome-wide binding sites for Nova family members on pre-mRNAs. The sequence of the CLIP tags (short RNA sequences directly crosslinked to Nova and cloned using this technique) has confirmed the specific binding site for Nova previously identified by in vitro RNA selection to be YCAY clusters. In addition, the location of the tags on a specific set of pre-mRNAs, combined with the results of in vivo splicing assays in mouse models, has provided a predictive "map" that

correctly predicts the splicing outcome of Nova-dependent targets. (Ule et al., 2003; Ule et al., 2006).

CLIP analysis offers a few advantages over previously used techniques in identifying bona fide *in vivo* RNA targets (Ule et al., 2005a; Ule et al., 2003). First, it uses UV to crosslink protein and RNA that directly interact with one another on the order of 1 angstrom apart in intact brain tissues. Second, the UV photocrosslinking step in the CLIP protocol forms irreversible covalent bonds between RNA and proteins, allowing for unusually rigorous purification of RNA-protein complexes in multiple steps, like stringent IP, boiling complexes in SDS-sample buffer, running complexes on SDS-PAGE gels and transferring to nitrocellulose, through which non-specific free RNA can be removed, lowering the false-positive rate. Third, limited RNase digestion allows for the isolation of the sequence involved in protein binding, providing a snapshot of where an RBP is bound in vivo, which conventional IP techniques cannot provide. Therefore, we set out to use CLIP to identify FMRP RNA targets.

Results

Adaptation of CLIP for FMRP to identify RNA targets

The first step of adapting CLIP for FMRP was to work out the IP condition for FMRP. Several changes in the protocol optimized for the Nova experiments had to be altered. First, we had to lower the ultracentrifugation step from 60,000rpm to 30,000rpm (TLA 120.2 rotor), an experimental step to separate large ribosomal particles from protein-RNA complexes before the IP. At 60,000rpm, half of the FMRP was lost in the pellet. After a 30,000rpm spin however, the vast majority of FMRP was retained in the supernatant (**Figure 4.2A)**. Second, it was necessary to screen for a good FMRP-specific antibody that could IP under stringent conditions. Out of 7G1-1, 2F5, 6B5 and 7B8, only 7G1-1 was able to IP FMRP in 1XPXL buffer which contains 0.5% NP-40, 0.5% Na deoxycholate as well as 0.1% SDS **(Figure 4.2B)**. Furthermore, 7G1-1 antibody showed no cross-reactivity with, (Brown et al., 2001) and did not co-IP, FXR1P or FXR2P in the1XPXL buffer **(Figure 4.3B)**. We further optimized IP efficiency by testing a number of parameters: dynal beads vs. sepharose beads, protein A vs. protein A and G mix, with or without rabbit anti-mouse Fcγ bridging antibody, monoclonal supernatant vs. mouse

ascites, and the amount of 7G1-1 antibody optimal for each IP. 7G1-1 antibody of IgG isotype 2b has a moderately strong affinity for protein A. Rabbit bridging antibody strengthened binding to protein A beads and doubled the bead capacity. We found that 400ul dynal A beads with 120ug rabbit anti-mouse Fcγ antibody and 8ul of 7G1-1 mouse ascites at 5mg/ml gave the optimal FMRP IP **(Figure 4.2C)** where the majority of FMRP was depleted **(Figure 4.3B and 4.4B)**.

We used postnatal day 8 mouse brains for FMRP CLIP since dendritic spine abnormalities in Fmr1 knockout mice have been reported to be the most severe at one week of age and subside by postnatal two to three weeks (Nimchinsky et al., 2001). Non-crosslinked wild type mouse brain and crosslinked Fmr1 knockout brain were processed in parallel as negative controls. Non-crosslinked wild type mouse brain lysate didn't have any radiolabeled RNA signal **(Figure 4.3A)**. Free RNAs, if not covalently crosslinked to a protein, were "filtered" out through various purification steps of the CLIP procedure. In wild type crosslinked samples, RNA signal in complex with FMRP was observed concentrated at molecular sizes greater than the M_r of FMRP **(Figure 4.3A)**. In comparison, the Fmr1 knockout sample had a much reduced RNA signal **(Figure 4.3A)**. We excised the region of FMRP-RNA complex from the protein gel and from comparable regions in Fmr1 knockout and non-crosslinked wild type sample **(Figure 4.3A)**, digested the protein, added the 5'linker, RT-PCR amplified the RNA, and separated the PCR products on a denaturing polyacrylamide gel. We obtained a strong nucleic acid (NA) smear from wild type sample, very little signal from Fmr1 knockout, and none from non-crosslinked sample **(Figure 4.3C)**.

CLIP experiments on Nova have demonstrated that RNA:protein complexes run quite true to size on SDS-PAGE gels. For example, RNA-protein complexes that contain RNAs of ~50-70 nts run ~15-20 kDa larger than the Mr of the protein alone (Ule et al., 2005a). We next explored whether the size of RNAs we obtained corresponded to the predicted migration of RNA-FMRP complexes on the protein gel. We excised a few thin bands corresponding molecular weights of 85, 90, 95, and 115 kDa from both wild type and Fmr1 knockout samples **(Figure 4.4A)**. As in the previous experiment, after RT-PCR amplification, NA signals were present in wild type and very little in FMR-1 knockout sample **(Figure 4.4C)**. As the size of RNA-protein complexes increased from 90 to 95

kDa, NA smears also increased in size **(Figure 4.4C)**. 95 kDa RNA-FMRP complexes would have predicted RNA size of 60 nts (95 kDa minus 75 kDa for FMRP leaves 20,000 Da, which correspond to ~60 nts). Indeed we recovered RNAs of an average of 64 nts (average of 44 nts CLIP tag plus 20 nts of 3' linker). The size of the RT-PCR product contained both linkers. So the PCR products appeared to be about 80mers. Our data suggest RNAs extracted from 95 kDa as well as 90 kDa are RNAs directly crosslinked to FMRP. To our surprise, the 115 kDa FMRP:RNA band generated sharp NA bands instead of the smears present in both wild type and Fmr1 knockout samples. The size of these NAs was unexpectedly small. They appear to be approximately 55-60 nts in length on the gel, corresponding to original RNA tags of 19-24 nts plus linkers totally 36 nts. We pursued this observation and found that commercially available 7G1-1 antibody we used for FMRP CLIP was contaminated by a pan-Argonaute antibody (described in detail in Chapter 5). The sharp NA bands present in both wild type and Fmr1 knockout were in fact microRNAs. Here microRNA CLIP, serving as an elegant control for FMRP CLIP, further confirmed that the NA signal amplified from wild type but not knockout mice, derives from RNAs specifically bound by FMRP, not other RBPs. Otherwise, like microRNAs, RNAs would be amplified from both wild type and Fmr1 knockout samples.

FMRP CLIP was repeated with three biological replicates, all at postnatal day 8. A total of 1698 unique wild type FMRP RNA tags were collected from these three experiments. In order to clone from the faint RNA signal from Fmr1 knockout, we had to amplify 5 more RT-PCR cycles than for wild type. We collected 1106 unique Fmr1 knockout RNA tags, which served as a control for background noise of our CLIP experiment. We used a subtractive method (WT minus KO) to obtain a list of FMRP CLIP targets.

FMRP CLIP tags distribute evenly on mature mRNAs

Out of 1698 wild type CLIP tags, 1013 were in known genes and of these, 66% were exonic hits **(Figure 4.5)**. In contrast, only 27% of 1106 Fmr1 knockout RNA tags were exonic (164 out of 613 tags in known genes). In comparison, we have previously done CLIP on the nuclear splicing factors, Nova and bPTB, which had 24% and 8% of exonic hits respectively.

Out of the FMRP exonic hits, 30 (5%) tags were located in 5'UTRs, 510 (76%) tags in coding sequence, and 128 (19%) in 3'UTRs. The number of FMRP exonic hits was plotted with respect to their positions on mRNAs, which was best fitted for linear regression with r^2=0.99 **(Figure 4.6A)**, indicating FMRP likely binds evenly along the length of mRNA.

Our top FMRP candidate gene based on number of sequenced tags is adenomatosis polyposis coli (APC) had 31 hits, which were also distributed all over the APC mRNA **(Figure 4.6B)**, consistent with our analysis of all FMRP CLIP tags.

CLIP identifies Mtap1b and a few previously identified targets

The UCSC mouse genome browser, mm8 (updated in Feb 2006), was used to annotate all of our CLIP tags. Combining P8 biological replicates for a total 1698 FMRP tags, we generated a list of FMRP candidate genes, having ≥2 RNA tags in the wild type sample **(Table 4.I)**, while under-represented in the Fmr1 knockout sample. This list of FMRP targets was quite reproducible between biological replicates; many of them were identified from more than one CLIP experiment. The adenomatosis polyposis coli (APC) mRNA was our top target as it had a total of 31 hits and was identified in all three CLIP experiments. The previously identified and validated target Mtap1b (Brown et al., 2001; Darnell et al., 2001; Zhang et al., 2001b) was one of our top candidates. In addition, genes like Spnb3 (5 hits by our FMRP CLIP), Rab6ip1 (3 hits), Aatk (2 hits), Lphn1 (1 hit), Bai2 (1 hit), Munc13a (1 hit), Cacna1d (1 hit) and Psd95 (1 hit) on our list overlapped with previous findings (Brown et al., 2001; Chen et al., 2003; Todd et al., 2003). Abundant non-specific sequences, like ribosomal RNA, were seldom hit and did not out-compete the low abundance of true target mRNA sequences.

Total brain CLIP targets overlap well with polyribosome CLIP

One concern with the FMRP CLIP experiment from total mouse brain was the low but present background signal in Fmr1 knockout sample. Our lab has worked out a new and improved approach to solve the background issue by using polyribosome associated FMRP for the CLIP experiment (Darnell, JC personal communication). This method not only removes the nuclei, where many RNA binding proteins are present, but

also takes advantage of sucrose gradient fractionation as an additional step of purification of FMRP:RNA complexes. Furthermore, high throughput sequencing was used to obtain hundreds of thousands of FMRP CLIP tags. Polyribosome FMRP CLIP was performed at multiple developmental ages, using a FMRP-specific polyclonal antibody in addition to the 7G1-1 antibody.

FMRP CLIP targets obtained from total mouse brain at P8 matched extremely well with targets of polyribosome CLIP using both antibodies **(Table 4.I)**. Many of the top listed FMRP targets from total brain CLIP also had a considerable number of hits from polyribosome CLIP **(Table 4.I)**. 21 of top 30 polyribosome targets were present in the total brain CLIP. Fourteen of the top 30 polyribosome targets, Bsn, Adcy1, Kif1a, Kif1b, Mtap1b, Atp2b2, Apc, Ptprs, Kif5a, Fasn, BC067047, Huwe1, Itpr1, and Grin2b were hit ≥2 times in the total brain CLIP. Therefore, we have obtained a reliable set of FMRP targets.

Function categories of FMRP targets

We used GOminer (Gene Ontology) to categorize encoded functions of our top FMRP targets (hits≥2) **(Table 4.II and Figure 4.7)**, an unbiased assessment of strict statistical analysis. Age matched mouse brain total RNA was used as the control set (data from D. Licatalosi, Darnell lab). We found FMRP targets were highly enriched in function categories of cytoskeleton organization, microtubule based processes, synaptic transmission, neurotransmitter secretion, and cell-cell signaling ($p < 0.001$ and false discovery rate < 0.03).

GOminer analysis was further supported by more detailed individual annotation by Pubmed search confirming FMRP targets encode for proteins enriched in coherent functions related to cytoskeleton organization, cytoskeleton-based intracellular movement and microtubule-based movement, and the neuronal synapse **(Table 4.III)**. The category of cytoskeletal organization and movements included FMRP target genes Mtap1b, Kif1a, Kif1b, Kif5a, Kif5c, Dnchc1, Dncic1, Myo5a, Dst, Macf1, Plec1, Spnb2, Spnb3, and Hdh. Interestingly, these genes also belonged to closely related superfamilies, e.g. the kinesin family (microtubule plus end motors), the dynein family (microtubule minus end motors), and myosin (actin based motors). The category of synaptic functions included

Gabbr1 (2 hits), Grin2a (2 hits), Grin2b (2 hits), Psd95 (1 hit), Akap6 (4 hits), Dap-3 (1 hit), Pak1 (1 hit), Pak6 (1 hit), Camk2a (1 hit), Arhgap5 (2 hits), Nlgn2 (2 hits), Nlgn 3 (1 hit), Itsn (2 hits) found at the postsynaptic side of the synapse, and Bsn (3 hits), Pclo (5 hits), Munc13a (1 hit), Syn1 (1 hit), Syn3 (2 hits), Caskin1 (3 hits), Cacna1e (2 hits), Cacna1d (1 hit), Stxbp1 (1 hit), Nrxn1 (1 hit), VAMP2 (1 hit) which are presynaptically localized **(Table 4.III)**. Some of these targets closely interact with one another forming a network **(Figure 4.8)**. Although FMRP is widely thought to play a role in postsynaptic local translation effecting changes in synaptic strength in response to synaptic input , our data suggest FMRP may also have a role in regulating presynaptic functions.

Validation of FMRP CLIP targets

Knowing the set of RNAs that FMRP binds to *in vivo*, we are interested in asking what regulatory roles FMRP has on these targets. The precise physiological function of FMRP has not been defined. The most likely function of FMRP, given the sum of the current literature in the field is in translational regulation perhaps coupled with delivery of mRNAs to neuronal processes and possibly regulated export from the nucleus. A strong piece of evidence is that FMRP is associated with polyribosomes in cell culture and mouse brain, in an RNA dependent manner (Corbin et al., 1997; Feng et al., 1997a; Feng et al., 1997b; Khandjian et al., 1996; Khandjian et al., 2004; Stefani et al., 2004). FMRP has been shown to be a translational inhibitor in rabbit reticulocyte lysate and when over-expressed in cell culture, but these studies used candidate mRNAs which have little overlap with identified FMRP targets (Laggerbauer et al., 2001b; Li et al., 2001; Mazroui et al., 2002; Zhang et al., 2001b). Both systems are also considerably different from endogenous cellular environment. Overexpressed FMRP appears to nonspecifically repress translation. The best *in vivo* evidence for a role in translational control in neurons comes from combined biochemical data and Drosophila genetics. Mutations of futsch/mtap1b or dfxr alone lead to aberrations in architecture of neuronal synapses, but double mutation restores synaptic architecture (Zhang et al., 2001b). Together with the finding that Mtap1b mRNA is co-IPed with FMRP and has increased association with polyribosomes (Brown et al., 2001), these data support a role for FMRP as a translational repressor of mtap1b mRNA.

-Western analysis of target protein levels

In order to asses whether the lack of FMRP could lead to changes in steady state protein levels of FMRP targets, we used Western blots to examine protein levels encoded by FMRP top targets in wild type vs. Fmr1 knockout mouse whole brain at P8, the same developmental age as we performed CLIP experiment. No significant difference was observed. We then repeated the Western analysis at different developmental ages: P8, P14, and P40, and in finer brain regions: cortex, cerebellum, hippocampus, diencephalon, and brain stem. Protein levels of APC, Kif1a, Kif5a, Akap6, Grin2b, Munc13 **(data not shown)** as well as an APC downstream effector, phosphorylated beta-catenin, were examined. But no significant difference in protein levels were found in wild type vs. Fmr1 knockout littermates **(Figure 4.9)**. Kif5a is shown as one example; data are not shown for the rest of the targets.

-Quantitative RT-PCR examination of target mRNA translational profiles

In many cases, FMRP target mRNAs encode for very large proteins; e.g., APC is 313kDa, Kif1a 186kDa, Kif1b 195kDa, Mtap1b 271kDa, Macf1 488kDa, Bsn 434kDa, Pclo 550kDa, Akap6 255kDa, and Dst 592kDa. Aside from Western blot's heavy dependence on good antibodies, there is technical difficulty with electrophoresis and transfer of very large proteins. One alternative is to analyze the translational profile of FMRP targets by examining their mRNA distribution on polyribosome gradients. In many instances mRNAs will be present on polyribosomes when they are being actively translated but shift to monosome/ mRNP fractions if their translation is inhibited at the initiation stage.

Microarray screens of polyribosome-associated mRNAs have previously generated contrasting results. Using transformed human lymphoblastoid cells, 251 mRNAs have shown altered polyribosome distribution in fragile X patients vs. normal controls (Brown et al., 2001). On the other hand, polyribosome associated mRNAs from wild type and Fmr1 knockout mouse cerebral cortex show a remarkable lack of difference (Fraser, CE , PhD thesis). One possibility for these contradictory findings is that FMRP control of translational status of target mRNA is very subtle, such that

pooling polyribosome fractions masks the shift of mRNAs that shift only by one or more fractions rather than from polysomes to the mRNP fractions.

We optimized quantitative RT-PCR to examine mRNA levels in every fraction of the polyribosome gradient and tested the distribution of several FMRP mRNA targets. GAPDH was used as control mRNA that did not show distribution changes between wild type and Fmr1 knockout polyribosome gradients **(Figure 4.10A)**. Our data were consistent with mouse brain polyribosome microarrays in that FMRP target mRNAs showed remarkably similar distribution on polyribosome gradients in wild type vs. FMRP null littermate mouse brains **(Figure 4.10B, C, D, E and F)**, including Mtap1b mRNA **(Figure 4.10C)**.

In Chapter 3 we described the generation and characterization of a novel mouse model for Fragile X Syndrome, the introduction of the I304N KH2 domain mutation by homologous recombination. One of the goals of generating this mouse was to use it as another disease model in which to look at the metabolism of putative FMRP target mRNAs. Therefore we looked at the distribution of mtap1b mRNA in polyribosome gradients derived from the I304N mice compared with wild-type littermates. In this system, as in the Fmr1-null mice, Mtap1b mRNA was unchanged in its distribution on polyribosomes **(Figure 4.11)**.

-Use of Fmr1 and FXR2 double knockout mice

Fmr1 and its autosomal paralogs, FXR1 and FXR2 share the same conserved gene structure suggesting that they are derived from a common ancestral gene (Kirkpatrick et al., 2001). It is possible that the effect of loss of FMRP on its target mRNAs is compensated by the functional redundancy of FXR1P and FXR2P (Spencer et al., 2006). FXR1 and FXR2 knockout mouse models have both been successfully generated (Bontekoe et al., 2002; Mientjes et al., 2004). Because FXR1 knockout mice, which have a striated muscle defect, die shortly after birth due to cardiac or respiratory failure (Mientjes et al., 2004), we were not able to obtain a triple knockout of all three genes. We analyzed wild type vs. Fmr1/FXR2 double knockout mice (Dr. David Nelson provided the FXR2 knockout mice), which have been reported to have an exaggerated behavioral phenotype (Spencer et al., 2006). Western blot analysis was used to detect protein level

changes of APC, Akap6, Kif1a, Kif5a, Grin2b, and Munc13 in cortex, cerebellum and hippocampus at postnatal age of 10 days, but no significant differences were observed in double knockouts (n=5) vs. wild type mice (n=7). A few examples, Kif1a, Kif5a, and Grin2b protein levels in P10 hippocampus are shown **(Figure 4.12)**.

-Preliminary analysis of localized translation in synaptoneurosomes

FMRP has also been proposed to have a role in the transport of translationally dormant mRNA from cytoplasm to synapse and in the regulation of localized translation (Antar et al., 2004; Antar et al., 2005; De Diego Otero et al., 2002; Greenough et al., 2001; Muddashetty et al., 2007). We examined the steady state protein levels of the synaptically localized FMRP targets Akap6, Grin2b, Munc13, and Camk2a, in synaptoneurosome preparations from mouse brain (Shin et al., 2004), however no differences were found in wild type vs. Fmr1 knockout or Fmr1/FXR2 double knockout mice. A few examples of tested targets are shown **(Figure 4.13)**.

Discussion

Since the study of I304N mouse model suggests that a key function of FMRP in mediating normal cognition is sequence-specific RNA binding, the interest in identifying RNA ligands for FMRP is heightened. Despite the fact that many labs have attempted this with various approaches we still lack a reproducible and reliable set of FMRP targets due to intrinsic problems associated with each of these methods. CLIP, a newly developed methodology in our lab has several advantages over previous methods for identifying the in vivo RNA ligands of RBPs. These include crosslinking of RBPs to RNA ligands before cell lysis, and the stringent purification of specific RBPs possible because of the covalent association of RBP to RNA. Optimizing this method for FMRP, we obtained a set of FMRP RNA targets from mouse brain, including Mtap1b. Top targets of the set were reproducible between biological replicates and overlapped well with targets identified by FMRP polysome CLIP, a new and improved approach. Therefore, we have obtained a reliable set of RNA targets bound by FMRP. These RNA targets had coherent biological functions related to cytoskeleton organization and neuronal synapses, which fit well with fragile X biology. Knowing what set of RNAs

FMRP binds to *in vivo*, we were interested in asking what regulatory roles FMRP has on these targets. However, we encountered a hurdle. Despite our various attempts, we have not been able to detect changes in RNA metabolism of these targets. Since the precise functions of FMRP have not been defined, continuing efforts will focus on developing functional assays to eventually validate these targets in animal models.

CLIP tag locations likely indicate FMRP regulates elongation

CLIP not only identifies RNA targets, but the RNA binding sites bound by RBPs. It captures a snapshot of RNA sequences RBPs bind at the time of UV crosslinking. FMRP CLIP tags are distributed over the length of target mRNAs, indicating that FMRP likely binds all over mature mRNAs, without preference for UTRs or coding sequences. FMRP has been previously reported to be a translational inhibitor of its target RNAs (Laggerbauer et al., 2001b; Li et al., 2001; Mazroui et al., 2002; Zhang et al., 2001b) and it has been shown to associate with polyribosomes (Corbin et al., 1997; Feng et al., 1997a; Feng et al., 1997b; Khandjian et al., 1996; Khandjian et al., 2004; Stefani et al., 2004). Therefore, it is not likely that FMRP inhibits translation initiation, or else it would have been found in monomeric 80S ribosome fractions. Also, one would expect most of the CLIP tags to be found in the 5'UTR or near the initiator methionine if FMRP blocked initiation of translation. Indeed, even after puromycin treatment, FMRP cosedimented with the largest remaining polyribosomes containing three to four ribosomes rather than with the much more prominent peak of monomeric ribosomes (Stefani et al., 2004). These findings together with our data suggest that FMRP is more likely to modulate translation at the step of elongation, instead of at the initiation step.

Although FMRP CLIP tags were found to lie all over the length of target mRNAs, this finding does not rule out pockets of high affinity binding sites on mRNAs FMRP prefers. The number of tags we sequenced, even for APC, does not give a high enough sample size for us to discern these high affinity sites. High throughput sequencing is needed. FMRP has been shown to prefer binding to purines over pyrimidines; G-quartet and kissing complex RNAs have been identified as high affinity RNA motifs for FMRP RNA binding domains (Brown et al., 2001; Darnell et al., 2005a; Darnell et al., 2001; Schaeffer et al., 2001). Analysis of high throughput CLIP tag densities on mRNAs can

help to discern FMRP preferred binding sites *in vivo*, which can ultimately resemble identified *in vitro* motifs, as has been shown for the Nova family of RBPs (Ule et al., 2003; Ule et al., 2006; Ule et al., 2005b).

FMRP mRNA targets encode coherent functions--cytoskeletal organization and synaptic transmission

-Understanding APC

APC is our top target with a total of 31 hits. APC is best known as a tumor suppressor. APC forms a complex with AXIN/GSK-3β that phosphorylates β-catenin and leads to its degradation. Deletion of APC allows accumulation of β-catenin/Tcf-4 and activation of downstream growth promoting genes that lead to the development of inherited and sporadic forms of colorectal cancer. APC is also highly expressed in the brain (Brakeman et al., 1999). APC is especially enriched in the tips of neurites (Shi et al., 2004; Votin et al., 2005) and is required for Par3 localization to the axon tip, where Par3/Par6 are required for neuronal polarity (Shi et al., 2004). APC binds microtubules directly and indirectly through EB1, a microtubule plus-end-binding protein (Barth et al., 2002; Su et al., 1995). APC promotes microtubule assembly and bundling *in vitro* (Munemitsu et al., 1994; Zumbrunn et al., 2001) and its association with microtubules in the growth cone is important during axon outgrowth induced by nerve growth factor (NFG) (Zhou et al., 2004). Although initially surprising to us, APC indeed can be a potential target of FMRP. Its role in microtubule assembly and neurite outgrowth fit extremely well with the abnormal neurite morphology seen in fragile X patients as well as mouse and fly models of the disease.

-FMRP targets in the functional category of cytoskeletal organization

FMRP mRNA targets encode proteins with coherent biological functions. They are especially enriched in the categories of cytoskeletal organization and synaptic transmission. In the category of cytoskeleton organization, FMRP targets consist of giant cytoskeletal proteins that crosslink cytoskeletal filaments--spectraplakin family members, e.g. Dst, Macf1, and Plec1, which are able to interact with all three cytoskeletal elements: actins, microtubules, and intermediate filaments or proteins that crosslink cytoskeleton to

membrane receptors--spectrin family, e.g. Spnb2, Spnb3 (Roper et al., 2002). Mutation of *shot*, the only spectraplakin gene in Drosophila, causes defects in axon fasciculation and guidance and dendritic branching in embryonic CNS and PNS (Roper et al., 2002).

FMRP targets also include cytoskeletal motor proteins, which are microtubule plus end directed kinesins, e.g., Kif1a, Kif1b, Kif5a, Kif5c, microtubule minus end directed dyneins, e.g., Dnchc1, Dncic1, and actin based motors, e.g., Myo5a. These motor proteins transport organelles, proteins, or mRNA and tightly control subcellular localization of their cargoes, especially in highly polarized cells, like neurons (Guzik and Goldstein, 2004). Kif1a and Kif1b transport synaptic vesicle precursors containing synaptic vesicle proteins such as synaptotagmin, synaptophysin, Rabphilin3A; Kif5 transport vesicles that contain APPs (amyloid precursor proteins) and vesicles containing APOERs (apoliprotein E receptor 2) to the presynaptic terminals. Kif5 also participates in slow axonal transport of cytoskeletal proteins. In dendrites, AMPA glutamate receptors are transported by the motor Kif5, mediated by adaptor/scaffolding protein, glutamate receptor interacting protein 1 (Grip1) (Hirokawa, 2006; Hirokawa and Takemura, 2005). One proposed function of FMRP has been targeting of translationally dormant mRNAs from cytoplasm to synapses, where they await signaling that would allow local translation (Antar et al., 2005; De Diego Otero et al., 2002; Ferrari et al., 2007; Muddashetty et al., 2007), We speculate that FMRP may affect subcellular localization not only through a direct effect on mRNAs bound by FMRP, but also an indirect effect through its regulation on these cytoskeletal motor proteins.

-FMRP targets form a close network at neuronal synapse

Aside from cytoskeletal organization, FMRP mRNA targets encode proteins present at the neuronal synapse. Receptors in both excitatory and inhibitory synapses, Grin2a, Grin2b and Gabbr1 have been identified as FMRP targets. At the excitatory synapse, Grin (the NMDA receptor) is associated with post-synaptic MAGUK, e.g. PSD95, also a CLIP target, which anchored to the membrane via palmitoylation. Additionally, PSD95 interacts with a number of multi-domain scaffold proteins, e.g. A-kinase anchored proteins (AKAP) and guanylate kinase associated proteins (SAPAP/GKAPs)—Akap6 and Dap-3 that belong to these two families respectively have

been CLIPed as FMRP targets as well. This is one of many examples that FMRP can bind and regulate mRNAs encoding proteins that interact with one another in a functional pathway. AKAP recruits cAMP-dependent protein kinase A (PKA) and calcineurin/protein phosphatase 2B (CN/PP2B) which regulate many phosphorylation-dependent events that influence synaptic plasticity, e.g. actin regulation, membrane receptor anchorage or endocytosis, and etc. On the other hand, SAPAP/GKAPs recruits shank proteins, which possess numerous protein-protein interaction domains, thus linking the post-synaptic scaffold with a variety of signaling molecules. One of the protein families that shank recruits to the excitatory synapse is p21-activated kinase (PAK) and, interestingly, we CLIPed Pak1 and Pak6 as well. A cascade of phosphorylation from PAK to LIMK to cofilin occurs, which inhibits cofilin's actin severing activity and reduces depolymerization of actin filaments (Carlisle and Kennedy, 2005; Schubert and Dotti, 2007). Thus, our finding that FMRP targets encode proteins upstream to the regulation of actin dynamics fits extremely well with dendritic spine biology of the fragile X syndrome.

Moreover, many FMRP RNA targets are pre-synaptic cytomatrix proteins. Bsn, Pclo, Munc13a are specifically localized in the active zone where neurotransmitter-containing vesicles (SVs) dock, fuse, release their content and then recycle. Bsn and Pclo, two very large proteins structurally related and highly specifically localized near the site of neurotransmitter release, are postulated to be members of the ensemble of proteins orchestrating events at the active zone. Munc13a binds the second messenger diacylglycerol (DAG). At increase concentration of DAG, Munc13 regulates the fusion of SVs with plasma membrane. Munc13a binds SV-associated protein Doc2 and induces the open conformation of syntaxin in the plasma membrane, thereby promoting the formation of a loose SNARE complex for neurotransmitter release (Dresbach et al., 2001; Schoch and Gundelfinger, 2006). Interestingly, syntaxin binding protein 1 (stxbp1 or munc18) has also been CLIPed as a FMRP target. This is another example that FMRP targets encode proteins that interact with one another. Yet another example is that presynaptic Caskin1, Nrxn1, Cacna1e, Cacna1d, postsynaptic Nlgn, and PSD95, which form a close network, have all been CLIPed as FMRP targets. CASK and MaGuK (membrane associated guanylate kinase) family members in complex with Veli/Mint1 at

the presynapse interact with presynaptic voltage caged Ca^{2+} channels and adhesion molecule Nrxn. Nrxn binds postsynaptic adhesion molecule Nlgn, which in turn is linked to the postsynaptic MAGUK, PSD95 (Dresbach et al., 2001; Schoch and Gundelfinger, 2006). Therefore, we find this theme that FMRP targets encode proteins forming an interacting network at the synapse.

Presynaptic FMRP targets were initially surprising to us, since majority of findings on fragile X biology focus on dendritic, postsynaptic abnormalities. Recently FMRP has been shown to localize in developing axons of cultured hippocampal neurons and growth cones had more filopodia and were less dynamic in Fmr1 null neurons (Antar et al., 2006). Therefore, FMRP may have a broader role than we thought, having both dendritic and axonal functions that converge at the developing synapse.

In conclusion, FMRP targets encoding coherent functions in cytoskeletal organization and synaptic transmission fit extremely well with fragile X biology. Misregulation of cytoskeletal proteins, cytoskeletal motor proteins, pre- or post-synaptic proteins due to lack of FMRP can lead to distorted synaptic architecture and signaling, causing dendritic spine phenotype (Comery et al., 1997; Nimchinsky et al., 2001) and altered synaptic plasticity (Bear et al., 2004; Hou et al., 2006; Huber et al., 2002; Koekkoek et al., 2005; Nosyreva and Huber, 2006) observed in fragile X patients and mouse models.

Future Directions for validation of FMRP RNA targets

Knowing what set of RNAs FMRP binds to *in vivo*, we are interested in asking what regulatory roles FMRP has on these targets. However, we have encountered a hurdle. The precise physiological function of FMRP has not been defined. The most plausible function of FMRP known to us so far is translational regulation. And the best piece of evidence is that FMRP is associated with polyribosomes in cell culture and mouse brain (Corbin et al., 1997; Feng et al., 1997a; Feng et al., 1997b; Khandjian et al., 1996; Khandjian et al., 2004; Stefani et al., 2004). Validation for even the best-understood target, Mtap1b, is not trivial. Biochemically we cannot reproduce the change of Mtap1b mRNA levels in polyribosomes (Brown et al., 2001), using different fragile X

mouse models. Changes in protein levels has been shown to be very subtle (Li et al., 2001).

Our validation assays have focused on assessing the translational status of FMRP mRNA targets. The encoded protein levels are measured by Western blot and their translational profiles over polyribosome gradients are assessed by quantitative RT-PCR. We have attempted to validate these targets not only in wild type mice vs. Fmr1 knockout mice, but also in Fmr1/FXR2 double knockout mice, considering the functional redundancy of Fmr1 paralogs. However, we have not succeeded in detecting changes in steady state protein levels, or steady state distribution of transcripts on polyribosome gradients thus far. Continuing efforts will focus on developing new functional assays to eventually validate these targets in animal models.

-Resolve Redundancy from autosomal paralogs

Although we are trying to overcome the functional redundancy of Fmr1 paralogs by using Fmr1/FXR2 double knockout mice, the remaining FXR1P may still be able to compensate for the loss of FMRP and FXR2P to a great extent, therefore, still significantly attenuating the effect of lack of FMRP on its targets.

FXR1 mice die immediately after birth likely due to respiratory or cardiac failure to due to their striated muscle defect (Mientjes et al., 2004). One way to overcome this is to generate a conditional FXR1 knockout mouse model, so that Fmr1/FXR1/FXR2 triple knockout mice can be obtained and used for validation. A more immediate solution is to use siRNA pools to knockdown the expression of FMRP, FXR1P, and FXR2P in cell lines or primary neurons, but the drawback is that tissue culture cannot mimic true *in vivo* synapses or cell-cell signaling in brain. Another solution is to use Drosophila for validation. A single homologue, dFXR, exists for all three mammalian FMRP family members. Similar to Fmr1 knockout mice in many ways, dfxr mutant flies exhibit increased synaptic growth and branching at the neuromuscular junction, impaired coordinated behavior, arrhythmic circadian activity, and reduced courtship (Inoue et al., 2002; Ishizuka et al., 2002; Morales et al., 2002; Zhang et al., 2001b). Significantly, the futsch/Mtap1b mRNA and dFXR protein interaction was validated using Drosophila genetics (Zhang et al., 2001b).

-More approaches to assess mRNA trafficking and localized translation

Preliminary analysis of role of FMRP in trafficking and localized translation of its mRNA targets has been done by examining protein levels in synaptoneurosome preparation. No difference so far has been observed for a few synaptically localized targets in wild type vs. Fmr1 knockout or Fmr1/FXR2 double knockout mice. Our synaptoneurosome protocol is enriching for resealed pre- and post-synaptic vesicles; however, it is far from pure. Currently available synaptoneurosome protocols suffer from either impurity or low yields. Our lab has been generating BAC transgenic mice expressing EGFP tagged Gabbr2, which is present in both excitatory and inhibitory synapses. These mice can be a very useful tool toward getting purer synaptoneurosomes by IP of tagged EGFP and can facilitate better validation of FMRP targets.

FISH to assess mRNA trafficking and immunofluorescence to examine localized protein levels on either primary neuron culture or brain slices are also plausible approaches to validate FMRP targets.

Our lab has also worked out a protocol for laser capture microdissection of dendrites in layer I in cortex, and molecular layers in cerebellum, from their cell bodies. This technology could be applied to wild type vs. Fmr1 knockout or Fmr1/FXR2 double knockout mice. If FMRP were to regulate trafficking of mRNA to dendrites, we might be able to observe a difference in mRNA levels in layer I or molecular layer between wild type vs. knockout or double knockout mice. Instead of target-by-target approach, microarray analysis of RNA present in these compartments can give us a more comprehensive list that we can use to overlap with our CLIP target list. Some of the mRNA changes, if any, could be from direct effect of FMRP on its target RNA while others could be an indirect effect.

-FMRP functions could be activity dependent

Last but not least, activity-dependent changes in the functional interaction between FMRP and the translational apparatus have been proposed by a number of groups (Greenough et al., 2001; Hou et al., 2006; Huber et al., 2002; Muddashetty et al., 2007; Weiler et al., 1997). Group I mGluR-dependent LTD is increased in hippocampal and cerebellum slices of Fmr1 knockout mice and is no longer protein synthesis

dependent (Huber et al., 2002; Koekkoek et al., 2005; Nosyreva and Huber, 2006). It is likely that we need to incorporate activity into our various validation assays in order to see an enhanced or transient effect of FMRP on its targets. Primary neuron cultures can be treated with KCl or DHPG and brain slices can either be treated with DHPG or stimulated with paired pulses before we perform our validation assays. Furthermore, our lab has previously explored seizures induced in mice by MECS or pilocarpine treatment. Preliminary data has shown that seizures altered mRNA localization in dendrites and alternative splicing pattern of certain genes (O'Donovan, K, Wickiser, JK and Wang, H). Furthermore, Fmr1 knockout mice were reported to be susceptible to audiogenic epileptic seizures (Chen and Toth, 2001; Musumeci et al., 2000). Therefore, treatment of MECS or pilocarpine can possibly help our validation assays by enhancing FMRP effects. If so, it allows us to test our FMRP targets in mouse brain, the most physiologically relevant system.

-An open mind for FMRP functions

FMRP may be a multi-functional protein, contributing to different steps of gene expression. So far, a few functional roles have already been proposed, e.g., translational regulation, including localized or via microRNAs, transport of mRNA, and mRNA turnover. Anecdotally, we have observed FMRP targets to encode extremely large proteins. Just to name a few of them; APC is 313kDa, Kif1a 186kDa, Kif1b 195kDa, Mtap1b 271kDa, Macf1 488kDa, Bsn 434kDa, Pclo 550kDa, Akap6 255kDa, and Dst 592kDa. FMRP may function as a molecular chaperone, facilitate the folding of these large proteins co-translationally. Moreover, FMRP, although largely cytoplasmic, does have a NES and NLS signal. We thus far have focused on FMRP exonic CLIP tags, but analysis of intronic CLIP tags enriched in wild type over Fmr1 knockout may cast light on a nuclear role for FMRP.

Gene Symbols

Aatk	Apoptosis-associated tyrosine kinase
Akap6	A kinase anchor protein
Apc	Adenomatosis polyposis coli
Arf3	ADP-ribosylation factor 3
Arhgap5	Rho GTPase activating protein 5
Bai2	Brain-specific angiogenesis inhibitor 2
Bsn	Bassoon
Cacna1d	Calcium channel, voltage-dependent, L type, alpha 1D subunit
Cacna1e	Calcium channel, voltage-dependent, R type, alpha 1E subunit
Camk2a	Calcium/calmodulin-dependent protein kinase II alpha
Dap-3	Disks large associated protein 3
Dnchc1	Dynein, cytoplasmic, heavy chain 1
Dncic1	Dynein, cytoplasmic, intermediate chain 1
Dst	Dystonin
Gabbr1	Gamma-aminobutyric acid receptor 1
Grin2a	Glutamate receptor, ionotropic, NMDA2A (epsilon 1)
Grin2b	Glutamate receptor, ionotropic, NMDA2B (epsilon 2)
Grip1	Glutamate receptor interacting protein 1
Hdh	Huntington disease gene homolog
Itsn	Intersectin
Kif1a	Kinesin family member 1A
Kif1b	Kinesin family member 1B
Kif5a	Kinesin family member 5A
Kif5c	Kinesin family member 5C
Lphn1	Latrophilin 1
Macf1	Microtubule-actin crosslinking factor 1
Mtap1b	Microtubule-associated protein 1 B
Munc13a	Mammalian homolog of Unc-13 A (C. elegans)
Myo5a	Myosin Va
Nlgn2	Neuroligin 2

Nlgn3	Neuroligin 3
Nrxn1	Neurexin 1
Pak1	p-21 activated kinase 1
Pak6	p-21 activated kinase 6
Pclo	Piccolo
Plec1	Plectin 1
Psd95	Discs large homolog 4 (Drosophila)
Spnb2	Spectrin beta 2
Spnb3	Spectrin beta 3
Stxbp1	Syntaxin binding protein 1
Syn1	Synapsin 1
Syn3	Synapsin 3
Vamp2	Vesicle-associated membrane protein 2

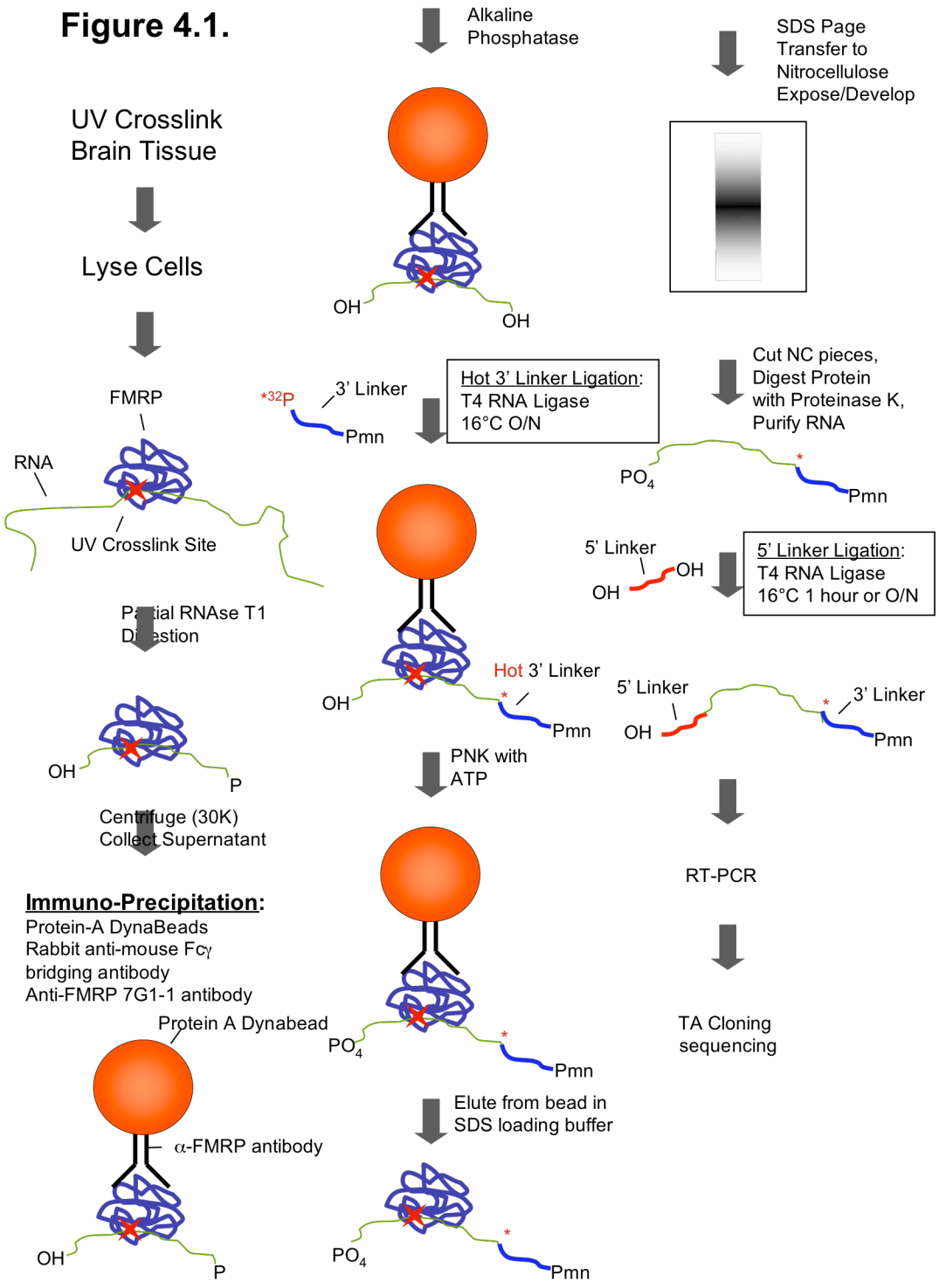

Figure 4.1. A schematic illustration of FMRP CLIP method. The diagram represents the FMRP CLIP method adapted from (Ule et al., 2005a), described in detail in Chapter 2 Materials and Methods.

Figure 4.2.

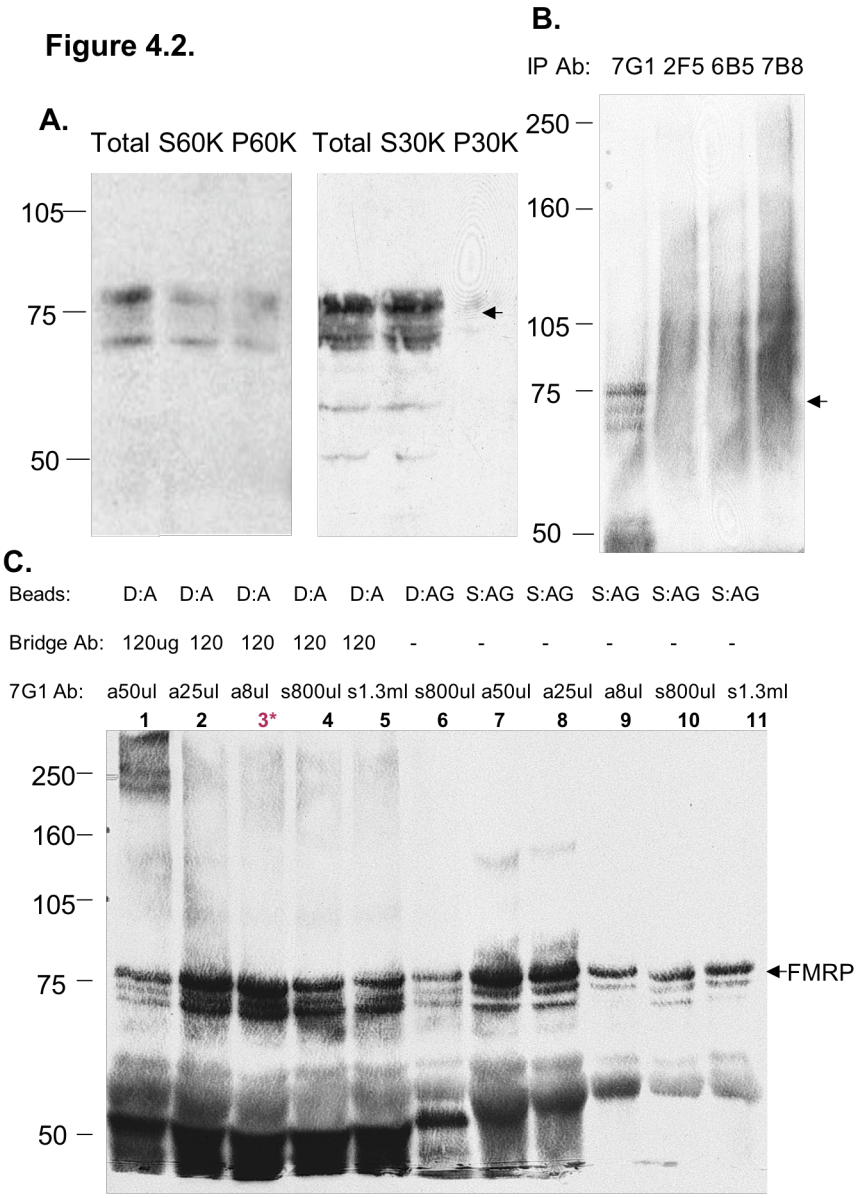

Figure 4.2. Optimization of FMRP IP condition. (A) Western analysis of FMRP (1C3 antibody) in mouse brain lysates before and after ultracentrifugation at 60,000rpm vs. 30,000rpm spin (TLA 120.2 rotor), supernatant (S60K, S30K) vs. pellet (P60K, P30K). At 60,000rpm, half of FMRP was lost to the pellet. At 30,000rpm, the majority of FMRP was retained in the supernatant; and became the input to IP. **(B)** Testing various FMRP specific antibodies for IP. Only 7G1-1 antibody was able to IP FMRP in 1XPXL buffer. **(C)** Testing various IP parameters: dynal (D) vs. sepharose (S) beads, protein A (A) vs. protein A and G mix (AG), with or without rabbit anti-mouse Fcγ bridging antibody, 7G1-1 ascites fluid (a) vs. monoclonal supernatant (s) and titration of 7G1-1 antibody. Condition 3* (dynal protein A beads, 120ug bridging antibody, 8ul 5mg/ml 7G1-1 mouse ascites) gave the best IP efficiency.

Figure 4.3.

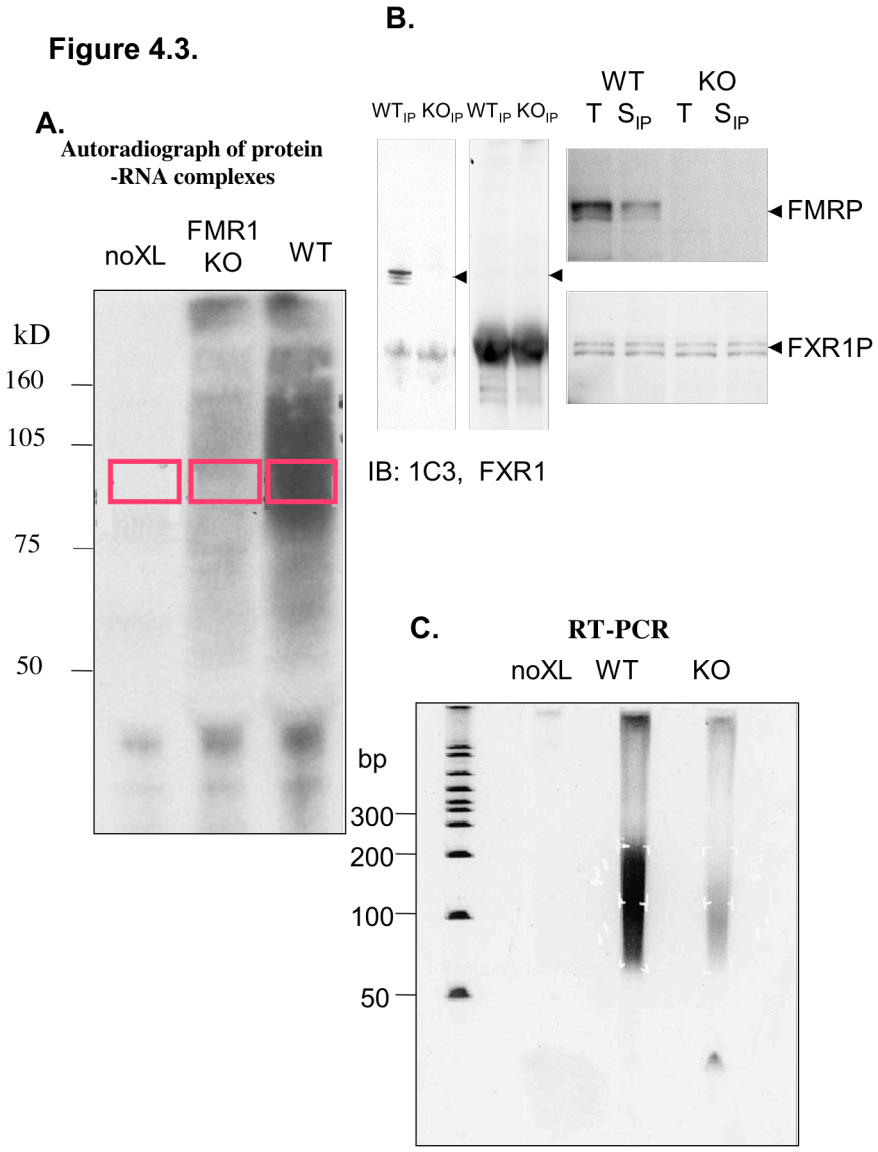

Figure 4.3. FMRP CLIP. (A) Postnatal day 8 mouse brains were UV irradiated, protein:RNA complexes IPed with FMRP specific 7G1-1 monoclonal antibody, RNA ligated with ^{32}P labeled 3' linker, and complexes separated by SDS-PAGE, transferred to nitrocellulose, and visualized by autoradiography. Either wild type (WT), Fmr1 knockout (KO), or non-crosslinked wild type (noXL) brain lysates were used. CLIP performed using wild type brain revealed radiolabeled signal from RNA-FMRP complexes at molecular sizes greater than M_r of FMRP. RNA signal was much fainter from Fmr1 knockout sample and absent from non-crosslinked sample. **(B)** 7G1-1 IP under our optimized condition was able to clear majority of FMRP while it did not IP or co-IP FXR1P. **(C)** RNA-FMRP complexes were cut out from areas of the membrane boxed in red from wild type sample. Proteins were digested. RNAs were RT-PCR amplified and separated on a polyacrylamide gel. Bands from Fmr1 knockout and non-crosslinked samples were processed in parallel but gave little signal.

Figure 4.4.

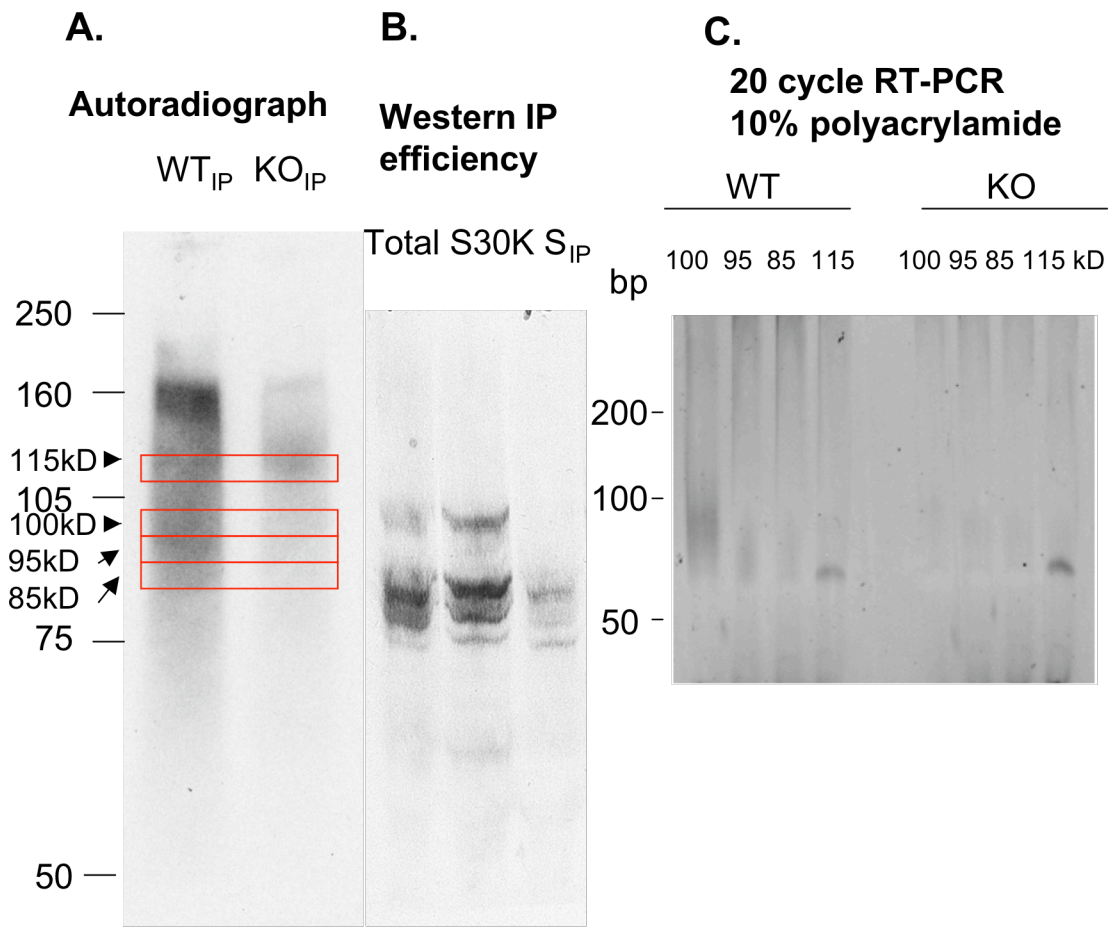

Figure 4.4. FMRP-RNA complexes migrate according to the sizes of the crosslinked RNA tags. (A) P8 mouse brain FMRP CLIP autoradiograph. Bands corresponding to different molecular weights of protein-RNA complexes were cut out from the membrane. Excised areas are designated by a red box. **(B)** Optimized 7G1-1 IP condition depleted the majority of FMRP. "Total" reflects the input to the IP, "S30K" is the supernatant after a 30K spin and "S-IP" is the supernatant after IP. **(C)** RNAs were RT-PCR amplified and separated by denaturing PAGE. Significantly the peak of RT-PCR product from the bands excised from the gel in 4.4A increase in size with increasing Mr, as would be expected for RNAs of increasing size crosslinked to a protein of constant size. Little RT-PCR product is seen in the KO for the 85kDa, 95kDa and 115 kDa bands. The sharp band of approximately 60 nts is seen in both WT and KO mice.

Figure 4.5.

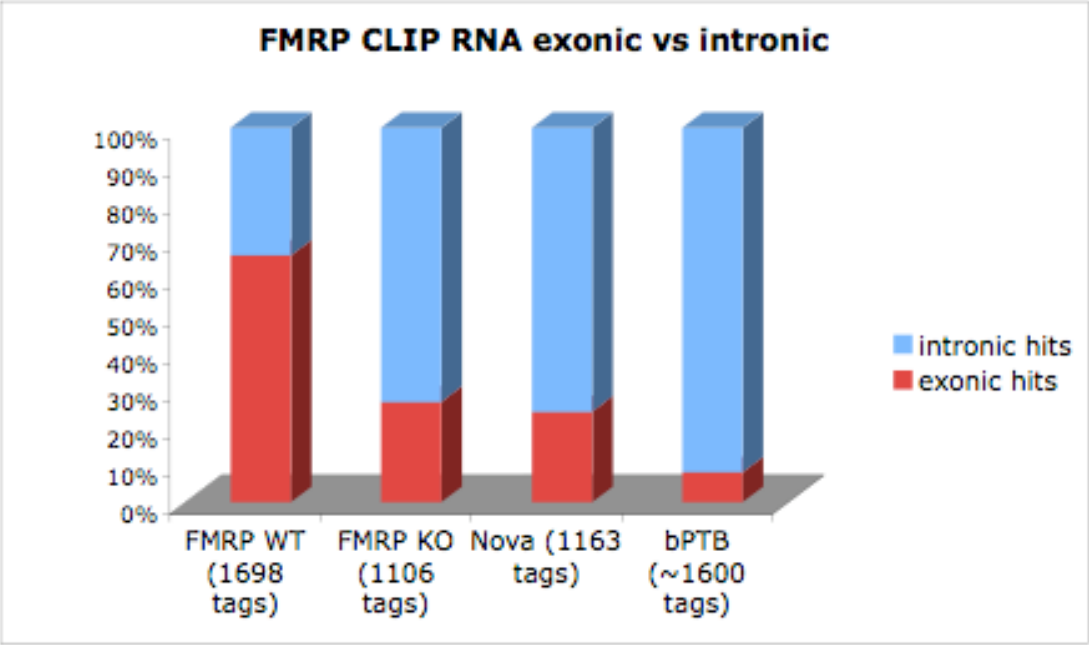

Figure 4.5. The majority of FMRP CLIP tags are exonic. Out of 1698 unique FMRP CLIP tags from the wild type sample, 66% were exonic hits, in comparison to only 27% of exonic hits in Fmr1 knockout sample, which served as the background of our CLIP experiment. Nuclear splicing factors, Nova and bPTB had 24% and 8% of exonic hits respectively.

Figure 4.6.

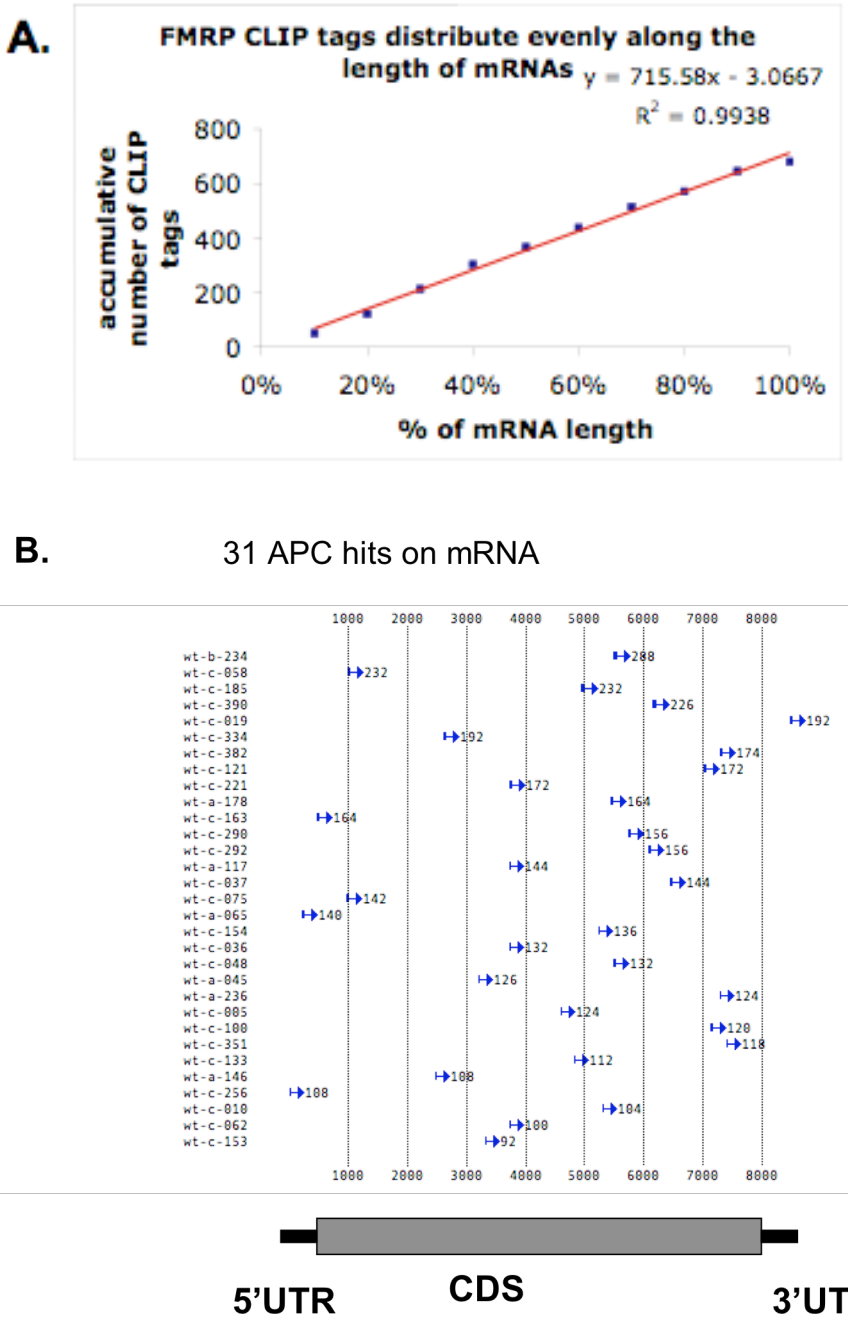

Figure 4.6. FMRP CLIP tags distribute evenly along the length of mRNA. **(A)** Number of cumulative FMRP tags were plotted against mRNA length. The distribution was best fit for a linear regression with r^2=0.99. **(B)** Plot of 31 tags on adenomatosis polyposis coli (APC) mRNA, the top hit among our FMRP targets.

Table 4.I. List of FMRP top mRNA targets from three independent CLIP experiments (hits≥2), from P8 mouse brain. Genes are ranked according to their enrichment in WT compared to KO (net WT exonic hits=WT-exonic hits minus KO-exonic hits). Previously validated target in Drosophila, Mtap1b (Zhang et al., 2001b), was one of our top targets. Rab6ip1, Spnb3, and Aatk on this list also overlapped with previously identified FMRP targets (Brown et al., 2001). The last column "polysome CLIP hits" tallies the results of one experiment on p25 mice using high-throughput sequencing to identify RNA ligands crosslinked to FMRP on polysomes in brain. Total brain FMRP targets overlapped well with polysome FMRP targets.

GeneSymbol	GeneName	Net-WT Exon	WT-Exon	WT-Intron	KO-exon	KO-intron	Polysome CLIP hits
APC	adnomatous polyposis coli	30	31	1	1	0	60
Kif1a	kinesin family member 1A	10	10	3	0	0	84
Mtap1b	microtubule-associated protein 1 B	8	10	0	2	0	78
macf1	microtubule-actin crosslinking factor 1	6	7	1	1	0	7
Adcy1	adenylate cyclase 1	5	5	0	0	0	101
Pclo	piccolo	5	5	0	0	0	26
Spnb3	spectrin beta 3	5	5	0	0	0	24
Kif1b	kinesin family member 1B	4	4	0	0	0	61
Kif5a	kinesin family member 5A	4	4	0	0	0	54
Nlgn2	neuroligin 2	4	4	0	0	0	28
Hivep2	human immunodeficiency virus type I enhancer binding protein 2	4	4	1	0	2	24
Akap6	A kinase (PRKA) anchor protein 6	4	4	0	0	0	24
Kif5c	kinesin family member 5C	4	4	0	0	0	17
Bsn	bassoon	3	3	0	0	0	110
Fasn	fatty acid synthase	3	3	0	0	0	46
Itpr1	inositol 1,4,5-triphosphate receptor 1	3	3	1	0	1	39
Huwe1	HECT, UBA and WWE domain containing 1	3	3	0	0	1	33
Rab6ip1	Rab6 interacting protein 1	3	3	0	0	0	32
Hdh	Huntington disease gene homolog	3	3	0	0	0	31
Phr1	PAM, HIGHWIRE, RPM 1	3	3	1	0	1	23
Dst	dystonin	3	3	0	0	0	17
Caskin1	CASK interacting protein 1	3	3	0	0	0	15
1110007H17Rik		3	3	0	0	0	7
Igfbp5	insulin-like growth factor binding protein 5	3	3	0	0	0	1
Atp2b2	ATPase, Ca++ transporting, plasma membrane 2	2	2	0	0	0	65
Ptprs	protein tyrosine phosphatase, receptor type, S	2	2	1	0	0	52
2610507B11Rik		2	2	0	0	0	39
BC067047		2	2	0	0	0	33
Aatk	apoptosis-associated tyrosine kinase	2	2	0	0	0	33
Eef2	eukaryotic translation elongation factor 2	2	2	0	0	0	33
Grin2b	glutamate receptor, ionotropic, NMDA2B (epsilon 2)	2	2	1	0	0	32
Abr	active BCR-related gene	2	2	0	0	0	29
Grin2a	glutamate receptor, ionotropic, NMDA2A (epsilon 1)	2	2	0	0	0	26
Myo5a	myosin Va	2	2	1	0	0	24
Ptprt	protein tyrosine phosphatase, receptor type, T	2	2	1	0	0	19
2900052E22Rik		2	2	0	0	0	19

GeneSymbol	GeneName	Net-WT Exon	WT-Exon	WT-Intron	KO-exon	KO-intron	Polysome CLIP hits
AA536749		2	2	1	0	0	17
Disp2	dispatched homolog 2 (Drosophila)	2	2	0	0	0	16
Dbccr1	deleted in bladder cancer chromosome region candidate 1 (human)	2	2	0	0	0	15
Slc22a12	solute carrier family 22 (organic anion/cation transporter), member 12	2	2	0	0	0	15
Cacna1e	calcium channel, voltage-dependent, R type, alpha 1E subunit	2	2	0	0	0	14
Odz3	odd Oz/ten-m homolog 3 (Drosophila)	2	2	0	0	0	14
2310014B11Rik		2	2	0	0	0	13
Dnchc1	dynein, cytoplasmic, heavy chain 1	2	2	0	0	0	12
4930544G21Rik		2	2	0	0	0	12
4733401O11Rik		2	2	0	0	0	12
Ankrd12	ankyrin repeat domain 12-like	2	2	0	0	0	12
Trrap	transformation/transcription domain associated protein	2	2	0	0	0	11
Gprin1	G protein-regulated inducer of neurite outgrowth 1	2	2	0	0	0	10
A830007M12		2	2	0	0	0	10
Gabbr1	GAMMA-AMINOBUTYRIC ACID (GABA-B) RECEPTOR, 1	2	2	0	0	0	9
Slc4a3	solute carrier family 4 (anion exchange), member 3	2	2	0	0	0	9
D330037A14Rik		2	2	0	0	0	8
Itsn	intersectin (SH3 domain protein 1A)	2	2	0	0	0	7
Scd2	stearoyl-Coenzyme A desaturase 2	2	2	0	0	0	7
9030205A07		2	2	0	0	0	7
0710001E19Rik		2	2	0	0	0	7
D630003G22Rik		2	2	1	0	0	6
2500002E12Rik		2	2	0	0	0	6
Arf3	ADP-ribosylation factor 3	2	2	0	0	0	5
Sez6l	seizure related 6 homolog like	2	2	0	0	0	5
Arhgap5	Rho GTPase activating protein 5	2	2	0	0	0	4
Birc6	baculoviral IAP repeat-containing 6	2	2	0	0	0	4
Nr3c1	nuclear receptor subfamily 3, group C, member 1	2	2	0	0	0	3
4932408F19		2	2	0	0	0	3
1110037D04Rik		2	2	0	0	0	3
Ids	iduronate 2-sulfatase	2	2	0	0	0	2
Ankfy1	ankyrin repeat and FYVE domain containing 1	2	2	0	0	0	1
Clcn4-2	chloride channel 4-2	2	2	0	0	0	1
Syn3	synapsin III	2	2	0	0	0	-
TPRD	tetratricopeptide repeat domain 3	2	2	0	0	0	-
Unc5c	UNC-5 homolog C	2	2	0	0	0	-
2410089E03Rik		2	2	0	0	0	-

Table 4.II. GoMiner analysis of molecular functions of FMRP target genes with hits ≥2. The top 73 FMRP target genes were analyzed by the GoMiner program, using total brain RNAs as a control set. For each gene ontology, the total number of genes in control set and FMRP targets were shown. p values represented the significance of enrichment of genes within gene ontologies of FMRP targets relative to the control group. p values lower than 0.001, which represented the most significant enrichment, were marked in red.

GO categories	total genes (out of 8169 brain RNA)	FMRP CLIP target genes (hit>1)	enrichment	p value
cytoskeleton dependent intracellular transport	82	8	13.9	8.0E-08
cytoskeleton organization and biogenesis	445	15	4.8	2.1E-07
microtubule based movement	70	7	14.2	4.7E-07
transmission of nerve impulses	328	12	5.2	1.9E-06
microtubule based processes	170	9	7.5	2.2E-06
synaptic transmission	291	10	4.9	2.7E-05
neurotransmitter secretion	526	13	3.5	4.7E-05
cell-cell signaling	495	12	3.4	1.2E-04
neurotransmitter secretion	79	5	9.0	2.1E-04
regulated secretory pathway	82	5	8.7	2.5E-04
organelle organization and biogenesis	1008	17	2.4	3.2E-04
regulation of neurotransmitter levels	109	5	6.5	9.4E-04
cellular metabolism	4472	22	0.7	1.0E+00
cellular biogenesis	934	5	0.8	8.0E-01
transcription	1305	7	0.8	8.4E-01
DNA repair	185	1	0.8	7.3E-01
signal transduction	1954	22	1.6	8.6E-03
cell cycle	721	6	1.2	4.0E-01
cell death	589	6	1.4	2.3E-01

Figure 4.7.

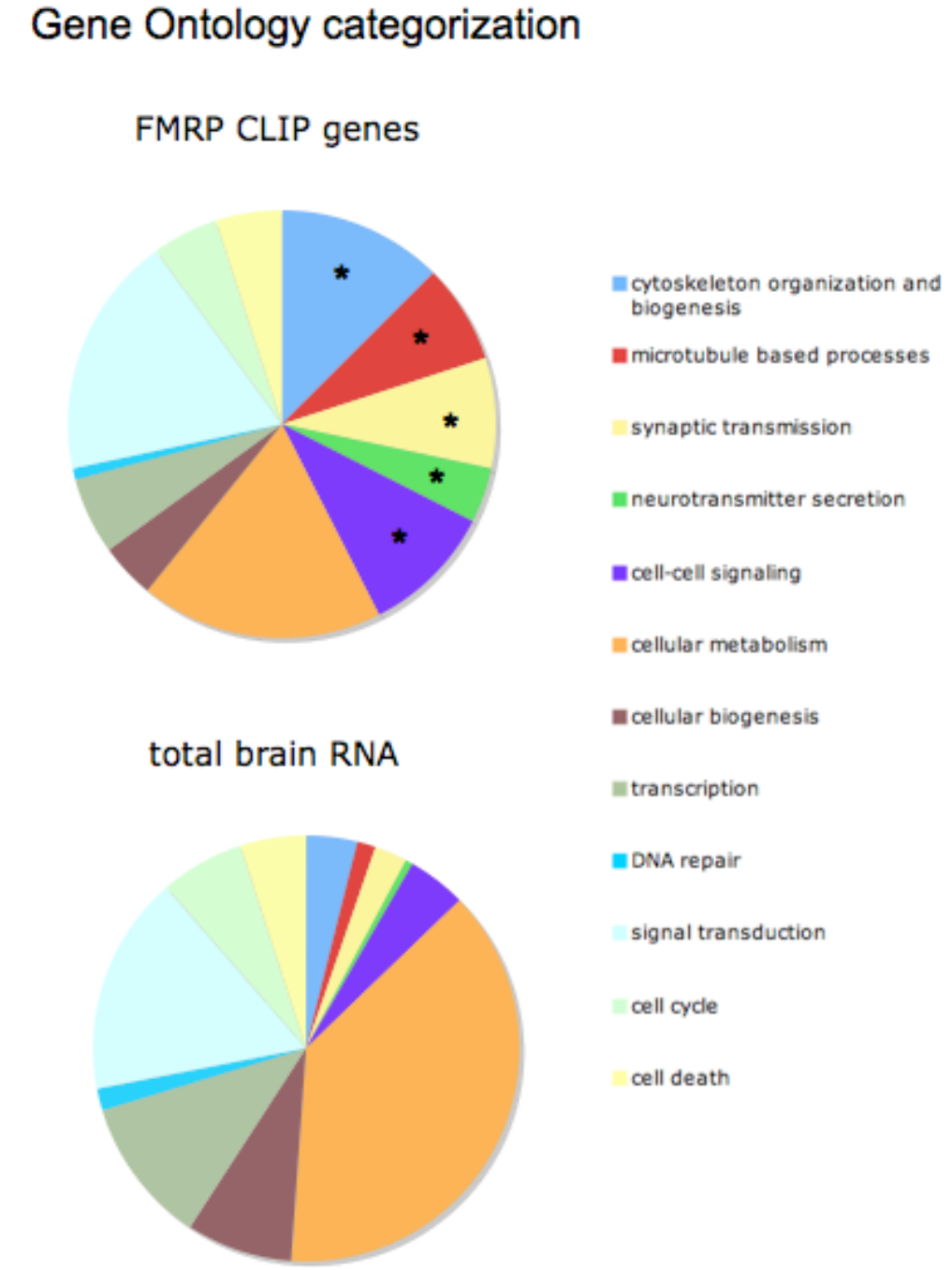

Figure 4.7. FMRP target genes encoding coherent functions. Relative representation of selected molecular functions (as defined by GoMiner) for the total set of genes in mouse brain and 73 FMRP CLIP targets (hits ≥2), illustrating coherent functions of FMRP bound mRNA targets (* indicates $p<0.001$).

Table 4.III. List of representative FMRP targets in their function categories. Grouping of FMRP CLIP targets was determined by GoMiner and published literature. Genes listed in bold had hits ≥2.

Cytoskeleton organization	**Mtap1b**; microtubule + end motor : **Kif1a, Kif1b, Kif5a, Kif5c**; microtubule - end motor: **Dnchc1**, Dncic1; actin motor: **Myo5a**; spectraplakin family: **Dst, Macf1**, Plec1; spectrin family: Spnb2, **Spnb3**; **Hdh**
Post-synaptic function	**Gabbr1**, **Grin2a, Grin2b,** Psd-95, **Akap6,** Dap-3, Pak1, Pak6, Camk2a, **Arhgap5, Nlgn2**, Nlgn3, **Itsn**,
Pre-synaptic function	**Bsn, Pclo**, Munc13a, Stxbp1, Vamp2, **Caskin1**, Nrxn1, **Cacna1e**, Cacna1d, Syn1, **Syn3**

Figure 4.8.

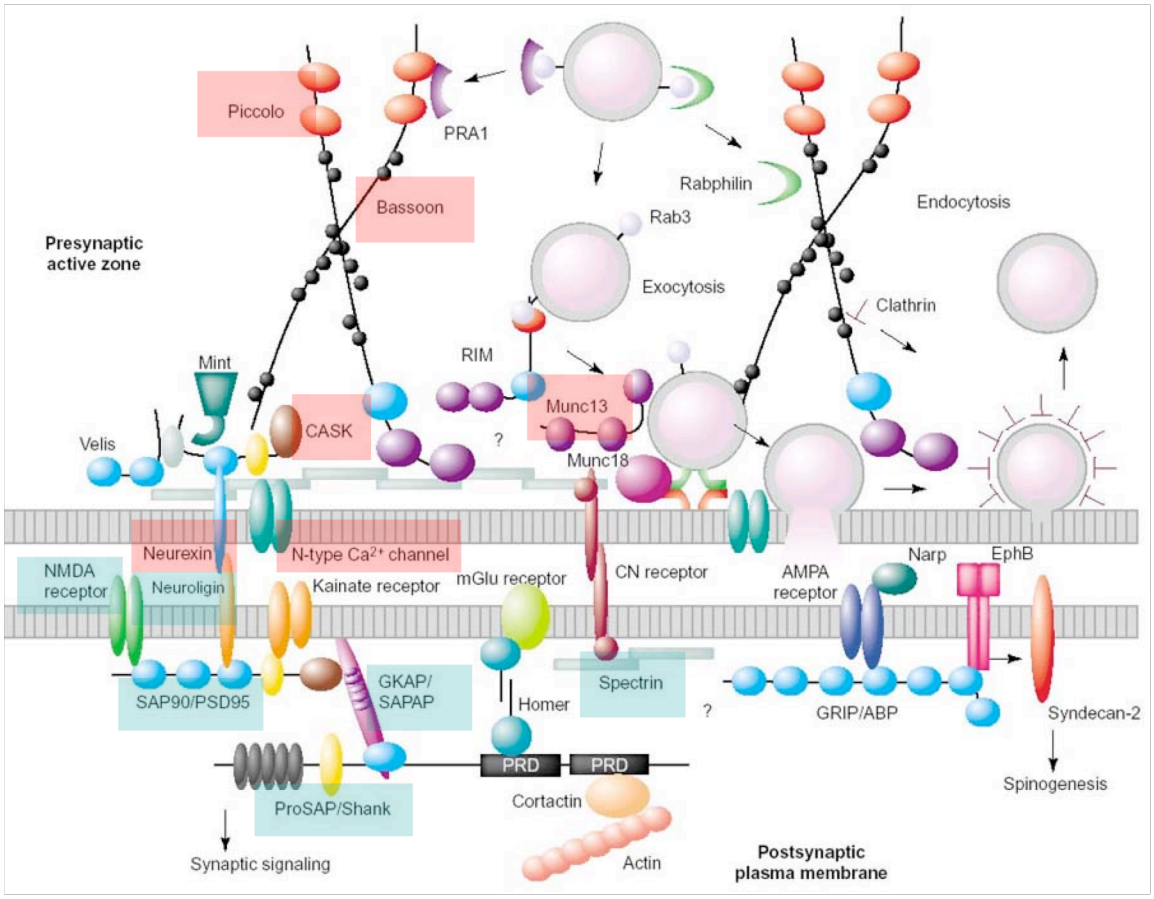

Figure 4.8. FMRP targets encode proteins that interact with one another forming a network at the synapse. Shaded genes were FMRP CLIP targets, pink color for targets expressed at presynapse while blue color for postsynaptically expressed targets.

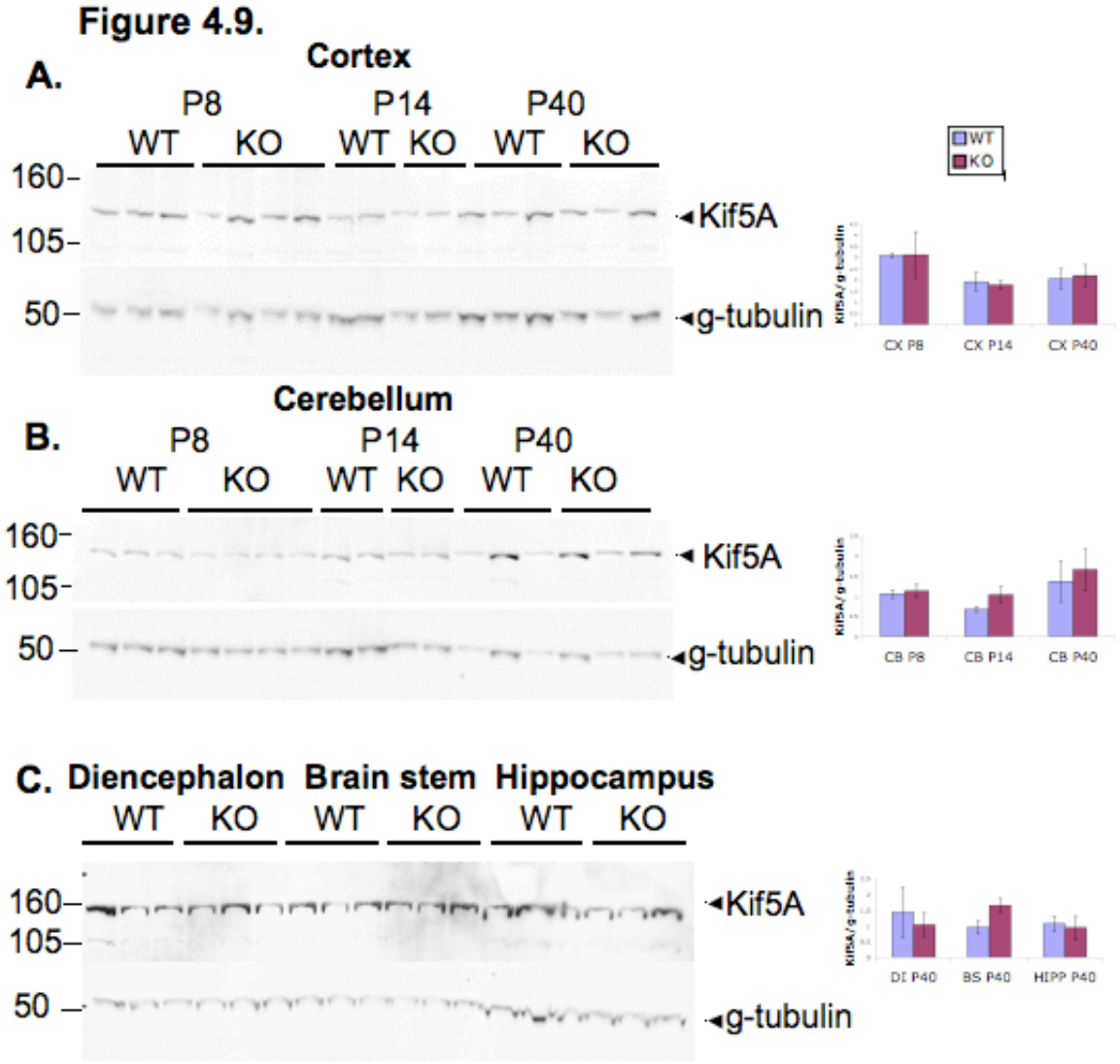

Figure 4.9. Kif5A protein levels showed no significant difference in wild type vs. Fmr1 knockout mouse brains. Western blot and quantification of **(A)** P8, P14, and P40 cortex, **(B)** P8, P14, and P40 cerebellum, **(C)** P40 diencephalon, brain stem, hippocampus. Chemiluminescence was quantified using Versa Doc imaging, Kif1A signal was normalized to loading control γ-tubulin. The same Western analysis was applied to APC, Kif5a, Akap6, Grin2b, and Munc13 and no significant difference in their protein levels was observed (data not shown).

Figure 4.10.

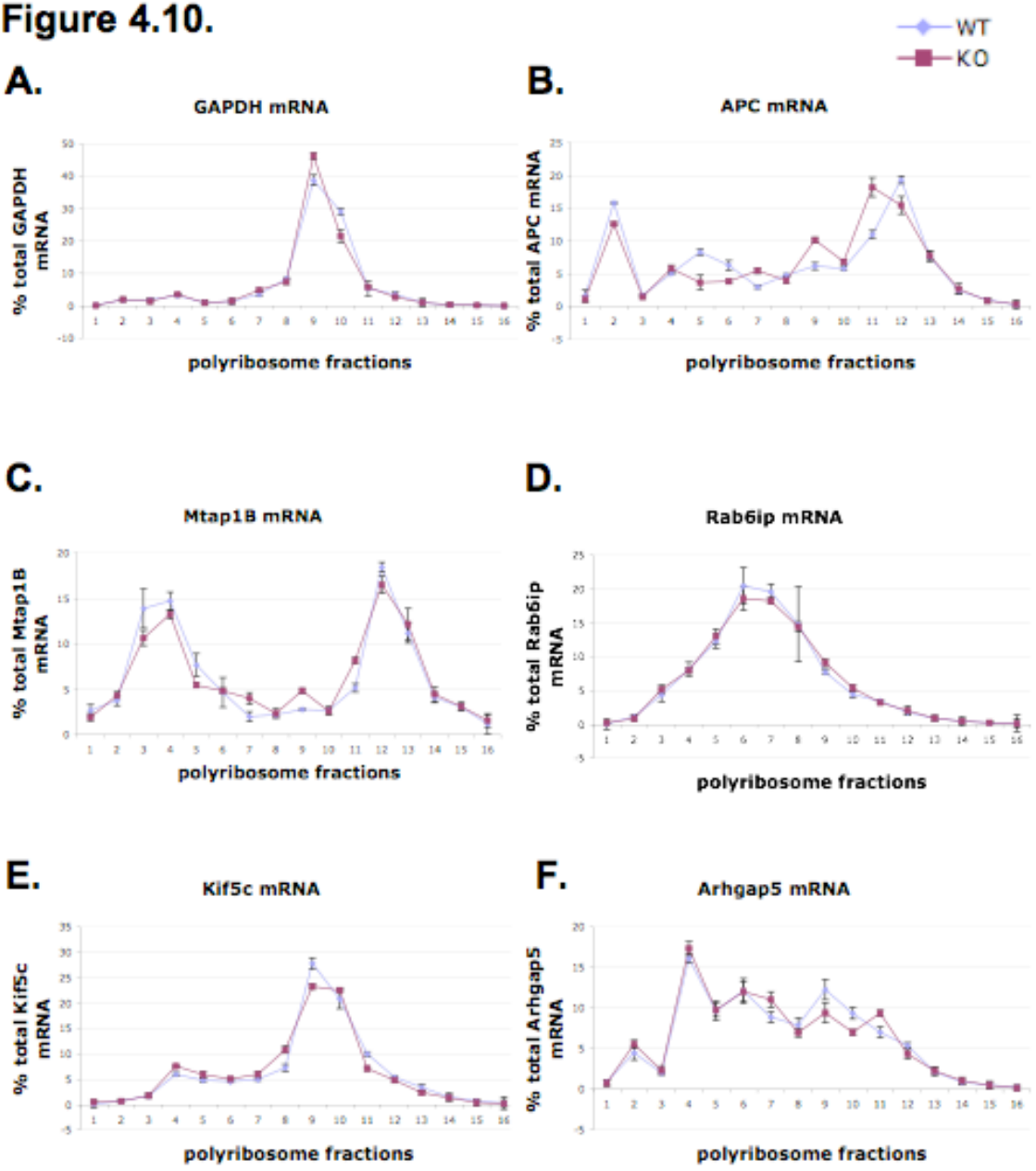

Figure 4.10. Translational profiles of a few FMRP target mRNAs were not significantly different between wild type vs. Fmr1 knockout polyribosome gradients. Wild type and knockout mouse brain cytoplasmic lysates were centrifuged on a w/w 20-50% linear sucrose gradients. Gradients were fractionated and RNAs were collected from each fraction. Quantitative RT-PCR was performed (ΔΔCt method) for each mRNA target. Relative mRNA levels in each fraction were plotted as a percentage of the total of a given mRNA to illustrate its distribution over the polyribosome gradient. GAPDH **(A)** was the control mRNA that did not show distribution changes over wild type vs. knockout polyribosome gradient. **(B)** APC mRNA, **(C)** Mtap1b mRNA, **(D)** Rab6ip mRNA, **(E)** Kif5c mRNA, **(F)** Arhgap5 mRNA.

Figure 4.11.

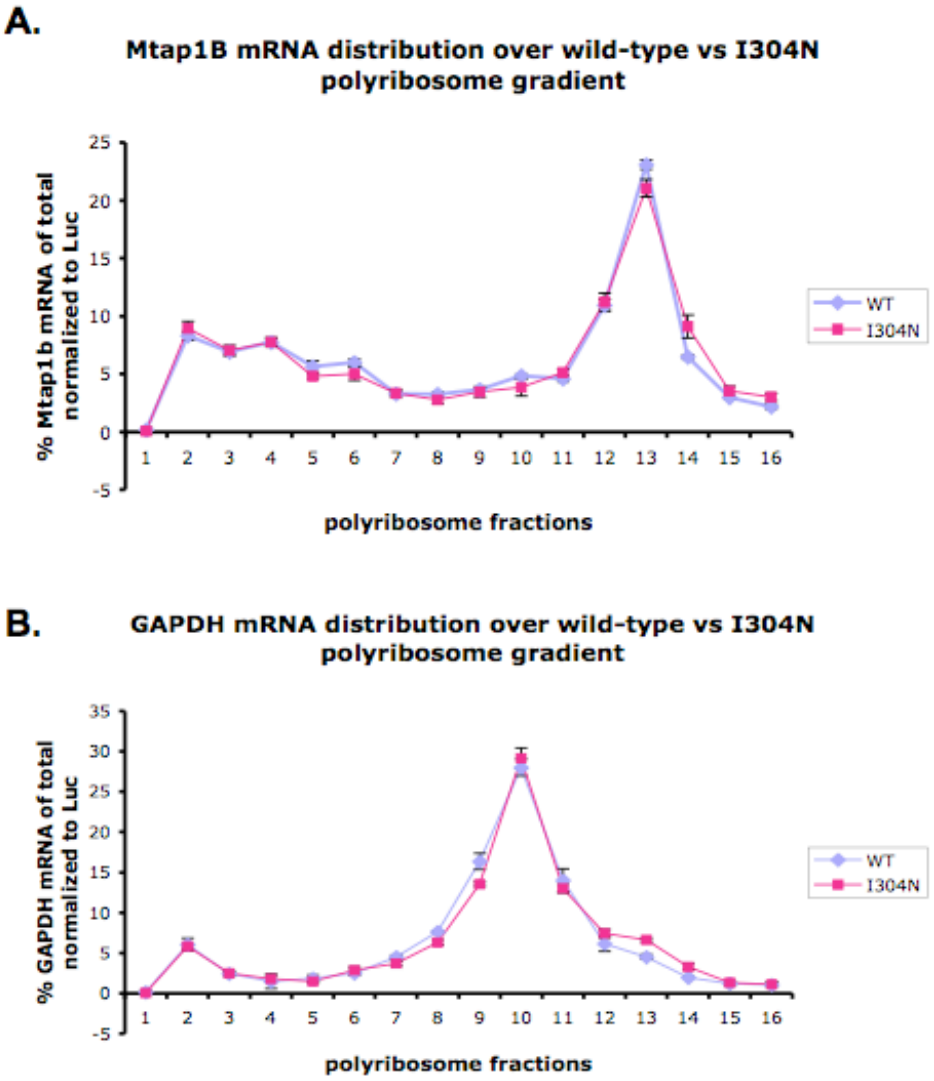

Figure 4.11. Translational profile of Mtap1b mRNA was not significantly different between wild type vs. I304N knock-in polyribosome gradients. Wild type and I304N mouse brain cytoplasmic lysates were centrifuged on w/w 20-50% linear sucrose gradients. Gradients were fractionated and RNA was collected from each fraction. Quantitative RT-PCR was performed (ΔΔCt method) for Mtap1b mRNA **(A)**. Relative mRNA levels in each fraction were plotted as a percentage of the total mRNA to illustrate its distribution over the polyribosome gradient. GAPDH **(B)** was the control mRNA that did not show distribution changes over wild type vs. I304N polyribosome gradient.

Figure 4.12.

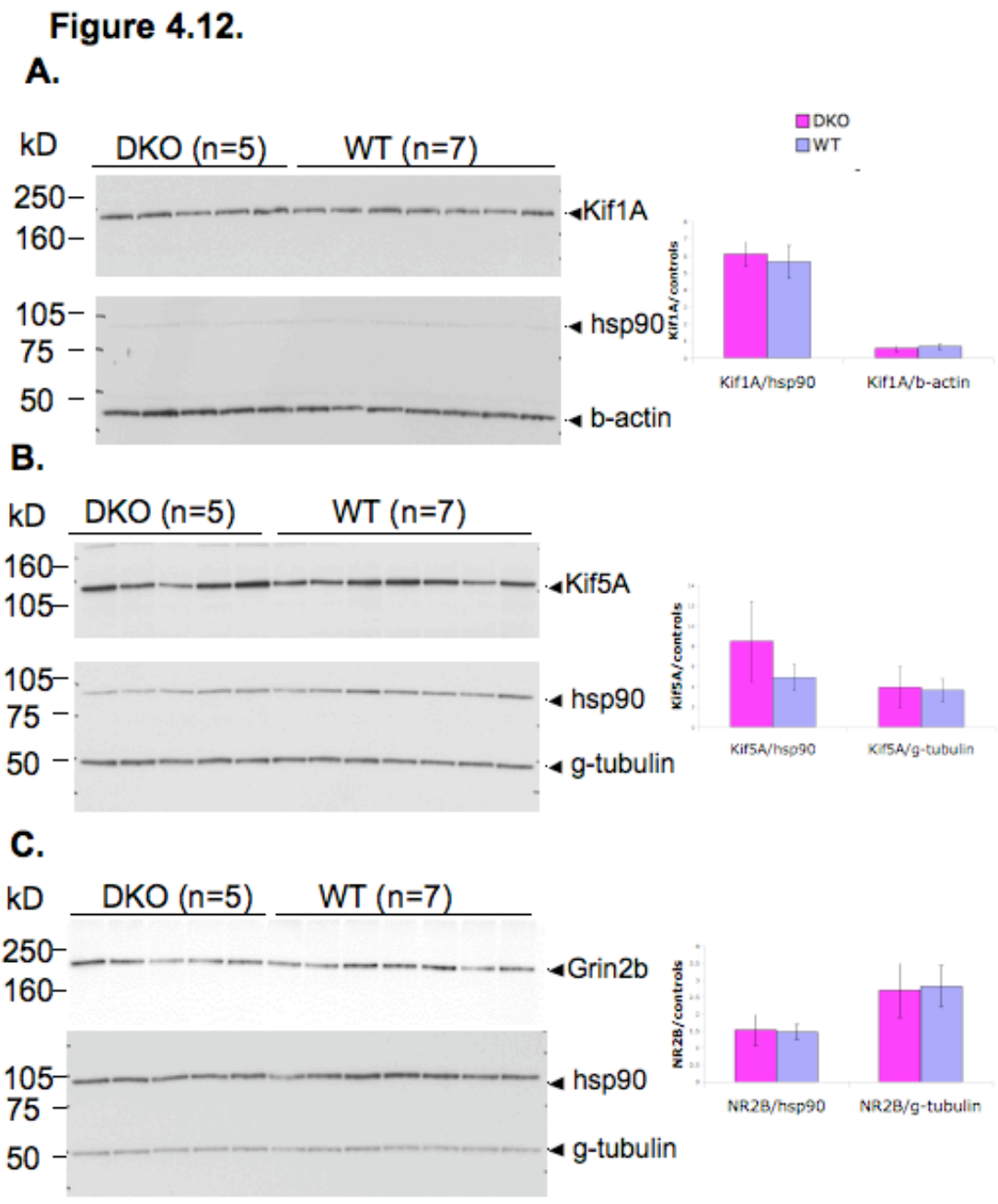

Figure 4.12. Protein levels of Kif1a, Kif5a, Grin2b were not significantly different in wild type vs. Fmr1/FXR2 double knockout mouse brains. Western blot and quantification of **(A)** Kif1a, **(B)** Kif5a, and **(C)** Grin2b expression in P8 hippocampus; WT n=7 and DKO n=5. Additional targets APC, Akap6, and Munc13 were subject to the same Western analysis and no significant difference in their protein levels was observed (data not shown).

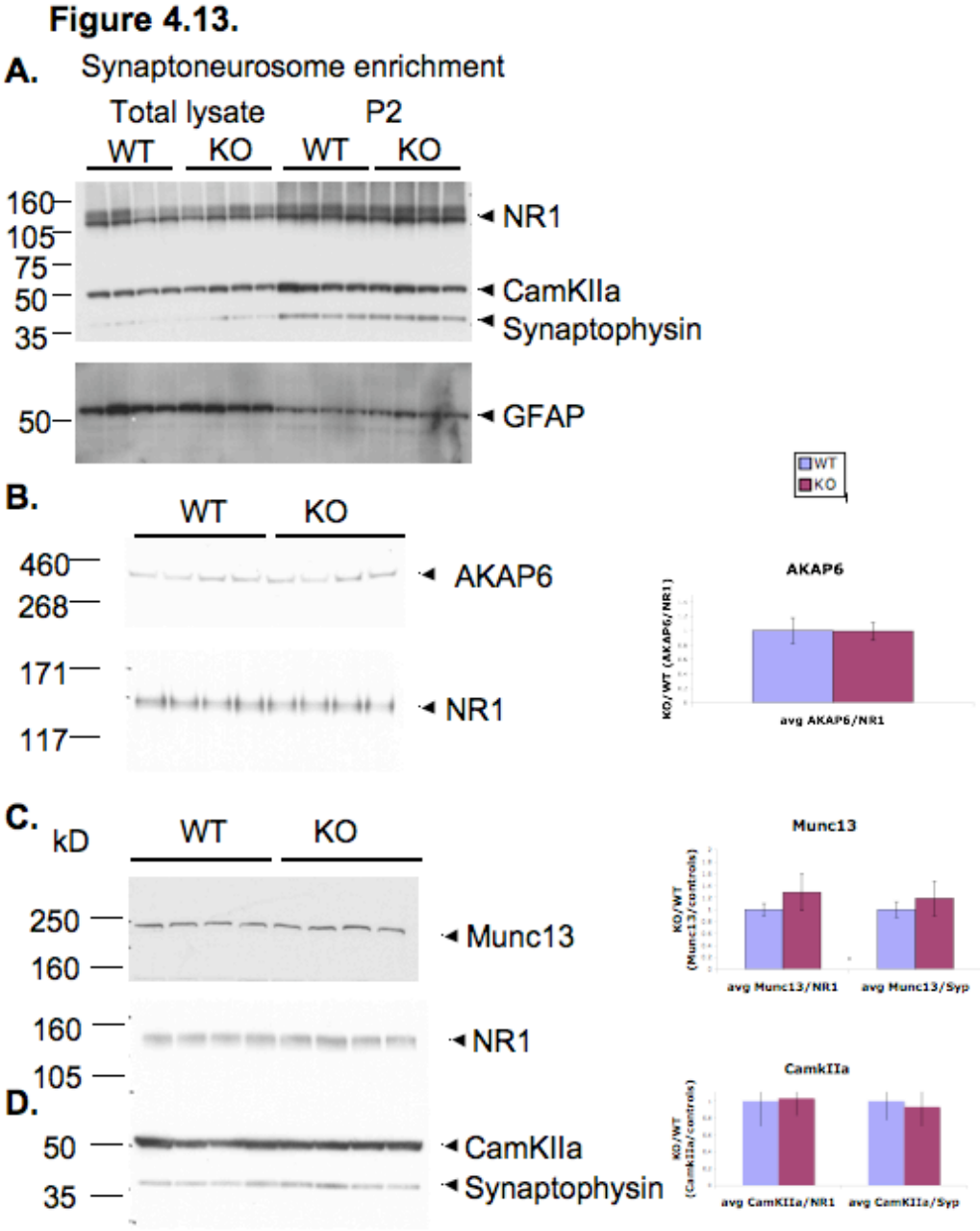

Figure 4.13. A few synaptically localized FMRP targets had similar expression levels in wild type vs. Fmr1 knockout synaptoneurosomes. (A) Synaptoneurosome preparation enriched NR1, Camk2a, and synaptophysin, while the glial marker GFAP was depleted, shown by Western blot. **(B)** Akap6, **(C)** Munc13, **(D)** Camk2a expression in synaptoneurosomes prepared from P15 wild type vs. Fmr1 knockout mice revealed no difference. Expression levels of these targets were also examined in wild type vs. double knockout synaptoneurosomes and no significant difference was found (data not shown).

CHAPTER V. COMPARISON OF ARGOUNATE BOUND miRNAs IN WILD TYPE AND Fmr1-NULL MOUSE BRAINS

Introduction

We have become interested in miRNAs because several reports have linked FMRP to the RNA-induced silencing complex (RISC). In Drosophila, dFXR has been found to interact biochemically with Argonaute 2 (dAgo2) (Caudy et al., 2003; Caudy et al., 2002; Ishizuka et al., 2002) and genetically with Argonaute 1 (dAgo1) (Jin et al., 2004). In mammalian cell culture, FMRP and FXR1P have been shown to co-immunoprecipitate with mAgo2, the mammalian ortholog of dAgo1 (Jin et al., 2004; Vasudevan and Steitz, 2007). These findings suggest that there may be a connection between the functions of FXR family members and miRNA involved processes.

MicroRNAs (miRNA) are a class of evolutionarily conserved non-coding RNA sequences of approximately 22 nts. They play an important role in regulating translation and degradation of mRNAs through base pairing to sites that are partially complementary on mRNAs. miRNA genes are often located in clusters that are transcribed by RNA polymerase II or III as polycistrons (Borchert et al., 2006; Lee et al., 2004). Primary miRNA transcripts (pri-miRNAs) are cleaved by RNase III enzyme, Drosha, liberating stem loop structured precursors (pre-miRNAs) of roughly 70 nucleotides in length (Lee et al., 2003). Pre-miRNAs are exported out of the nucleus via Exportin 5 in a Ran-GTP dependent manner (Bohnsack et al., 2004; Lund et al., 2004; Yi et al., 2003). In the cytoplasm, pre-miRNAs are further processed by another RNase III enzyme, Dicer, to produce a shorted-lived double-stranded miRNA/miRNA* complex of 22 nucleotides composed of one guide strand, the mature miRNA, and one passenger strand, miRNA* (Lee et al., 2002; Park et al., 2002). Following cleavage, RDE-4/R2D2 facilitates the transfer of miRNA/miRNA* to the RISC complex, which is the effector complex of miRNA action and is composed of Argonaute proteins and a number of accessory factors. The passenger strand, miRNA*, is cleaved quickly and is subsequently degraded (Matranga et al., 2005). The remaining mature miRNA recognizes complementary binding sites located in 3'UTRs of target mRNAs and functions as a guide for effectors,

such as Argonaute proteins, to regulate mRNA stability or repress translation (Pillai et al., 2007).

Although several reports have shown interactions of FMRP with Argonautes through biochemical assays and Drosophila genetics, it is largely unknown whether FMRP has any role on miRNA maturation, Argonaute loading, guidance of RISC effector complex to mRNA, or miRNA mediated regulation of gene expression. Through a serendipitous discovery during our study on the RNA binding properties of FMRP, we found that a commercially available FMRP antibody, 7G1-1, was contaminated by a pan-Argonaute antibody. Using this antibody and CLIP methodology, we successfully cloned Argonaute bound miRNAs from mouse brains. Preliminary data showed similar miRNA expression in wild type vs. Fmr1 knockout mouse brains, consistent with Landgraf et al. (Landgraf et al., 2007), suggesting that FMRP likely does not play a role in miRNA maturation or miRNA:Ago assembly.

Characterization of FMRP 7G1-1 antibody

We found that a commercially available FMRP antibody, 7G1-1, was able to immunoprecipitate Argonaute proteins during the troubleshooting for the FMRP-CLIP experiment. After covalently crosslinking RBPs to their RNA targets using ultraviolet light, multiple steps of stringent purification can be used for the purification of RBP-RNA complexes and non-crosslinked free RNA is "filtered" out. When we used the 7G1-1 antibody, we observed there were still some RNA signals in the Fmr1 knockout sample concentrated at approximately 115 kDa **(Figure 5.1)**. Therefore, we analyzed the purity of 7G1-1 immunoprecipitates with protein staining, and the protein bands were identified with mass spectrometry **(Figure 5.2)**. As we expected, FMRP (band 1) was immunoprecipitated from wild type while absent from Fmr1 knockout brains. To our surprise, 7G1-1 antibody also was able to immunoprecipitate Argonautes 1 to 4 (band 4). We confirmed the mass spectrometry result by Western analysis; 7G1-1 antibody immunoprecipitated Argonaute1 and Argonaute2 from wild type, I304N knock-in, and Fmr1 knockout mouse brain lysates **(Figure 5.3A)**. Since the Argonaute proteins were immunoprecipitated in the absence of FMRP, we speculated that the 7G1-1 antibody we used for our experiments recognized Argonaute proteins directly, instead of co-

immunoprecipitating them. As a negative control, another FMRP antibody, 17722, did not immunoprecipitate Argonaute proteins under the same conditions **(Figure 5.3B)**. We further confirmed the direct reactivity of 7G1-1 antibody to Argonautes by immunoprecipitating recombinant Ago2 protein from crude bacterial lysates **(Figure 5.3C)**.

There are two possibilities for the 7G1-1 antibody to recognize Argonaute proteins. 7G1-1 could cross-react with the Argonautes, or it could be contaminated with an unknown source of anti-Ago antibody. We distinguished these two possibilities by blocking 7G1-1 immunoprecipitation using a competing peptide, the 15 amino acid epitope of FMRP (Brown et al., 2001; Ceman et al., 2003b). The peptide successfully competed away FMRP immunoprecipitation, but has no effect on Ago protein immunoprecipitation **(Figure 5.4A)**. Our data suggests that FMRP and Argonautes do not share the same 7G1-1 epitope. Instead, this specific batch of commercial 7G1-1 may not be a true monoclonal, but a mixture of two antibodies, one for FMRP and the other for the Argonautes. Indeed, a batch of 7G1-1 antibody obtained from Dr. Stephanie Ceman no longer recognized Ago proteins **(Figure 5.4B)**.

miRNA CLIP

Utilizing CLIP methodology and the 7G1-1 antibody which also immunoprecipitates Argonaute proteins, we not only cloned FMRP-bound mRNAs, but we also serendipitously cloned Argonaute-bound miRNAs from mouse brain. CLIP experiments on Nova have demonstrated that RNA-protein complexes run quite true to size on SDS-PAGE gels. For example, RNA-protein complexes that contain RNAs of between 50-70 nts run approximately15-20 kDa larger than the M_r of the protein alone (Ule et al., 2005a). We excised a few thin bands corresponding to molecular weights of 85, 90, 95, and 115 kDa from both wild type and Fmr1 knockout samples **(Figure 4.4A in Chapter IV)**. After RT-PCR amplification, nucleic acid (NA) signals were present in wild type and very little in FMR-1 knockout sample. As the size of RNA-protein complexes increased from 90 to 95 kDa, NA smears also increased in size **(Figure 4.4C in Chapter IV)**. The average size of RNAs cloned from 90 and 95 kDa corresponded well with the expected size of RNAs directly crosslinked to FMRP. However, 115 kDa

generated sharp NA bands present in both wild type and Fmr1 knockout samples. The sizes of these NAs were unexpectedly small, approximately 55-60 nts in length, corresponding to original RNA tags of 19-24 nts plus linkers totaling 36 nts. Taken together with the finding that the 7G1-1 antibody was contaminated with a pan-Argonaute antibody, these small RNAs from 115 kDa are most likely crosslinked to Argonautes. The uniform length of the NAs indicated that they could be miRNAs, which was confirmed by cloning and sequencing. More than 80% of the RNAs corresponding to 115 kDa were matched to known miRNAs in the miRNA registry. miR-124a, miR-30c, and let-7 were the three miRNAs that were the most frequently cloned in P8 mouse brains **(Table 5.I)**. Assuming the number of tags sequenced is reflective of the abundance, our data suggests that they are likely the most abundant mouse brain miRNAs at postnatal day 8.

We then attempted to compare miRNA expression in wild type vs. Fmr1 knockout mouse brains. Preliminary data from ~350 sequenced miRNAs showed that the top most abundant miRNAs have similar expression in wild type vs. Fmr1 knockout brains **(Table 5.I)**. In order to draw a definitive conclusion, we needed a larger set of sequences. A repeat of the Ago CLIP experiment using P16 mouse brains was submitted for high throughput sequencing. 198,236 sequences were obtained from Fmr1 knockout. Of these, 165,168 were matched to known miRNAs. Unfortunately, due to sequencing errors, only 2706 sequences from wild type, 2275 of which were matched to known miRNAs, were obtained. Our data showed that the frequencies of miRNAs CLIPed were largely similar between wild type and knockout mouse brains, consistent with Landgraf et al. **(Table 5.II)** (Landgraf et al., 2007). However, the disparity in the total numbers of these two data sets and the low number of sequences obtained from the wild type set prevented us from drawing a definitive conclusion at present. The sequencing of wild type miRNA sample would need to be repeated. On the other hand, the expression patterns of miRNAs at P8 and P16 were found to be different. For instance, miR-124a was found to be the most abundant miRNA consisting of ~30% of total miRNAs obtained at P8 in both wild type and Fmr1 knockout brains, but it represented only ~3-6% of total miRNAs in P16 mouse brains, suggesting miRNA expression may be developmentally regulated.

Conclusion

Taking advantage of an antibody that unexpectedly immunoprecipitates Argonaute proteins, we have extended CLIP methodology to the purification of miRNAs, and we have demonstrated that miRNAs are directly bound to Argonaute proteins. Furthermore, since more than 80% of the sequences cloned from Argonaute CLIP match to known miRNAs, we have confirmed the high specificity of CLIP methodology for the purification of bona fide RNA targets bound to RNA binding proteins. Although the remaining sequences have not been matched to known miRNAs so far, more analysis will be done for the identification of new miRNAs. The two Argonaute CLIP experiments on mouse brains from two developmental ages, P8 and P16, have shown different miRNA expression patterns, consistent with Neilson et al. (Neilson et al., 2007), suggesting that miRNA expression is dynamically regulated at different developmental stages. Furthermore, our preliminary data have shown that miRNA expression is largely similar in wild type and Fmr1 knockout mouse brains, indicating FMRP probably does not play a role in miRNA maturation or miRNA-Ago assembly. Whether FMRP has a role in the later processes, such as facilitating mRNA cognition or miRNA mediated regulation of gene expression, will be a very interesting area of study for future exploration.

Figure 5.1.

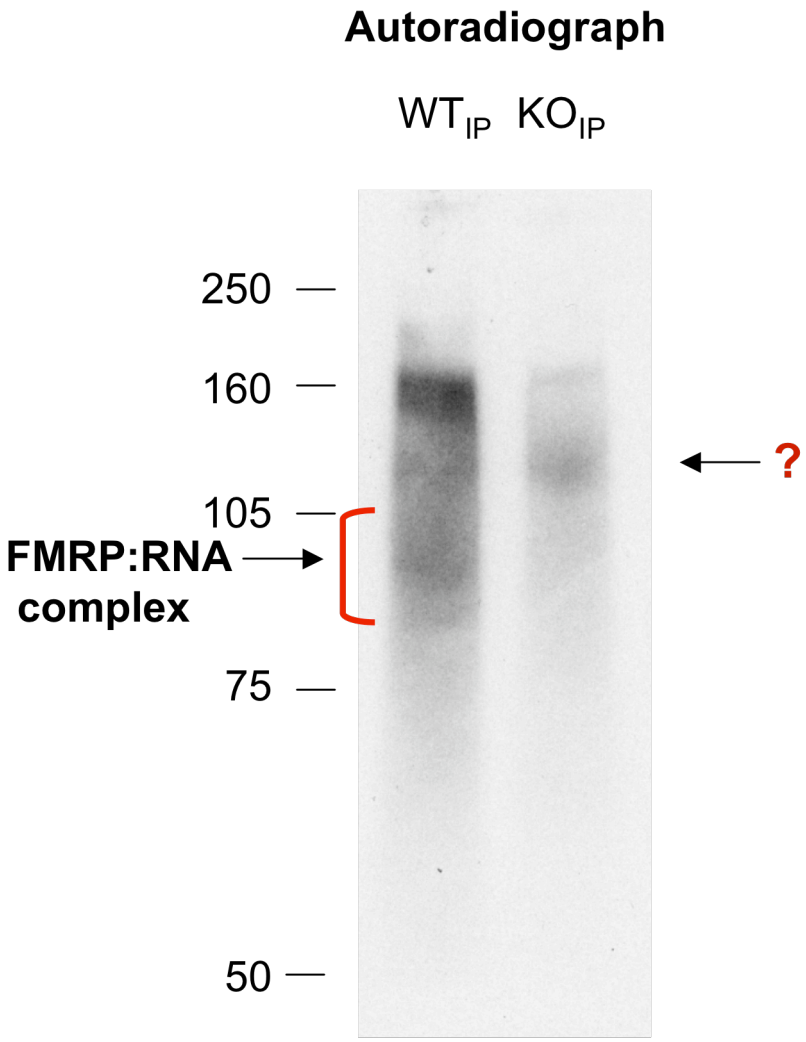

Figure 5.1. Autoradiograph of FMRP CLIP shows unexpected RNA signals in Fmr1 knockout sample. Postnatal day 8 wild type (WT) and Fmr1 knockout (KO) mouse brains were UV irradiated, protein:RNA complexes immunoprecipitated with FMRP-specific 7G1-1 monoclonal antibody, RNA-ligated with ^{32}P labeled 3' linker, and separated by SDS-PAGE, transferred to nitrocellulose, and visualized by autoradiography. CLIP performed using wild type brain revealed radiolabeled signals from RNA-FMRP complexes. However, we still observed RNA signals in the Fmr1 knockout sample, with most intensity at ~115 kDa.

Figure 5.2.

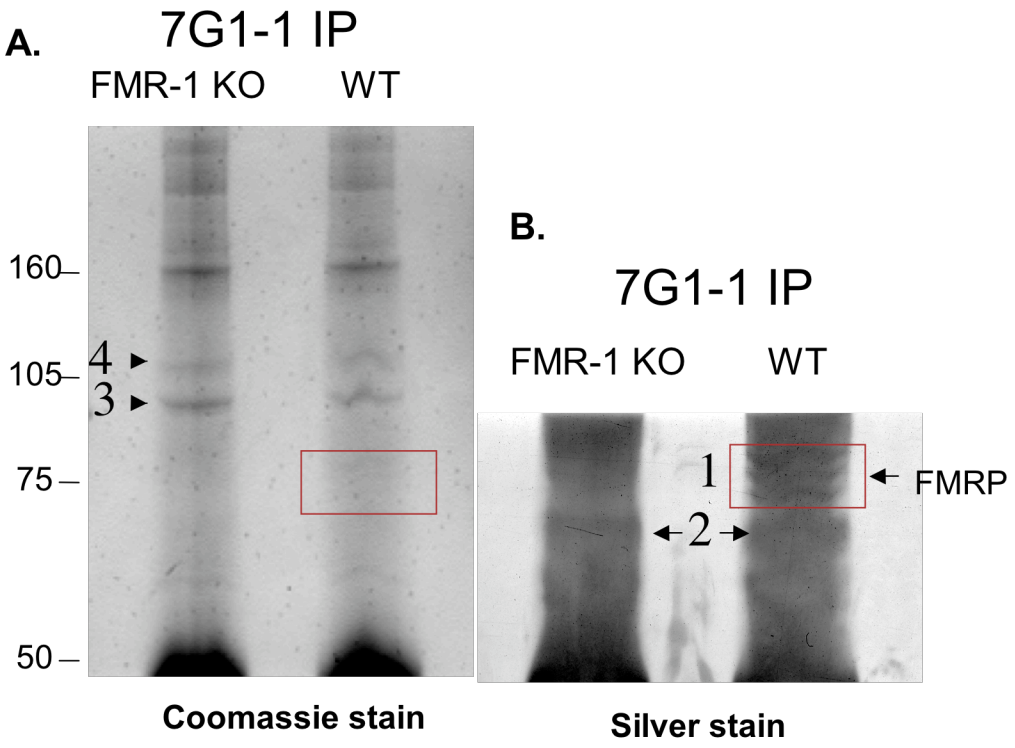

C.

1. **FMRP** score 368, queries matched 9;
2. **Albumin 1** score 554, queries matched 13;
3. **Glycosyl-phosphatidyl-inositol anchored protein p137**, score 341, queries matched 9
4. **eIF2C2** score 723, queries matched 20,
   eIF2C1 score 285, queires matched 11,
   eIF2C3 score 183, queries matched 7;
   eIF2C4 score 95, queries matched 5

Figure 5.2. Protein staining and mass spectrometry identify that 7G1-1 antibody immunoprecipitates Argonaute proteins. Wild type and Fmr1 knockout brain lysates were immunoprecipitated under FMRP CLIP condition. Immunoprecipitates were run on a 4-12% Tris-glycine protein gel, stained with Coomassie stain **(A)** and followed with silver stain **(B)**. Triplet protein bands (band 1), which corresponds to M_r of FMRP, were observed in wild type, but not in knockout, immunoprecipitates. Mass spectrometry confirmed it was FMRP. Band 4 was identified as Ago proteins 1-4, present in both wild type and Fmr1 knockout immunoprecipitates. Details of MS identification are listed in **(C)**.

Figure 5.3.

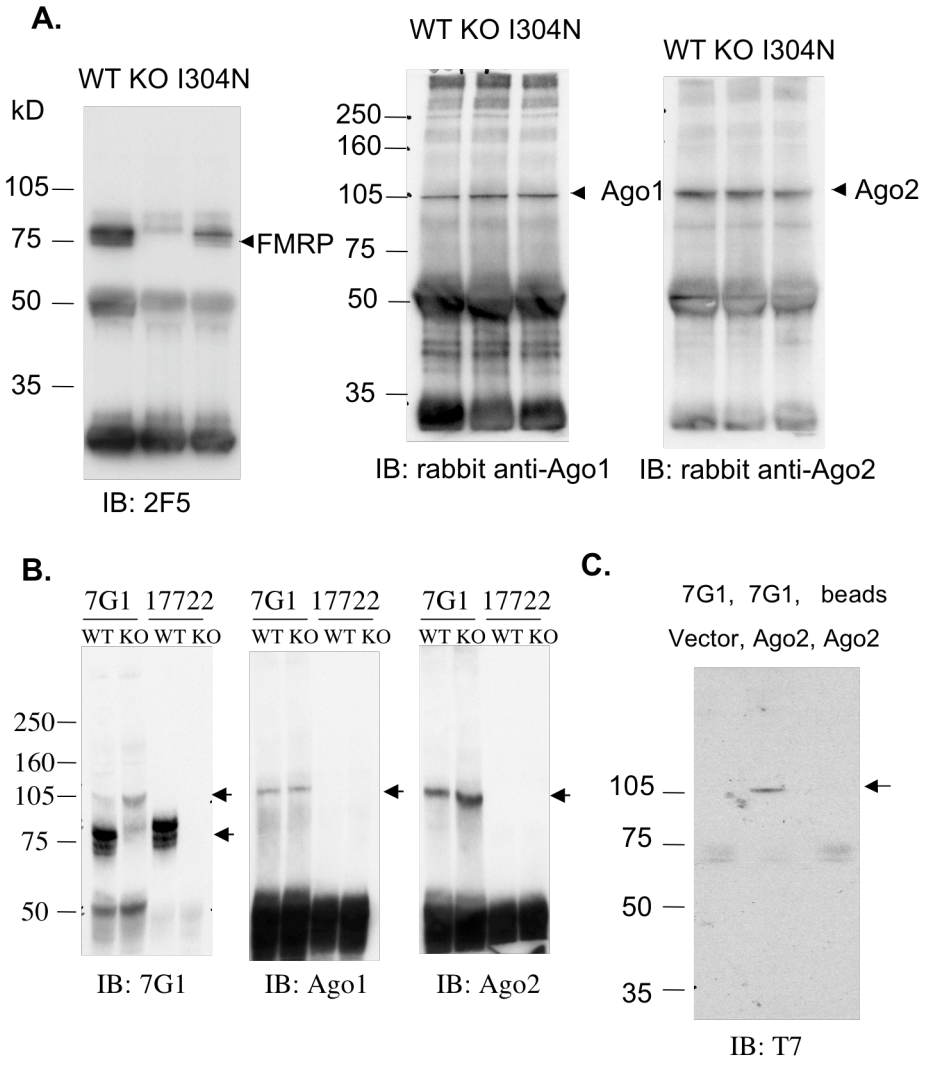

Figure 5.3. Confirmation that 7G1-1 recognizes Argonaute proteins. (A) Wild type (WT), Fmr1 knockout (KO), and I304N knock-in (I304N) mouse brain lysates were IPed with 7G1-1 antibody under FMRP CLIP condition. Immunoprecipitates were analyzed by Western for FMRP, probed with 2F5 antibody, Argonaute 1 and Argonaute 2. **(B)** Immunoprecipitation was done under the same conditions with another FMRP antibody, rabbit polyclonal 17722, and Western analysis showed that 17722 did not immunoprecipitate Argonaute 1 or Argonaute 2, in contrast to 7G1-1 antibody. **(C)** Recombinant T7-tagged human Argonaute 2 (obtained from Addgene) or empty T7 vector were expressed in BL21 E coli. Bacteria were lysed with Bugbuster mastermix. Lysates were sonicated and pelleted at 27,200xg to separate soluble proteins from inclusion bodies. 7G1-1 antibody was able to immunoprecipitate recombinant Argonaute 2 protein, detected by Western blot probed with a T7 antibody. As negative controls, 7G1-1 immunoprecipitation from the bacterial lysate of the empty T7 vector and immunoprecipitation using only beads did not generate any signal.

Figure 5.4.

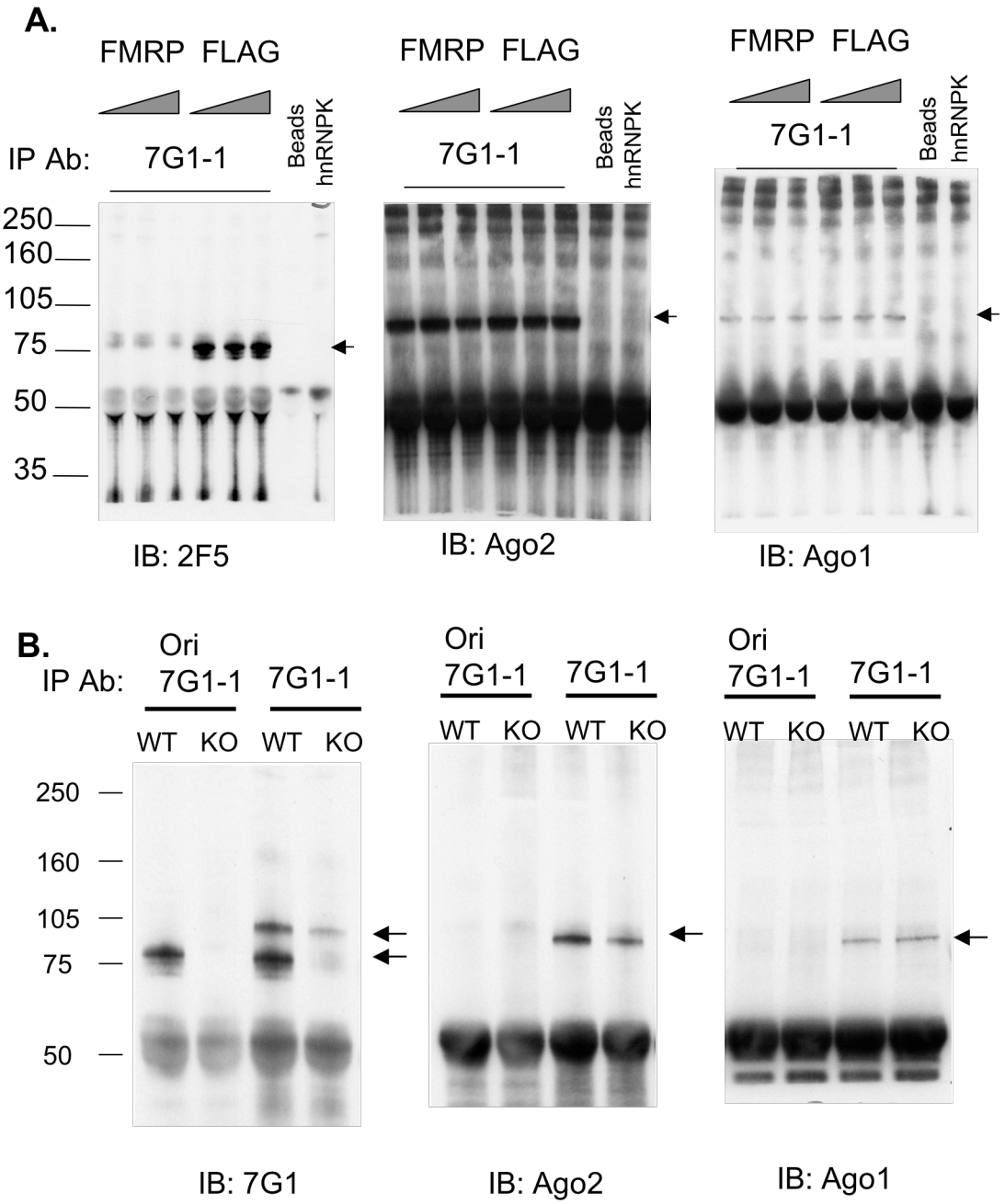

Figure 5.4. "7G1-1" is contaminated with an unknown source of Argonaute antibody. (A) 7G1-1 antibody was pre-incubated with 20ug, 200ug or 2mg (50 fold excess) of FMRP 354-KHLDTKENTHFSQPN-368 peptide, the epitope 7G1-1 recognizes (Brown et al., 2001; Ceman et al., 2003b), or an irrelevant FLAG peptide. FMRP peptide, but not FLAG peptide, was sufficient to completely block FMRP immunoprecipitation from mouse brain. FMRP peptide even at 2mg had no effect on Argonaute 1 or Argonaute 2 immunoprecipitation. **(B)** Original batch of 7G1-1 antibody immunoprecipitate Arogounate 1 or Argounate 2 from mouse brain.

Table 5.I. List of miRNAs cloned from Argonaute CLIP using P8 wild type vs. Fmr1 knockout mouse brains. miRNAs were listed for both wild type and Fmr1 knockout according to the number of times being sequenced. The percentage as the total was calculated for top ranked miRNAs.

mature miR	WT	FMR1 KO	WT (% total)	FMR1 KO (% total)
miR-124a	46	62	30.9	31.2
miR-30c	14	25	9.4	12.6
let-7 family	5	14	3.4	7.0
miR-9	9	8	6.0	4.0
miR-434	5	10	3.4	5.0
miR-487	8	7	5.4	3.5
miR-125b	2	8	1.3	4.0
miR-125a	5	3	2.5	1.5
miR-26a, b	6	2	3.0	1.0
miR-376a, b	2	4	1.0	2.0
miR-204	4	1		
miR-300	0	5		
miR-126-3p, 5p	2	2		
miR-127	1	3		
miR-219	2	2		
miR-323	1	3		
miR-99b	0	4		
miR-137	3	0		
miR-187	1	2		
miR-193	1	2		
miR-296	1	2		
miR-485	1	2		
miR-541	2	1		
miR-138	1	1		
miR-142-3p	0	2		
miR-181a	0	2		
miR-19b	0	2		
miR-23b	2	0		
miR-27a, b	1	1		
miR-30a	1	1		
miR-30b	1	1		
miR-30e	1	1		
miR-346	2	0		
miR-384	2	0		
miR-433	0	2		
miR-484	1	1		
miR-92	2	0		
miR-100	0	1		
miR-132	1	0		
miR-135a	1	0		
miR-139	2	0		
miR-141	1	0		
miR-143	0	1		
miR-150	1	0		
miR-151	1	0		
miR-154	0	1		
miR-16	0	1		
miR-199a	0	1		
miR-20	1	0		
miR-301	0	1		
miR-30d	1	0		
miR-326	1	0		
miR-328	0	1		
miR-33	0	1		
miR-337	1	0		
miR-339	0	1		
miR-350	0	1		
miR-351	1	0		
miR-369	0	1		
miR-409	1	0		
miR-429	0	1		
miR-451	1	0		
miR-540	0	1		
miR-93	1	0		
miR-466	0	1		
total	150	200		

Table 5.II. List of top 35 miRNAs cloned from Argonaute CLIP using P16 wild type vs. Fmr1 knockout mouse brains.

miRNAs P16 brains	KO hits	WT hits	KO(%)	WT(%)	KO rank	WT rank
mmu-mir-30e	24230	397	14.7	17.5	1	1
mmu-mir-30d	16878	297	10.2	13.1	2	2
mmu-mir-27a	14248	163	8.6	7.2	3	5
mmu-mir-26a	11062	287	6.7	12.6	4	3
mmu-mir-30a	10998	197	6.7	8.7	5	4
mmu-mir-708	10077	92	6.1	4.0	6	6
mmu-mir-124a	9110	67	5.5	2.9	7	9
mmu-mir-181a	6332	71	3.8	3.1	8	7
mmu-mir-9-1	6056	68	3.7	3.0	9	8
mmu-let-7i	3772	57	2.3	2.5	10	10
mmu-mir-181b	3320	37	2.0	1.6	11	11
mmu-mir-138	3156	17	1.9	0.7	12	17
mmu-let-7c-2	2866	32	1.7	1.4	13	12
mmu-let-7b	2395	21	1.5	0.9	14	14
mmu-mir-449	2215	23	1.3	1.0	15	13
mmu-mir-344	1775	15	1.1	0.7	16	18
mmu-mir-22	1590	10	1.0	0.4	17	23
mmu-mir-153	1305	21	0.8	0.9	18	15
mmu-mir-324	1156	5	0.7	0.2	19	34
mmu-mir-27b	1042	15	0.6	0.7	20	19
mmu-mir-101b	896	5	0.5	0.2	21	35
mmu-mir-34a	825	10	0.5	0.4	22	24
mmu-mir-16	811	10	0.5	0.4	23	25
mmu-let-7g	785	6	0.5	0.3	24	30
mmu-mir-221	781	6	0.5	0.3	25	31
mmu-mir-125b	778	20	0.5	0.9	26	16
mmu-mir-31	745	11	0.5	0.5	27	20
mmu-mir-383	698	11	0.4	0.5	28	21
mmu-mir-106b	691	5	0.4	0.2	29	36
mmu-mir-21	640	4	0.4	0.2	30	38
mmu-mir-136	617	6	0.4	0.3	31	32
mmu-mir-101a	604	2	0.4	0.1	32	65
mmu-mir-30c	546	4	0.3	0.2	33	39
mmu-mir-338	526	4	0.3	0.2	34	40
mmu-mir-340	525	6	0.3	0.3	35	33

CHAPTER VI. GENERAL DISCUSSION

This thesis is devoted to the understanding of functional roles of FMRP in normal neuronal development and in the pathogenesis of the Fragile X Syndrome. Particularly we have focused on the study of FMRP RNA binding properties, using both mouse models and biochemical analysis. We have generated and characterized mouse models of a functionally important point mutation in FMRP KH-type RNA binding domain that recapitulate the fragile X phenotype. We have biochemically purified a reliable set of FMRP RNA targets of coherent biological functions related to cytoskeletal organization and synaptic transmission. Our data suggest RNA binding is a key function of FMRP, through which it controls gene expression of a defined set of mRNA targets to mediate normal cognition.

Point mutation mouse models of the Fragile X Syndrome reveal KH2 domain specific RNA binding is a key function of FMRP

Characterization of dysfunctional genes at the molecular level has unraveled the causes of many diseases in the recent years. Naturally occurring mutations found in patients, particularly point mutations that often define the loss of an important functional domain, have facilitated the understanding of the pathogenesis of many diseases. For instance, frontotemporal dementia and parkinsonism linked to chromosome 17 (FTDP-17) is associated with mutations of the Tau protein. Thirty-nine mutations in Tau have been identified with majority of them present in its coding region. Most mutations are located in the microtubule-binding region, defining it as an important domain for Tau to mediate microtubule assembly. There are also mutations in the N-terminus of Tau, a domain that is found to be responsible for Tau trafficking and compartmentalization (van Swieten and Spillantini, 2007). Another example is autosomal recessive juvenile parkinsonism (ARJP). Mutations of Parkin (PARK2) are the predominant cause of the disease. At least ten familial-associated Parkin mutations have been reported and they are closely associated with the disruption of Parkin protein solubility, localization or ubiquitination (Wood-Kaczmar et al., 2006).

Fragile X Syndrome is one of the pioneer examples of one mutation being responsible for one disease. In most cases the disease is caused by the CGG repeat expansion in the 5'UTR of the Fmr1 gene and methylation of CpG islands that lead to subsequent loss of FMRP expression (Jin and Warren, 2000, 2003; O'Donnell and Warren, 2002). Conventional Fragile X DNA tests are designed to detect the triplet repeat expansion in the 5'UTR of the gene, and as a result of that, there is only one missense mutation found in a single patient known to us to this day. This single severely affected patient harbors a conserved I->N mutation (I304N) within the KH2 RNA binding domain (DeBoulle et al., 1993). Nevertheless this clinical case has offered us hope of focusing FMRP studies in a key functional domain. This I->N mutation has previously been shown to abolish RNA binding by this and similar KH domains (Lewis et al., 2000; Liu et al., 2001; Ramos et al., 2003). Symptoms in this patient therefore suggest that the disease is caused by a loss of FMRP KH2 domain specific RNA binding. However, this interpretation has been complicated by questions of whether such a mutation might lead to an unfolded protein that is completely functionless (Lewis et al., 1999; Musco et al., 1997; Musco et al., 1996) rather than a correctly folded protein (Liu et al., 2001; Pozdnyakova and Regan, 2005), in which RNA binding function is specifically lost. Moreover, one case of a single patient who also has a confounding liver disease (DeBoulle et al., 1993) limits us to draw any definitive conclusions.

To address these questions, we have introduced this mutation in mouse models and phenocopied the disease. I304N knock-in mice have FMRP null-like behavioral deficits and altered synaptic plasticity. The mutant protein is present, albeit at somewhat reduced levels in adult mice. The protein retains some normal activities, as it is competent to bind both protein partners such as FXR1 and FXR2 and, via its RGG-domain, to G-quartet RNA (Darnell et al., 2001), confirming it is not a completely functionless denatured protein. However, I304N protein is defective in RNA binding, as we have predicted, and is dissociated from polyribosomes, hence proper translational control is likely lost in the I304N mouse brain. We have not been able to examine homodimerization of the I304N protein in mouse brain, which has been reported to be defective using ZZ-tagged recombinant protein (Laggerbauer et al., 2001b). This study using fusion proteins may or may not correctly depict *in vivo* interactions. Our findings

that mouse brain I304N FMRP is capable of heterodimerization with FXR1P and FXR2P and is in a RNase resistant particle significantly larger than the monomer size suggest the N-terminal protein interaction domain, NDF or PPId (Mazroui et al., 2003; Ramos et al., 2006), may be unaffected by the mutation and direct protein-protein interaction may be retained. The loss of polyribosome association is likely primarily due to a loss of KH2 domain specific RNA binding. Taken together I304N knock-in mice bearing a Fmr1-null-like phenotype, our findings support the suggestion that a key function of FMRP in mediating normal cognition is KH2 domain sequence specific RNA binding.

This I304N patient and our mouse models also point to the need for more thorough and inclusive diagnostic tests, like DNA tests for detection of mutations in the Fmr1 coding region or antibody staining for peripheral blood smears. Therefore more potential candidates of Fragile X Syndrome can be correctly diagnosed and clinically managed. In return, clinical cases of patients who have mutations that have not been previously identified can supply new information for the understanding of the disease.

Moreover, our I304N knock-in mouse, in addition to the Fmr1 null, conditional null mice, and Fmr1/FXR2 double knockout mice, is a new mouse model for the Fragile X Syndrome. It can be used together with wild type and Fmr1 knockout mice for validation assays to test RNA metabolism mediated by FMRP functions. Lastly, trials of clinical treatment can also be tested on these mice, since the mice provide a physiologically relevant living system that closely resembles fragile X patients.

FMRP may spatially and temporally regulate a coherent set of mRNAs in a precise, robust and instantaneous fashion

Since the study of I304N mouse models suggests that a critical function of FMRP is mediating sequence-specific RNA binding, the need to identify RNA ligands for FMRP is heightened. Many laboratories have attempted various approaches (Brown et al., 2001; Chen et al., 2003; Darnell et al., 2005a; Darnell et al., 2001; Dolzhanskaya et al., 2003; Miyashiro et al., 2003; Muddashetty et al., 2007; Sung et al., 2003; Todd et al., 2003; Xu et al., 2004; Zalfa et al., 2003; Zhang et al., 2001b). A long list of RNA candidates has been generated. However, due to some intrinsic uncertainties underlying each technique, these targets have limited overlap, making it difficult to distinguish true

FMRP targets from falsely identified ones. To overcome this, our laboratory has developed *in vivo* UV crosslinking and immunoprecipitation (CLIP) analysis (Ule et al., 2005a; Ule et al., 2003). It has been used successfully to identify the genome-wide binding sites for Nova family members on pre-mRNAs (Ule et al., 2003; Ule et al., 2006).

We have successfully adapted CLIP methodology for FMRP and identified a reliable list of mRNAs bound by FMRP, including previously validated Mtap1b mRNA (Brown et al., 2001; Zhang et al., 2001b). This defined set of RNA targets encodes proteins of coherent functions, such as cytoskeletal organization and synaptic transmission, suggesting FMRP may regulate cytoskeletal dynamics, dendritic and axonal functions that all converge at the developing synapse. Knowing what set of RNAs FMRP binds to *in vivo*, we were interested in asking what regulatory roles FMRP has on these targets. Given the sum of the current literature in the field, the most likely function of FMRP on these RNA targets is in translational regulation, perhaps coupled with delivery of mRNAs to neuronal processes. Binding and regulating gene expression of this defined set of RNA targets is likely a key function of FMRP. We propose FMRP may spatially and temporally fine-tune gene expression of its mRNA targets, but the regulation is precise, robust and instantaneous.

Gene expression in a living system especially in highly specialized cells like neurons is very complex, but precise. Knowing what mRNAs FMRP binds to, we propose two modalities that may help to achieve precise and robust means of regulation. First, many mRNAs FMRP binds encode proteins within the same functional category. One example is that a few FMRP mRNAs encode cytoskeletal motor proteins. Microtubule plus-end directed kinesins, Kif1a, Kif1b, Kif5a, and Kif5c, microtubule minus-end directed dyneins, Dnchc1, and Dncic1, and actin based motor, Myo5a have all been identified to be bound by FMRP. Therefore FMRP may regulate them in parallel pathways, which can provide redundancy. A second modality is that FMRP regulates mRNA targets encoding proteins in a network. For example, presynaptic Caskin1, Nrxn1, Cacna1e, Cacna1d, postsynaptic Nlgn, and Psd-95 closely interact with one another and have all been identified as FMRP targets. CASK and MAGUK (membrane associated guanylate kinase) family members at the presynapse, in complex with Veli/Mint1,

interact with presynaptic voltage-caged Ca^{2+} channels and adhesion molecule Nrxn. Nrxn binds postsynaptic adhesion molecule Nlgn, which in turn is linked to postsynaptic MAGUK, PSD-95 (Dresbach et al., 2001; Schoch and Gundelfinger, 2006). When FMRP regulates targets within a network, individual components may be fragile in their responsiveness to changes, but due to their interconnection, the entire network functions synergistically and is highly resistant to perturbations. Therefore, FMRP achieves a robust and precise regulation of gene expression in the nervous system.

Our data also show FMRP binds all over mature mRNAs, without preference for UTRs or coding sequences, suggesting that FMRP likely does not inhibit translation initiation, or else one would expect most of the CLIP tags to be found in the 5'UTR or near the initiator methionine. FMRP has been shown to associate with polyribosomes (Corbin et al., 1997; Feng et al., 1997a; Feng et al., 1997b; Khandjian et al., 1996; Khandjian et al., 2004; Stefani et al., 2004). Even after puromycin treatment, FMRP co-sedimented with the largest remaining polyribosomes containing three to four ribosomes rather than with the much more prominent peak of monomeric ribosomes (Stefani et al., 2004). These findings together with our data suggest that FMRP is more likely to modulate translation at the step of elongation. Regulation at the elongation step confers several advantages. First, since the elongation step is the most energy-consuming step of translation, regulation at elongation likely acts as the final checkpoint for inhibiting unwanted protein synthesis to conserve energy expenditure. Second, regulation at elongation allows translation to pause or resume rapidly, because when the elongation step is regulated, polyribosomes are still retained, which will allow translation to resume rapidly. Fast translational control may be particularly important for neurons to respond to a synaptic stimulus. FMRP has been shown to regulate the translation of synaptically localized proteins in response to mGluR signaling. (Muddashetty et al., 2007). mGluR-dependent LTD is enhanced in fragile X mouse models (Huber et al., 2002; Koekkoek et al., 2005). In steady state, FMRP may suppress protein synthesis to conserve the energy for more important use; but in response to a synaptic stimulus, FMRP bound mRNAs that are already associated with polyribosomes and translational machinery can instantaneously resume translation, bypassing the rate limiting initiation step. Therefore,

FMRP instant control of translation in response to a stimulus can be crucial for synaptic plasticity.

Furthermore, lack of FMRP does not alter the global translational status, as the polyribosome profile is unchanged in Fmr1 null mice. Using assays like Western blots to examine protein levels and quantitative RT-PCR to examine mRNA translation profile over polyribosomes, we haven't been able to validate any FMRP mRNA targets. A genome wide screen by microarray analysis has revealed no significant difference in the levels of polyribosome associated mRNAs between wild type and Fmr1 knockout mice (Fraser, CE thesis). These negative data indicate that global effects of FMRP in terms of translational control at steady state is extremely subtle. Effects of FMRP may be local as it is suggested by many studies that FMRP traffics mRNAs to synapses for local translational regulation (Antar et al., 2004; Antar et al., 2005; De Diego Otero et al., 2002; Muddashetty et al., 2007). Effects of FMRP may also be transient and activity dependent (Hou et al., 2006; Todd et al., 2003). Therefore FMRP may spatially and temporally fine-tune gene expression of its target mRNAs. Although globally we have not been able to observe the changes of FMRP target metabolism, if we were able to capture the right subcellular compartment at the right time, the effect of FMRP may not be so subtle.

Last but not least, gene expression in eukaryotes undergoes many different control steps regulated by various multi-protein complexes. In contrast to a simple linear assembly line, a complex and extensive coupled network has evolved to coordinate the activities of the different protein complexes (Maniatis and Reed, 2002). Studies of other RBPs have shown that one RBP can have more than one role. The best understood function of Hu is regulation of mRNA stability by binding to AU rich element in 3'UTR of messages (Brennan et al., 2000; Deschenes-Furry et al., 2006; Keene, 1999). But other functions have also been shown. When shuttling of HuD is blocked, neurite elongation is severely impeded, suggesting that HuD plays an important role in trafficking and localizing its transcripts, e.g. Tau mRNA is targeted to axons and GAP-43 to growth cones (Deschenes-Furry et al., 2006). In our lab, Hu has also been shown to regulate splicing of certain RNAs. Another example is Nova, a well characterized tissue specific mammalian RNA-binding protein that regulates alternative splicing (Dredge and Darnell,

2003; Ule et al., 2003; Ule et al., 2006). A genome wide screen has shown that 24% of Nova-binding sites map to mature RNAs, most of them to the 3'UTR regions. Two thirds of Nova proteins are present in the cytoplasm, indicating Nova may have functions in cytoplasm, too. This may apply to FMRP as well. FMRP may be a multifunctional protein contributing to different steps of gene expression.

Conclusion

In conclusion, we have combined mouse models and biochemical analysis to demonstrate that RNA binding is a key function of FMRP. Particularly we have shown in the mouse that loss of KH2 domain specific RNA binding is likely the primary cause for polyribosome dissociation and thus loss of proper translational control, which in turn contributes to the synaptic dysfunction underlying the cognitive and behavioral deficits observed in the Fragile X Syndrome. Through RNA binding, FMRP regulates a defined set of mRNA targets involved in cytoskeletal and synaptic functions to mediate normal cognition. We propose FMRP may spatially and temporally fine-tune gene expression of its mRNA targets, but in a precise, robust and instantaneous fashion.

REFERENCES

Adinolfi, S., Bagni, C., Musco, G., Gibson, T., Mazzarella, L., and Pastore, A. (1999). Dissecting Fmr1, the protein responsible for fragile X syndrome, in its structural and functional domains. RNA *5*, 1248-1258.

Adinolfi, S., Ramos, A., Martin, S.R., Dal Piaz, F., Pucci, P., Bardoni, B., Mandel, J.L., and Pastore, A. (2003). The N-terminus of the fragile X mental retardation protein contains a novel domain involved in dimerization and RNA binding. Biochemistry *42*, 10437-10444.

Akamatsu, W., Fujihara, H., Mitsuhashi, T., Yano, M., Shibata, S., Hayakawa, Y., Okano, H.J., Sakakibara, S., Takano, H., Takano, T.*, et al.* (2005). The RNA-binding protein HuD regulates neuronal cell identity and maturation. Proc Natl Acad Sci U S A *102*, 4625-4630.

Albert, M.L., Austin, L.M., and Darnell, R.B. (2000). Detection and treatment of activated T cells in the cerebrospinal fluid of patients with paraneoplastic cerebellar degeneration. Ann Neurol *47*, 9-17.

Albert, M.L., Darnell, J.C., Bender, A., Francisco, L.M., Bhardwaj, N., and Darnell, R.B. (1998). Tumor-specific killer cells in paraneoplastic cerebellar degeneration. Nat Med *4*, 1321-1324.

Antar, L.N., Afroz, R., Dictenberg, J.B., Carroll, R.C., and Bassell, G.J. (2004). Metabotropic glutamate receptor activation regulates fragile x mental retardation protein and Fmr1 mRNA localization differentially in dendrites and at synapses. J Neurosci *24*, 2648-2655.

Antar, L.N., Dictenberg, J.B., Plociniak, M., Afroz, R., and Bassell, G.J. (2005). Localization of FMRP-associated mRNA granules and requirement of microtubules for activity-dependent trafficking in hippocampal neurons. Genes, brain, and behavior *4*, 350-359.

Antar, L.N., Li, C., Zhang, H., Carroll, R.C., and Bassell, G.J. (2006). Local functions for FMRP in axon growth cone motility and activity-dependent regulation of filopodia and spine synapses. Mol Cell Neurosci *32*, 37-48.

Ashley, C.T., Sutcliffe, J.S., Kunst, C.B., Leiner, H.A., Eichler, E.E., Nelson, D.L., and Warren, S.T. (1993a). Human and murine FMR-1: alternative splicing and translational initiation downstream of the CGG-repeat. Nature Genet *4*, 244-251.

Ashley, C.T., Wilkinson, K.D., Reines, D., and Warren, S.T. (1993b). FMR-1 protein: conserved RNP family domains and selective RNA binding. Science *262*, 563-566.

Banerjee, P., Nayar, S., Hebbar, S., Fox, C.F., Jacobs, M.C., Park, J.H., Fernandes, J.J., and Dockendorff, T.C. (2007). Substitution of Critical Isoleucines in the KH Domains of Drosophila Fragile X Protein Results in Partial Loss-of-Function Phenotypes. Genetics *175*, 1241-1250.

Bardoni, B., Castets, M., Huot, M.E., Schenck, A., Adinolfi, S., Corbin, F., Pastore, A., Khandjian, E.W., and Mandel, J.L. (2003). 82-FIP, a novel FMRP (fragile X mental retardation protein) interacting protein, shows a cell cycle-dependent intracellular localization. Hum Mol Genet *12*, 1689-1698.

Bardoni, B., Schenck, A., and Mandel, J.L. (1999). A novel RNA-binding nuclear protein that interacts with the fragile X mental retardation (Fmr1) protein. Hum Mol Genet *8*, 2557-2566.

Barth, A.I., Siemers, K.A., and Nelson, W.J. (2002). Dissecting interactions between EB1, microtubules and APC in cortical clusters at the plasma membrane. J Cell Sci *115*, 1583-1590.

Bassell, G.J., Zhang, H., Byrd, A.L., Femino, A.M., Singer, R.H., Taneja, K.L., Lifshitz, L.M., Herman, I.M., and Kosik, K.S. (1998). Sorting of beta-actin mRNA and protein to neurites and growth cones in culture. J Neurosci *18*, 251-265.

Bear, M.F., Huber, K.M., and Warren, S.T. (2004). The mGluR theory of fragile X mental retardation. Trends Neurosci *27*, 370-377.

Bohnsack, M.T., Czaplinski, K., and Gorlich, D. (2004). Exportin 5 is a RanGTP-dependent dsRNA-binding protein that mediates nuclear export of pre-miRNAs. Rna *10*, 185-191.

Bontekoe, C.J., McIlwain, K.L., Nieuwenhuizen, I.M., Yuva-Paylor, L.A., Nellis, A., Willemsen, R., Fang, Z., Kirkpatrick, L., Bakker, C.E., McAninch, R.*, et al.* (2002). Knockout mouse model for Fxr2: a model for mental retardation. Hum Mol Genet *11*, 487-498.

Borchert, G.M., Lanier, W., and Davidson, B.L. (2006). RNA polymerase III transcribes human microRNAs. Nature structural & molecular biology *13*, 1097-1101.

Brakeman, J.S., Gu, S.H., Wang, X.B., Dolin, G., and Baraban, J.M. (1999). Neuronal localization of the Adenomatous polyposis coli tumor suppressor protein. Neuroscience *91*, 661-672.

Brennan, C.M., Gallouzi, I.E., and Steitz, J.A. (2000). Protein ligands to HuR modulate its interaction with target mRNAs in vivo. J Cell Biol *151*, 1-14.

Brennan, F.X., Albeck, D.S., and Paylor, R. (2006). Fmr1 knockout mice are impaired in a leverpress escape/avoidance task. Genes, brain, and behavior *5*, 467-471.

Brown, V., Jin, P., Ceman, S., Darnell, J.C., O'Donnell, W.T., Tenenbaum, S.A., Jin, X., Feng, Y., Wilkinson, K.D., Keene, J.D., *et al.* (2001). Microarray identification of FMRP-associated brain mRNAs and altered mRNA translational profiles in Fragile X Syndrome. Cell *107*, 477-487.

Brown, V., Small, K., Lakkis, L., Feng, Y., Gunter, C., Wilkinson, K.D., and Warren, S.T. (1998). Purified recombinant Fmrp exhibits selective RNA binding as an intrinsic property of the fragile X mental retardation protein. J Biol Chem *273*, 15521-15527.

Buckanovich, R.J., Posner, J.B., and Darnell, R.B. (1993). Nova, the paraneoplastic Ri antigen, is homologous to an RNA-binding protein and is specifically expressed in the developing motor system. Neuron *11*, 657-672.

Bunting, M., Bernstein, K.E., Greer, J.M., Capecchi, M.R., and Thomas, K.R. (1999). Targeting genes for self-excision in the germ line. Genes Dev *13*, 1524-1528.

Burd, C.G., and Dreyfuss, G. (1994). Conserved structures and diversity of functions of RNA-binding proteins. Science *265*, 615-621.

Carlisle, H.J., and Kennedy, M.B. (2005). Spine architecture and synaptic plasticity. Trends Neurosci *28*, 182-187.

Carr-Schmid, A., Valente, L., Loik, V.I., Williams, T., Starita, L.M., and Kinzy, T.G. (1999). Mutations in elongation factor 1beta, a guanine nucleotide exchange factor, enhance translational fidelity. Mol Cell Biol *19*, 5257-5266.

Caudy, A.A., Ketting, R.F., Hammond, S.M., Denli, A.M., Bathoorn, A.M., Tops, B.B., Silva, J.M., Myers, M.M., Hannon, G.J., and Plasterk, R.H. (2003). A micrococcal nuclease homologue in RNAi effector complexes. Nature *425*, 411-414.

Caudy, A.A., Myers, M., Hannon, G.J., and Hammond, S.M. (2002). Fragile X-related protein and VIG associate with the RNA interference machinery. Genes Dev *16*, 2491-2496.

Ceman, S., Brown, V., and Warren, S.T. (1999). Isolation of an FMRP-associated messenger ribonucleoprotein particle and identification of nucleolin and the fragile X-related proteins as components of the complex. Mol Cell Biol *19*, 7925-7932.

Ceman, S., Nelson, R., and Warren, S.T. (2000). Identification of mouse YB1/p50 as a component of the FMRP-associated mRNP particle. Biochem Biophys Res Commun *279*, 904-908.

Ceman, S., O'Donnell, W.T., Reed, M., Patton, S., Pohl, J., and Warren, S.T. (2003a). Phosphorylation influences the translation state of FMRP-associated polyribosomes. Hum Mol Genet *12*, 3295-3305.

Ceman, S., Zhang, F., Johnson, T., and Warren, S.T. (2003b). Development and characterization of antibodies that immunoprecipitate the Fmr1 protein. Methods in molecular biology (Clifton, NJ *217*, 345-354.

Chen, L., and Toth, M. (2001). Fragile X mice develop sensory hyperreactivity to auditory stimuli. Neuroscience *103*, 1043-1050.

Chen, L., Yun, S.W., Seto, J., Liu, W., and Toth, M. (2003). The fragile X mental retardation protein binds and regulates a novel class of mRNAs containing U rich target sequences. Neuroscience *120*, 1005-1017.

Chen, R.Z., Akbarian, S., Tudor, M., and Jaenisch, R. (2001). Deficiency of methyl-CpG binding protein-2 in CNS neurons results in a Rett-like phenotype in mice. Nat Genet *27*, 327-331.

Cifuentes-Diaz, C., Frugier, T., Tiziano, F.D., Lacene, E., Roblot, N., Joshi, V., Moreau, M.H., and Melki, J. (2001). Deletion of murine SMN exon 7 directed to skeletal muscle leads to severe muscular dystrophy. J Cell Biol *152*, 1107-1114.

Comery, T.A., Harris, J.B., Willems, P.J., Oostra, B.A., Irwin, S.A., Weiler, I.J., and Greenough, W.T. (1997). Abnormal dendritic spines in fragile X knockout mice: maturation and pruning deficits. Proc Natl Acad Sci U S A *94*, 5401-5404.

Corbin, F., Bouillon, M., Fortin, A., Morin, S., Rousseau, F., and Khandjian, E.W. (1997). The fragile X mental retardation protein is associated with poly(A)+ mRNA in actively translating polyribosomes. Hum Mol Genet *6*, 1465-1472.

Darnell, J.C., Fraser, C.E., Mostovetsky, O., Stefani, G., Jones, T.A., Eddy, S.R., and Darnell, R.B. (2005a). Kissing complex RNAs mediate interaction between the Fragile-X mental retardation protein KH2 domain and brain polyribosomes. Genes Dev *19*, 903-918.

Darnell, J.C., Jensen, K.B., Jin, P., Brown, V., Warren, S.T., and Darnell, R.B. (2001). Fragile X mental retardation protein targets G Quartet mRNAs important for neuronal function. Cell *107*, 489-499.

Darnell, J.C., Mostovetsky, O., and Darnell, R.B. (2005b). FMRP RNA targets: identification and validation. Genes, brain, and behavior *4*, 341-349.

Darnell, R.B. (2004). Paraneoplastic neurologic disorders: windows into neuronal function and tumor immunity. Arch Neurol *61*, 30-32.

Darnell, R.B. (2006). Developing global insight into RNA regulation. Cold Spring Harb Symp Quant Biol *71*, 321-327.

Darnell, R.B., and Posner, J.B. (2003). Observing the invisible: successful tumor immunity in humans. Nat Immunol *4*, 201.

De Diego Otero, Y., Severijnen, L.A., van Cappellen, G., Schrier, M., Oostra, B., and Willemsen, R. (2002). Transport of fragile X mental retardation protein via granules in neurites of PC12 cells. Mol Cell Biol *22*, 8332-8341.

DeBoulle, K., Verkerk, A., Reyniers, E., Vits, L., Hendrickx, J., Van Roy, B., Van Den Bos, F., de Graaff, E., Oostra, B., and Willems, P. (1993). A point mutation in the FMR-1 gene associated with fragile X mental retardation. Nature Genet *3*, 31-35.

Denman, R.B. (2002). Methylation of the arginine-glycine-rich region in the fragile X mental retardation protein FMRP differentially affects RNA binding. Cellular & molecular biology letters *7*, 877-883.

Deschenes-Furry, J., Perrone-Bizzozero, N., and Jasmin, B.J. (2006). The RNA-binding protein HuD: a regulator of neuronal differentiation, maintenance and plasticity. Bioessays *28*, 822-833.

Dockendorff, T.C., Su, H.S., McBride, S.M., Yang, Z., Choi, C.H., Siwicki, K.K., Sehgal, A., and Jongens, T.A. (2002). Drosophila lacking dfmr1 activity show defects in circadian output and fail to maintain courtship interest. Neuron *34*, 973-984.

Dolzhanskaya, N., Sung, Y.J., Conti, J., Currie, J.R., and Denman, R.B. (2003). The fragile X mental retardation protein interacts with U-rich RNAs in a yeast three-hybrid system. Biochem Biophys Res Commun *305*, 434-441.

Dredge, B.K., and Darnell, R.B. (2003). Nova regulates GABA(A) receptor gamma2 alternative splicing via a distal downstream UCAU-rich intronic splicing enhancer. Mol Cell Biol *23*, 4687-4700.

Dresbach, T., Qualmann, B., Kessels, M.M., Garner, C.C., and Gundelfinger, E.D. (2001). The presynaptic cytomatrix of brain synapses. Cell Mol Life Sci *58*, 94-116.

Dutch-Belgian Fragile X Consortium, T. (1994). Fmr1 knockout mice: a model to study fragile X mental retardation. Cell *78*, 23-33.

Eberhart, D.E., Malter, H.E., Feng, Y., and Warren, S.T. (1996). The fragile X mental retardation protein is a ribonucleoprotein containing both nuclear localization and nuclear export signals. Hum Mol Genet *5*, 1083-1091.

Eichler, E.E., Richards, S., Gibbs, R.A., and Nelson, D.L. (1993). Fine structure of the human Fmr1 gene. Hum Mol Genet *2*, 1147-1153.

Engels, B.M., and Hutvagner, G. (2006). Principles and effects of microRNA-mediated post-transcriptional gene regulation. Oncogene *25*, 6163-6169.

Eom, T., Antar, L.N., Singer, R.H., and Bassell, G.J. (2003). Localization of a beta-actin messenger ribonucleoprotein complex with zipcode-binding protein modulates the density of dendritic filopodia and filopodial synapses. J Neurosci *23*, 10433-10444.

Feng, Y., Absher, D., Eberhart, D.E., Brown, V., Malter, H.E., and Warren, S.T. (1997a). FMRP associates with polyribosomes as an mRNP, and the I304N mutation of severe fragile X syndrome abolishes this association. Mol Cell *1*, 109-118.

Feng, Y., Gutekunst, C.A., Eberhart, D.E., Yi, H., Warren, S.T., and Hersch, S.M. (1997b). Fragile X mental retardation protein--nucleocytoplasmic shuttling and association with somatodendritic ribosomes. J Neurosci *17*, 1539-1547.

Ferrari, F., Mercaldo, V., Piccoli, G., Sala, C., Cannata, S., Achsel, T., and Bagni, C. (2007). The fragile X mental retardation protein-RNP granules show an mGluR-dependent localization in the post-synaptic spines. Mol Cell Neurosci *34*, 343-354.

Frugier, T., Tiziano, F.D., Cifuentes-Diaz, C., Miniou, P., Roblot, N., Dierich, A., Le Meur, M., and Melki, J. (2000). Nuclear targeting defect of SMN lacking the C-terminus in a mouse model of spinal muscular atrophy. Hum Mol Genet *9*, 849-858.

Gabel, L.A., Won, S., Kawai, H., McKinney, M., Tartakoff, A.M., and Fallon, J.R. (2004). Visual experience regulates transient expression and dendritic localization of fragile X mental retardation protein. J Neurosci *24*, 10579-10583.

Gray, N.K., and Hentze, M.W. (1994). Iron regulatory protein prevents binding of the 43S translation pre-initiation complex to ferritin and eALAS mRNAs. Embo J *13*, 3882-3891.

Greenough, W.T., Klintsova, A.Y., Irwin, S.A., Galvez, R., Bates, K.E., and Weiler, I.J. (2001). Synaptic regulation of protein synthesis and the fragile X protein. Proc Natl Acad Sci U S A *98*, 7101-7106.

Guy, J., Hendrich, B., Holmes, M., Martin, J.E., and Bird, A. (2001). A mouse Mecp2-null mutation causes neurological symptoms that mimic Rett syndrome. Nat Genet *27*, 322-326.

Guzik, B.W., and Goldstein, L.S. (2004). Microtubule-dependent transport in neurons: steps towards an understanding of regulation, function and dysfunction. Curr Opin Cell Biol *16*, 443-450.

Heitz, D., Rousseau, F., Devys, D., Saccone, S., Abderrahim, H., Le Paslier, D., Cohen, D., Vincent, A., Toniolo, D., Della Valle, G.*, et al.* (1991). Isolation of sequences that span the fragile X and identification of a fragile X-related CpG island. Science *251*, 1236-1239.

Hirokawa, N. (2006). mRNA transport in dendrites: RNA granules, motors, and tracks. J Neurosci *26*, 7139-7142.

Hirokawa, N., and Takemura, R. (2005). Molecular motors and mechanisms of directional transport in neurons. Nat Rev Neurosci *6*, 201-214.

Hou, L., Antion, M.D., Hu, D., Spencer, C.M., Paylor, R., and Klann, E. (2006). Dynamic translational and proteasomal regulation of fragile X mental retardation protein controls mGluR-dependent long-term depression. Neuron *51*, 441-454.

Hsieh-Li, H.M., Chang, J.G., Jong, Y.J., Wu, M.H., Wang, N.M., Tsai, C.H., and Li, H. (2000). A mouse model for spinal muscular atrophy. Nat Genet *24*, 66-70.

Huang, C.S., Shi, S.H., Ule, J., Ruggiu, M., Barker, L.A., Darnell, R.B., Jan, Y.N., and Jan, L.Y. (2005). Common molecular pathways mediate long-term potentiation of synaptic excitation and slow synaptic inhibition. Cell *123*, 105-118.

Huang, Y.S., Jung, M.Y., Sarkissian, M., and Richter, J.D. (2002). N-methyl-D-aspartate receptor signaling results in Aurora kinase-catalyzed CPEB phosphorylation and alpha CaMKII mRNA polyadenylation at synapses. Embo J *21*, 2139-2148.

Huber, K.M., Gallagher, S.M., Warren, S.T., and Bear, M.F. (2002). Altered synaptic plasticity in a mouse model of fragile X mental retardation. Proc Natl Acad Sci U S A *99*, 7746-7750.

Humphreys, D.T., Westman, B.J., Martin, D.I., and Preiss, T. (2005). MicroRNAs control translation initiation by inhibiting eukaryotic initiation factor 4E/cap and poly(A) tail function. Proc Natl Acad Sci U S A *102*, 16961-16966.

Inoue, S., Shimoda, M., Nishinokubi, I., Siomi, M.C., Okamura, M., Nakamura, A., Kobayashi, S., Ishida, N., and Siomi, H. (2002). A role for the Drosophila fragile X-related gene in circadian output. Curr Biol *12*, 1331-1335.

Ishizuka, A., Siomi, M.C., and Siomi, H. (2002). A Drosophila fragile X protein interacts with components of RNAi and ribosomal proteins. Genes Dev *16*, 2497-2508.

Jackson, R.J., and Standart, N. (2007). How do microRNAs regulate gene expression? Sci STKE *2007*, re1.

Jensen, K.B., Dredge, B.K., Stefani, G., Zhong, R., Buckanovich, R.J., Okano, H.J., Yang, Y.Y., and Darnell, R.B. (2000a). Nova-1 regulates neuron-specific alternative splicing and is essential for neuronal viability. Neuron *25*, 359-371.

Jensen, K.B., Musunuru, K., Lewis, H.A., Burley, S.K., and Darnell, R.B. (2000b). The tetranucleotide UCAY directs the specific recognition of RNA by the Nova KH3 domain. Proc Natl Acad Sci *97*, 5740-5745.

Jin, P., and Warren, S.T. (2000). Understanding the molecular basis of fragile X syndrome. Hum Mol Genet *9*, 901-908.

Jin, P., and Warren, S.T. (2003). New insights into fragile X syndrome: from molecules to neurobehaviors. Trends Biochem Sci *28*, 152-158.

Jin, P., Zarnescu, D.C., Ceman, S., Nakamoto, M., Mowrey, J., Jongens, T.A., Nelson, D.L., Moses, K., and Warren, S.T. (2004). Biochemical and genetic interaction between the fragile X mental retardation protein and the microRNA pathway. Nat Neurosci *7*, 113-117.

Keene, J.D. (1999). Why is Hu where? Shuttling of early-response-gene messenger RNA subsets. Proc Natl Acad Sci U S A *96*, 5-7.

Khandjian, E.W., Corbin, F., Woerly, S., and Rousseau, F. (1996). The fragile X mental retardation protein is associated with ribosomes. Nat Genet *12*, 91-93.

Khandjian, E.W., Huot, M.E., Tremblay, S., Davidovic, L., Mazroui, R., and Bardoni, B. (2004). Biochemical evidence for the association of fragile X mental retardation protein with brain polyribosomal ribonucleoparticles. Proc Natl Acad Sci U S A *101*, 13357-13362.

Kirkpatrick, L.L., McIlwain, K.A., and Nelson, D.L. (2001). Comparative genomic sequence analysis of the FXR gene family: Fmr1, FXR1, and FXR2. Genomics *78*, 169-177.

Koekkoek, S.K., Yamaguchi, K., Milojkovic, B.A., Dortland, B.R., Ruigrok, T.J., Maex, R., De Graaf, W., Smit, A.E., VanderWerf, F., Bakker, C.E.*, et al.* (2005). Deletion of Fmr1 in Purkinje cells enhances parallel fiber LTD, enlarges spines, and attenuates cerebellar eyelid conditioning in Fragile X syndrome. Neuron *47*, 339-352.

Kooy, R.F. (2003). Of mice and the fragile X syndrome. Trends Genet *19*, 148-154.

Laggerbauer, B., Ostareck, D., Keidel, E.M., Ostareck-Lederer, A., and Fischer, U. (2001a). Evidence that fragile X mental retardation protein is a negative regulator of translation. Hum Mol Genet *10*, 329-338.

Laggerbauer, B., Ostareck, D., Keidel, E.M., Ostareck-Lederer, A., and Fischer, U. (2001b). Evidence that fragile X mental retardation protein is a negative regulator of translation. Hum Mol Genet *10*, 329-338.

Landgraf, P., Rusu, M., Sheridan, R., Sewer, A., Iovino, N., Aravin, A., Pfeffer, S., Rice, A., Kamphorst, A.O., Landthaler, M.*, et al.* (2007). A mammalian microRNA expression atlas based on small RNA library sequencing. Cell *129*, 1401-1414.

Lee, Y., Ahn, C., Han, J., Choi, H., Kim, J., Yim, J., Lee, J., Provost, P., Radmark, O., Kim, S., *et al.* (2003). The nuclear RNase III Drosha initiates microRNA processing. Nature *425*, 415-419.

Lee, Y., Jeon, K., Lee, J.T., Kim, S., and Kim, V.N. (2002). MicroRNA maturation: stepwise processing and subcellular localization. Embo J *21*, 4663-4670.

Lee, Y., Kim, M., Han, J., Yeom, K.H., Lee, S., Baek, S.H., and Kim, V.N. (2004). MicroRNA genes are transcribed by RNA polymerase II. Embo J *23*, 4051-4060.

Leulliot, N., and Varani, G. (2001). Current topics in RNA-protein recognition: control of specificity and biological function through induced fit and conformational capture. Biochemistry *40*, 7947-7956.

Lewis, H.A., Chen, H., Edo, C., Buckanovich, R.J., Yang, Y.Y., Musunuru, K., Zhong, R., Darnell, R.B., and Burley, S.K. (1999). Crystal structures of Nova-1 and Nova-2 K-homology RNA-binding domains. Structure *7*, 191-203.

Lewis, H.A., Musunuru, K., Jensen, K.B., Edo, C., Chen, H., Darnell, R.B., and Burley, S.K. (2000). Sequence-specific RNA binding by a Nova KH domain: implications for paraneoplastic disease and the fragile X syndrome. Cell *100*, 323-332.

Li, Z., Zhang, Y., Ku, L., Wilkinson, K.D., Warren, S.T., and Feng, Y. (2001). The fragile X mental retardation protein inhibits translation via interacting with mRNA. Nucleic Acids Res *29*, 2276-2283.

Liu, Z., Luyten, I., Bottomley, M.J., Messias, A.C., Houngninou-Molango, S., Sprangers, R., Zanier, K., Kramer, A., and Sattler, M. (2001). Structural basis for recognition of the intron branch site RNA by splicing factor 1. Science *294*, 1098-1102.

Lund, E., Guttinger, S., Calado, A., Dahlberg, J.E., and Kutay, U. (2004). Nuclear export of microRNA precursors. Science *303*, 95-98.

Lunde, B.M., Moore, C., and Varani, G. (2007). RNA-binding proteins: modular design for efficient function. Nature reviews *8*, 479-490.

Maniatis, T., and Reed, R. (2002). An extensive network of coupling among gene expression machines. Nature *416*, 499-506.

Matranga, C., Tomari, Y., Shin, C., Bartel, D.P., and Zamore, P.D. (2005). Passenger-strand cleavage facilitates assembly of siRNA into Ago2-containing RNAi enzyme complexes. Cell *123*, 607-620.

Mazroui, R., Huot, M.E., Tremblay, S., Boilard, N., Labelle, Y., and Khandjian, E.W. (2003). Fragile X Mental Retardation protein determinants required for its association with polyribosomal mRNPs. Hum Mol Genet *12*, 3087-3096.

Mazroui, R., Huot, M.E., Tremblay, S., Filion, C., Labelle, Y., and Khandjian, E.W. (2002). Trapping of messenger RNA by Fragile X Mental Retardation protein into cytoplasmic granules induces translation repression. Hum Mol Genet *11*, 3007-3017.

McLeod, L.E., Wang, L., and Proud, C.G. (2001). beta-Adrenergic agonists increase phosphorylation of elongation factor 2 in cardiomyocytes without eliciting calcium-independent eEF2 kinase activity. FEBS Lett *489*, 225-228.

Mientjes, E.J., Willemsen, R., Kirkpatrick, L.L., Nieuwenhuizen, I.M., Hoogeveen-Westerveld, M., Verweij, M., Reis, S., Bardoni, B., Hoogeveen, A.T., Oostra, B.A*., et al.* (2004). Fxr1 knockout mice show a striated muscle phenotype: implications for Fxr1p function in vivo. Hum Mol Genet *13*, 1291-1302.

Mili, S., and Steitz, J.A. (2004). Evidence for reassociation of RNA-binding proteins after cell lysis: implications for the interpretation of immunoprecipitation analyses. Rna *10*, 1692-1694.

Miyashiro, K.Y., Beckel-Mitchener, A., Purk, T.P., Becker, K.G., Barret, T., Liu, L., Carbonetto, S., Weiler, I.J., Greenough, W.T., and Eberwine, J. (2003). RNA cargoes associating with FMRP reveal deficits in cellular functioning in Fmr1 null mice. Neuron *37*, 417-431.

Monani, U.R., Sendtner, M., Coovert, D.D., Parsons, D.W., Andreassi, C., Le, T.T., Jablonka, S., Schrank, B., Rossol, W., Prior, T.W*., et al.* (2000). The human centromeric survival motor neuron gene (SMN2) rescues embryonic lethality in Smn(-/-) mice and results in a mouse with spinal muscular atrophy. Hum Mol Genet *9*, 333-339.

Morales, J., Hiesinger, P.R., Schroeder, A.J., Kume, K., Verstreken, P., Jackson, F.R., Nelson, D.L., and Hassan, B.A. (2002). Drosophila fragile X protein, DFXR, regulates neuronal morphology and function in the brain. Neuron *34*, 961-972.

Muckenthaler, M., Gray, N.K., and Hentze, M.W. (1998). IRP-1 binding to ferritin mRNA prevents the recruitment of the small ribosomal subunit by the cap-binding complex eIF4F. Mol Cell *2*, 383-388.

Muddashetty, R.S., Kelic, S., Gross, C., Xu, M., and Bassell, G.J. (2007). Dysregulated metabotropic glutamate receptor-dependent translation of AMPA receptor and postsynaptic density-95 mRNAs at synapses in a mouse model of fragile X syndrome. J Neurosci *27*, 5338-5348.

Munemitsu, S., Souza, B., Muller, O., Albert, I., Rubinfeld, B., and Polakis, P. (1994). The APC gene product associates with microtubules in vivo and promotes their assembly in vitro. Cancer Res *54*, 3676-3681.

Musco, G., Kharrat, A., Stier, G., Fraternali, F., Gibson, T.J., Nilges, M., and Pastore, A. (1997). The solution structure of the first KH domain of Fmr1, the protein responsible for the fragile X syndrome. Nat Struct Biol *4*, 712-716.

Musco, G., Stier, G., Joseph, C., Morelli, M.A.C., Nilges, M., Gibson, T., and Pastore, A. (1996). Three-dimensional structure and stability of the KH domain: molecular insights into the Fragile X syndrome. Cell *85*, 237-245.

Musumeci, S.A., Bosco, P., Calabrese, G., Bakker, C., De Sarro, G.B., Elia, M., Ferri, R., and Oostra, B.A. (2000). Audiogenic seizures susceptibility in transgenic mice with fragile X syndrome. Epilepsia *41*, 19-23.

Musunuru, K., and Darnell, R.B. (2001). Paraneoplastic neurologic disease antigens: RNA-binding proteins and signaling proteins in neuronal degeneration. Annu Rev Neurosci *24*, 239-262.

Neilson, J.R., Zheng, G.X., Burge, C.B., and Sharp, P.A. (2007). Dynamic regulation of miRNA expression in ordered stages of cellular development. Genes Dev *21*, 578-589.

Nimchinsky, E.A., Oberlander, A.M., and Svoboda, K. (2001). Abnormal development of dendritic spines in Fmr1 knock-out mice. J Neurosci *21*, 5139-5146.

Nosyreva, E.D., and Huber, K.M. (2006). Metabotropic receptor-dependent long-term depression persists in the absence of protein synthesis in the mouse model of fragile X syndrome. J Neurophysiol *95*, 3291-3295.

O'Donnell, W.T., and Warren, S.T. (2002). A decade of molecular studies of fragile X syndrome. Annu Rev Neurosci *25*, 315-338.

Ohashi, S., Koike, K., Omori, A., Ichinose, S., Ohara, S., Kobayashi, S., Sato, T.A., and Anzai, K. (2002). Identification of mRNA/protein (mRNP) complexes containing Puralpha, mStaufen, fragile X protein, and myosin Va and their association with rough endoplasmic reticulum equipped with a kinesin motor. J Biol Chem *277*, 37804-37810.

Okano, H.J., and Darnell, R.B. (1997). A hierarchy of Hu RNA binding proteins in developing and adult neurons. J Neurosci *17*, 3024-3037.

Ostareck, D.H., Ostareck-Lederer, A., Shatsky, I.N., and Hentze, M.W. (2001). Lipoxygenase mRNA silencing in erythroid differentiation: The 3'UTR regulatory complex controls 60S ribosomal subunit joining. Cell *104*, 281-290.

Ostareck, D.H., Ostareck-Lederer, A., Wilm, M., Thiele, B.J., Mann, M., and Hentze, M.W. (1997). mRNA silencing in erythroid differentiation: hnRNP K and hnRNP E1 regulate 15-lipoxygenase translation from the 3' end. Cell *89*, 597-606.

Ostareck-Lederer, A., and Ostareck, D.H. (2004). Control of mRNA translation and stability in haematopoietic cells: the function of hnRNPs K and E1/E2. Biology of the cell / under the auspices of the European Cell Biology Organization *96*, 407-411.

Park, W., Li, J., Song, R., Messing, J., and Chen, X. (2002). CARPEL FACTORY, a Dicer homolog, and HEN1, a novel protein, act in microRNA metabolism in Arabidopsis thaliana. Curr Biol *12*, 1484-1495.

Peier, A.M., McIlwain, K.L., Kenneson, A., Warren, S.T., Paylor, R., and Nelson, D.L. (2000). (Over)correction of Fmr1 deficiency with YAC transgenics: behavioral and physical features. Hum Mol Genet *9*, 1145-1159.

Pieretti, M., Zhang, F., Fu, Y., Warren, S., Oostra, B., Caskey, C., and Nelson, D. (1991). Absence of expression of the FMR-1 gene in fragile X syndrome. Cell *66*, 817-822.

Pillai, R.S., Bhattacharyya, S.N., Artus, C.G., Zoller, T., Cougot, N., Basyuk, E., Bertrand, E., and Filipowicz, W. (2005). Inhibition of translational initiation by Let-7 MicroRNA in human cells. Science *309*, 1573-1576.

Pillai, R.S., Bhattacharyya, S.N., and Filipowicz, W. (2007). Repression of protein synthesis by miRNAs: how many mechanisms? Trends Cell Biol *17*, 118-126.

Pozdnyakova, I., and Regan, L. (2005). New insights into Fragile X syndrome. Relating genotype to phenotype at the molecular level. The FEBS journal *272*, 872-878.

Ramos, A., Hollingworth, D., Adinolfi, S., Castets, M., Kelly, G., Frenkiel, T.A., Bardoni, B., and Pastore, A. (2006). The structure of the N-terminal domain of the fragile X mental retardation protein: a platform for protein-protein interaction. Structure *14*, 21-31.

Ramos, A., Hollingworth, D., and Pastore, A. (2003). The role of a clinically important mutation in the fold and RNA-binding properties of KH motifs. Rna *9*, 293-298.

Roper, K., Gregory, S.L., and Brown, N.H. (2002). The 'spectraplakins': cytoskeletal giants with characteristics of both spectrin and plakin families. J Cell Sci *115*, 4215-4225.

Ross, A.F., Oleynikov, Y., Kislauskis, E.H., Taneja, K.L., and Singer, R.H. (1997). Characterization of a beta-actin mRNA zipcode-binding protein. Mol Cell Biol *17*, 2158-2165.

Schaeffer, C., Bardoni, B., Mandel, J.L., Ehresmann, B., Ehresmann, C., and Moine, H. (2001). The fragile X mental retardation protein binds specifically to its mRNA via a purine quartet motif. Embo J *20*, 4803-4813.

Scheetz, A.J., Nairn, A.C., and Constantine-Paton, M. (1997). N-methyl-D-aspartate receptor activation and visual activity induce elongation factor-2 phosphorylation in

amphibian tecta: a role for N-methyl-D-aspartate receptors in controlling protein synthesis. Proc Natl Acad Sci U S A *94*, 14770-14775.

Scheetz, A.J., Nairn, A.C., and Constantine-Paton, M. (2000). NMDA receptor-mediated control of protein synthesis at developing synapses. Nat Neurosci *3*, 211-216.

Schenck, A., Bardoni, B., Langmann, C., Harden, N., Mandel, J.L., and Giangrande, A. (2003). CYFIP/Sra-1 controls neuronal connectivity in Drosophila and links the Rac1 GTPase pathway to the fragile X protein. Neuron *38*, 887-898.

Schenck, A., Bardoni, B., Moro, A., Bagni, C., and Mandel, J.L. (2001). A highly conserved protein family interacting with the fragile X mental retardation protein (FMRP) and displaying selective interactions with FMRP-related proteins FXR1P and FXR2P. Proc Natl Acad Sci U S A *98*, 8844-8849.

Schoch, S., and Gundelfinger, E.D. (2006). Molecular organization of the presynaptic active zone. Cell and tissue research *326*, 379-391.

Schrank, B., Gotz, R., Gunnersen, J.M., Ure, J.M., Toyka, K.V., Smith, A.G., and Sendtner, M. (1997). Inactivation of the survival motor neuron gene, a candidate gene for human spinal muscular atrophy, leads to massive cell death in early mouse embryos. Proc Natl Acad Sci U S A *94*, 9920-9925.

Schubert, V., and Dotti, C.G. (2007). Transmitting on actin: synaptic control of dendritic architecture. J Cell Sci *120*, 205-212.

Shahbazian, M., Young, J., Yuva-Paylor, L., Spencer, C., Antalffy, B., Noebels, J., Armstrong, D., Paylor, R., and Zoghbi, H. (2002). Mice with truncated MeCP2 recapitulate many Rett syndrome features and display hyperacetylation of histone H3. Neuron *35*, 243-254.

Shamoo, Y., Abdul-Manan, N., and Williams, K.R. (1995). Multiple RNA binding domains (RBDs) just don't add up. Nucleic Acids Res *23*, 725-728.

Shamoo, Y., Krueger, U., Rice, L.M., Williams, K.R., and Steitz, T.A. (1997). Crystal structure of the two RNA binding domains of human hnRNP A1 at 1.75 A resolution. Nat Struct Biol *4*, 215-222.

Shi, S.H., Cheng, T., Jan, L.Y., and Jan, Y.N. (2004). APC and GSK-3beta are involved in mPar3 targeting to the nascent axon and establishment of neuronal polarity. Curr Biol *14*, 2025-2032.

Shin, C.Y., Kundel, M., and Wells, D.G. (2004). Rapid, activity-induced increase in tissue plasminogen activator is mediated by metabotropic glutamate receptor-dependent mRNA translation. J Neurosci *24*, 9425-9433.

Siomi, H., Choi, M., Siomi, M., Nussbaum, R., and Dreyfuss, G. (1994). Essential role for KH domains in RNA binding: impaired RNA binding by a mutation in the KH domain of Fmr1 that causes fragile X syndrome. Cell *77*, 33-39.

Siomi, H., Matunis, M.J., Michael, W.M., and Dreyfuss, G. (1993a). The pre-mRNA binding K protein contains a novel evolutionarily conserved motif. Nucl Acids Res *21*, 1193-1198.

Siomi, H., Siomi, M., Nussbaum, R., and Dreyfuss, G. (1993b). The protein product of the fragile X gene, Fmr1, has characteristics of an RNA-binding protein. Cell *74*, 291-298.

Siomi, M.C., Siomi, H., Sauer, W.H., Srinivasan, S., Nussbaum, R.L., and Dreyfuss, G. (1995). FXR1, an autosomal homolog of the fragile X mental retardation gene. Embo J *14*, 2401-2408.

Sonenberg, N., Hershey, J.W.B., and Mathews, M.B. (2000). Translational control of gene expression.

Spencer, C.M., Alekseyenko, O., Serysheva, E., Yuva-Paylor, L.A., and Paylor, R. (2005). Altered anxiety-related and social behaviors in the Fmr1 knockout mouse model of fragile X syndrome. Genes, brain, and behavior *4*, 420-430.

Spencer, C.M., Serysheva, E., Yuva-Paylor, L.A., Oostra, B.A., Nelson, D.L., and Paylor, R. (2006). Exaggerated behavioral phenotypes in Fmr1/Fxr2 double knockout mice reveal a functional genetic interaction between Fragile X-related proteins. Hum Mol Genet *15*, 1984-1994.

Stefani, G., Fraser, C.E., Darnell, J.C., and Darnell, R.B. (2004). Fragile X mental retardation protein is associated with translating polyribosomes in neuronal cells. J Neurosci *24*, 7272-7276.

Stetler, A., Winograd, C., Sayegh, J., Cheever, A., Patton, E., Zhang, X., Clarke, S., and Ceman, S. (2006). Identification and characterization of the methyl arginines in the fragile X mental retardation protein Fmrp. Hum Mol Genet *15*, 87-96.

Su, L.K., Burrell, M., Hill, D.E., Gyuris, J., Brent, R., Wiltshire, R., Trent, J., Vogelstein, B., and Kinzler, K.W. (1995). APC binds to the novel protein EB1. Cancer Res *55*, 2972-2977.

Sung, Y.J., Dolzhanskaya, N., Nolin, S.L., Brown, T., Currie, J.R., and Denman, R.B. (2003). The fragile X mental retardation protein FMRP binds elongation factor 1A mRNA and negatively regulates its translation in vivo. J Biol Chem *278*, 15669-15678.

Takei, N., Inamura, N., Kawamura, M., Namba, H., Hara, K., Yonezawa, K., and Nawa, H. (2004). Brain-derived neurotrophic factor induces mammalian target of rapamycin-

dependent local activation of translation machinery and protein synthesis in neuronal dendrites. J Neurosci *24*, 9760-9769.

Takei, N., Kawamura, M., Hara, K., Yonezawa, K., and Nawa, H. (2001). Brain-derived neurotrophic factor enhances neuronal translation by activating multiple initiation processes: comparison with the effects of insulin. J Biol Chem *276*, 42818-42825.

Tamanini, F., Van Unen, L., Bakker, C., Sacchi, N., Galjaard, H., Oostra, B.A., and Hoogeveen, A.T. (1999). Oligomerization properties of fragile-X mental-retardation protein (FMRP) and the fragile-X-related proteins FXR1P and FXR2P. Biochem J *343 Pt 3*, 517-523.

Tassone, F., Hagerman, R.J., Ikle, D.N., Dyer, P.N., Lampe, M., Willemsen, R., Oostra, B.A., and Taylor, A.K. (1999). FMRP expression as a potential prognostic indicator in fragile X syndrome. Am J Med Genet *84*, 250-261.

Tassone, F., Hagerman, R.J., Loesch, D.Z., Lachiewicz, A., Taylor, A.K., and Hagerman, P.J. (2000). Fragile X males with unmethylated, full mutation trinucleotide repeat expansions have elevated levels of Fmr1 messenger RNA. Am J Med Genet *94*, 232-236.

Tassone, F., Hagerman, R.J., Taylor, A.K., and Hagerman, P.J. (2001). A majority of fragile X males with methylated, full mutation alleles have significant levels of Fmr1 messenger RNA. J Med Genet *38*, 453-456.

Todd, P.K., Mack, K.J., and Malter, J.S. (2003). The fragile X mental retardation protein is required for type-I metabotropic glutamate receptor-dependent translation of PSD-95. Proc Natl Acad Sci U S A *100*, 14374-14378.

Ule, J., Jensen, K., Mele, A., and Darnell, R.B. (2005a). CLIP: a method for identifying protein-RNA interaction sites in living cells. Methods *37*, 376-386.

Ule, J., Jensen, K.B., Ruggiu, M., Mele, A., Ule, A., and Darnell, R.B. (2003). CLIP identifies Nova-regulated RNA networks in the brain. Science *302*, 1212-1215.

Ule, J., Stefani, G., Mele, A., Ruggiu, M., Wang, X., Taneri, B., Gaasterland, T., Blencowe, B.J., and Darnell, R.B. (2006). An RNA map predicting Nova-dependent splicing regulation. Nature *444*, 580-586.

Ule, J., Ule, A., Spencer, J., Williams, A., Hu, J.S., Cline, M., Wang, H., Clark, T., Fraser, C., Ruggiu, M.*, et al.* (2005b). Nova regulates brain-specific splicing to shape the synapse. Nat Genet *37*, 844-852.

van Swieten, J., and Spillantini, M.G. (2007). Hereditary frontotemporal dementia caused by Tau gene mutations. Brain Pathol *17*, 63-73.

Vasudevan, S., and Steitz, J.A. (2007). AU-rich-element-mediated upregulation of translation by FXR1 and Argonaute 2. Cell *128*, 1105-1118.

Verkerk, A.J., Pieretti, M., Sutcliffe, J.S., Fu, Y.H., Kuhl, D.P., Pizzuti, A., Reiner, O., Richards, S., Victoria, M.F., Zhang, F.P.*, et al.* (1991). Identification of a gene (FMR-1) containing a CGG repeat coincident with a breakpoint cluster region exhibiting length variation in fragile X syndrome. Cell *65*, 905-914.

Votin, V., Nelson, W.J., and Barth, A.I. (2005). Neurite outgrowth involves adenomatous polyposis coli protein and beta-catenin. J Cell Sci *118*, 5699-5708.

Wan, L., Dockendorff, T.C., Jongens, T.A., and Dreyfuss, G. (2000). Characterization of dFmr1, a Drosophila melanogaster homolog of the fragile X mental retardation protein. Mol Cell Biol *20*, 8536-8547.

Weiler, I.J., Irwin, S.A., Klintsova, A.Y., Spencer, C.M., Brazelton, A.D., Miyashiro, K., Comery, T.A., Patel, B., Eberwine, J., and Greenough, W.T. (1997). Fragile X mental retardation protein is translated near synapses in response to neurotransmitter activation. Proc Natl Acad Sci U S A *94*, 5395-5400.

Wells, D.G., Dong, X., Quinlan, E.M., Huang, Y.S., Bear, M.F., Richter, J.D., and Fallon, J.R. (2001). A role for the cytoplasmic polyadenylation element in NMDA receptor-regulated mRNA translation in neurons. J Neurosci *21*, 9541-9548.

Willemsen, R., Bontekoe, C.J., Severijnen, L.A., and Oostra, B.A. (2002). Timing of the absence of Fmr1 expression in full mutation chorionic villi. Human genetics *110*, 601-605.

Willemsen, R., Smits, A., Mohkamsing, S., van Beerendonk, H., de Haan, A., de Vries, B., van den Ouweland, A., Sistermans, E., Galjaard, H., and Oostra, B.A. (1997). Rapid antibody test for diagnosing fragile X syndrome: a validation of the technique. Human genetics *99*, 308-311.

Williamson, J.R. (2000). Induced fit in RNA-protein recognition. Nat Struct Biol *7*, 834-837.

Wood-Kaczmar, A., Gandhi, S., and Wood, N.W. (2006). Understanding the molecular causes of Parkinson's disease. Trends Mol Med *12*, 521-528.

Wu, L., Wells, D., Tay, J., Mendis, D., Abbott, M.A., Barnitt, A., Quinlan, E., Heynen, A., Fallon, J.R., and Richter, J.D. (1998). CPEB-mediated cytoplasmic polyadenylation and the regulation of experience-dependent translation of alpha-CaMKII mRNA at synapses. Neuron *21*, 1129-1139.

Xu, K., Bogert, B.A., Li, W., Su, K., Lee, A., and Gao, F.B. (2004). The fragile X-related gene affects the crawling behavior of Drosophila larvae by regulating the mRNA level of the DEG/ENaC protein pickpocket1. Curr Biol *14*, 1025-1034.

Yang, X.W., Model, P., and Heintz, N. (1997). Homologous recombination based modification in Escherichia coli and germline transmission in transgenic mice of a bacterial artificial chromosome. Nat Biotechnol *15*, 859-865.

Yi, R., Qin, Y., Macara, I.G., and Cullen, B.R. (2003). Exportin-5 mediates the nuclear export of pre-microRNAs and short hairpin RNAs. Genes Dev *17*, 3011-3016.

Yisraeli, J.K. (2005). VICKZ proteins: a multi-talented family of regulatory RNA-binding proteins. Biology of the cell / under the auspices of the European Cell Biology Organization *97*, 87-96.

Zalfa, F., Adinolfi, S., Napoli, I., Kuhn-Holsken, E., Urlaub, H., Achsel, T., Pastore, A., and Bagni, C. (2005). Fragile X mental retardation protein (FMRP) binds specifically to the brain cytoplasmic RNAs BC1/BC200 via a novel RNA-binding motif. J Biol Chem *280*, 33403-33410.

Zalfa, F., Giorgi, M., Primerano, B., Moro, A., Di Penta, A., Reis, S., Oostra, B., and Bagni, C. (2003). The fragile X syndrome protein FMRP associates with BC1 RNA and regulates the translation of specific mRNAs at synapses. Cell *112*, 317-327.

Zhang, H.L., Eom, T., Oleynikov, Y., Shenoy, S.M., Liebelt, D.A., Dictenberg, J.B., Singer, R.H., and Bassell, G.J. (2001a). Neurotrophin-induced transport of a beta-actin mRNP complex increases beta-actin levels and stimulates growth cone motility. Neuron *31*, 261-275.

Zhang, Y., O'Conner, J.P., Siomi, M.C., Srinivasan, S., Dutra, A., Nussbaum, R.L., and Dreyfuss, G. (1995). The fragile X mental retardation syndrome protein interacts with novel homologs FXR1 and FXR2. EMBO J *14*, 5358-5366.

Zhang, Y.Q., Bailey, A.M., Matthies, H.J., Renden, R.B., Smith, M.A., Speese, S.D., Rubin, G.M., and Broadie, K. (2001b). Drosophila Fragile X-Related Gene Regulates the MAP1B Homolog Futsch to Control Synaptic Structure and Function. Cell *107*, 591-603.

Zhou, F.Q., Zhou, J., Dedhar, S., Wu, Y.H., and Snider, W.D. (2004). NGF-induced axon growth is mediated by localized inactivation of GSK-3beta and functions of the microtubule plus end binding protein APC. Neuron *42*, 897-912.

Zumbrunn, J., Kinoshita, K., Hyman, A.A., and Nathke, I.S. (2001). Binding of the adenomatous polyposis coli protein to microtubules increases microtubule stability and is regulated by GSK3 beta phosphorylation. Curr Biol *11*, 44-49.